STUDY OF FLAME HEATING OF STEEL PLATE

by

Eugene K. Johnson

STUDY OF FLAME HEATING OF STEEL PLATE

by

EUGENE KARNS JOHNSON

B.S., United States Coast Guard Academy

(1965)

SUBMITTED IN PARTIAL FULFILLMENT

OF THE REQUIREMENTS FOR THE DEGREES OF

NAVAL ENGINEER AND

MASTER OF SCIENCE IN

MECHANICAL ENGINEERING

at the

MASSACHUSETTS INSTITUTE OF TECHNOLOGY

May, 1971

STUDY OF FLAME HEATING OF STEEL PLATE

by

EUGENE KARNS JOHNSON

Submitted to the Department of Naval Architecture and Marine Engineering on May 14, 1971, in partial fulfillment of the requirements for the degrees of Naval Engineer in Naval Architecture and Marine Engineering and Master of Science in Mechanical Engineering.

ABSTRACT

The effects of welding and analytical procedures for predicting welding effects are discussed. The results of previous investigations of flame heating are analyzed. A flat plate was chosen as a model for this investigation so that the analytical techniques, developed for welding, could be applied to the flame heating. Line flame heating is employed because this closely resembles bead-on-plate welding. Three steels: AISI 1020, ASTM A-242, and ASTM A-514 were chosen as materials. Heating was performed with and without water cooling and continuous readings of strain and temperature were taken at selected positions.

The results of testing are presented in the form of temperature and strain plotted against time. Plots of experimental and analytical temperatures and strain are presented for comparison. It was found that flame heating with water cooling is more effective than without cooling, and the direction of the bending is controlled by the cooling. When water cooling is not employed, the flame heating is most effective on the mild steel. However, the direction of bending depends on the initial plate condition and is not controlled by the heating.

Comparison of the analytical predictions of temperatures and longitudinal strains with experimental data shows good correlation. However, transverse strains are large for the flame heating so a one dimensional analysis, assuming transverse stresses are negligible, is not satisfactory for flame heating. Welding programs, as they are developed, can be modified for flame heating. A full three dimensional analysis is needed to optimize flame heating.

It is recommended that further investigation of flame heating be delayed until a three dimensional analysis is developed. There is enough information available now on flame heating to make applications of this bending or straightening process more effective.

Thesis Supervisor: Prof. Koichi Masubuchi

Title: Associate Professor of Naval Architecture

ACKNOWLEDGEMENTS

I would like to thank the U. S. Coast Guard for sponsoring my studies at M.I.T. and this thesis.

I also thank Prof. Masubuchi and Prof. Argon for their assistance and many helpful suggestions throughout the course of this investigation. The assistance of Mr. A. Zona of the Materials Joining Laboratory was greatly appreciated. The technical assistance of Mr. F. Merlis while preparing for and conducting the experimental work was invaluable.

I would also like to thank Mr. W. Laughton of General Dynamics for allowing me to visit the Quincy Shipyard and observe how flame heating is used in practice.

Finally, I thank my wife, Lynne, for her efficient typing of this thesis.

TABLE OF CONTENTS

LIST OF FIGURES

LIST OF TABLES

NOMENCLATURE

$T\underline{x}$	Experimental temperature at position indicated by number $\underline{x}$
$AT\underline{x}$	Analytical temperature at position indicated by number $\underline{x}$
$EX\underline{x}$	Experimental strain in x-direction at position indicated by number $\underline{x}$
$EY\underline{x}$	Experimental strain in y-direction at position indicated by number $\underline{x}$
$AEX\underline{x}$	Analytical strain in x-direction at position indicated by number $\underline{x}$
x, y, z	Coordinates of the point
t	Temperature of the point
t_o	Initial temperature
s	Time
Q	Heat input
v	Velocity
g	Plate thickness
K	Thermal conductivity
λ	Thermal diffusivity
ρ	Density
c	Heat capacity
$\sigma_x, \sigma_y, \sigma_z$	Stress in direction indicated by coordinate
α	Coefficient of thermal expansion
Δ	Change in a quantity

I. INTRODUCTION

A. Background of Problem

In the shipbuilding industry, the fabrication process widely used is welding. This process is used for economic as well as structural reasons. However, in the application of this welding process undesired effects such as residual stresses and distortion, which may cause structural weakness, are induced.

In the past, the primary emphasis in research has been on how to prevent excessive residual stresses and distortion. Until recently the means by which this was accomplished has been more an art than a science. Observation of what occurred during particular welding processes lead to the development of design standards to allow tolerance for shrinkage and welding procedures to help minimize the residual stresses and distortion.

At present there is much effort being devoted to the development of analytical techniques for predicting the residual stresses and distortion that will occur for any given welding situation[1,2]. The program that has been developed at M.I.T. is a one dimensional analysis, Appendix B, and determines the strains induced by non-uniform heating during welding. Some experimental data has been obtained and correlated with this program and at present further experimental work is being carried on. Other investigations exclusively on the heating effects of welding and prediction of temperatures in metal plates have been performed[3,4].

Even if the best controls of the welding process are in effect, distortion will occur in a percentage of the welds made on a structure. The amount of distortion that occurs may be beyond acceptable limits and when this occurs it must be removed. There are many methods available for

removing the distortion but the primary method used in shipyards for ordinary carbon steels is flame heating. Flame heating is used because it is both an economical and easy method to employ as compared to all other available methods.

As practiced in the shipyards today, the flame heating technique for removing distortion is an art. Usually the senior welder determines where a distorted plate should be heated to remove the distortion. If the first application of heat fails, a second guess is made and heat again applied and so on until the distortion is removed or reduced to acceptable standards. One technique is spot heating an entire panel as shown in Figure (1). This method insures that the distortion is removed but is probably an excessive use of flame heating.

The cost of removing distortion can be very high as experienced by one shipyard where the cost of the distortion removal was half the total welding cost. In this instance, the welders utilized the method shown in Figure (1) for much of the distortion removal on 3/8 inch steel plates used for bulkheads.

Other heating techniques used to remove distortion are:

(1) Line heating of the panel. In this procedure, the area to be straightened is heated to approximately 1200^{o}F along narrow lines which may be water quenched after the heating.

(2) Line heating of the backs of the fillet welds. This procedure is similar to (1) except the flame is applied to the back of the weld.

(3) Line heating approximately three to four inches from the fillet weld along a single line. This method was developed in the German shipyards.

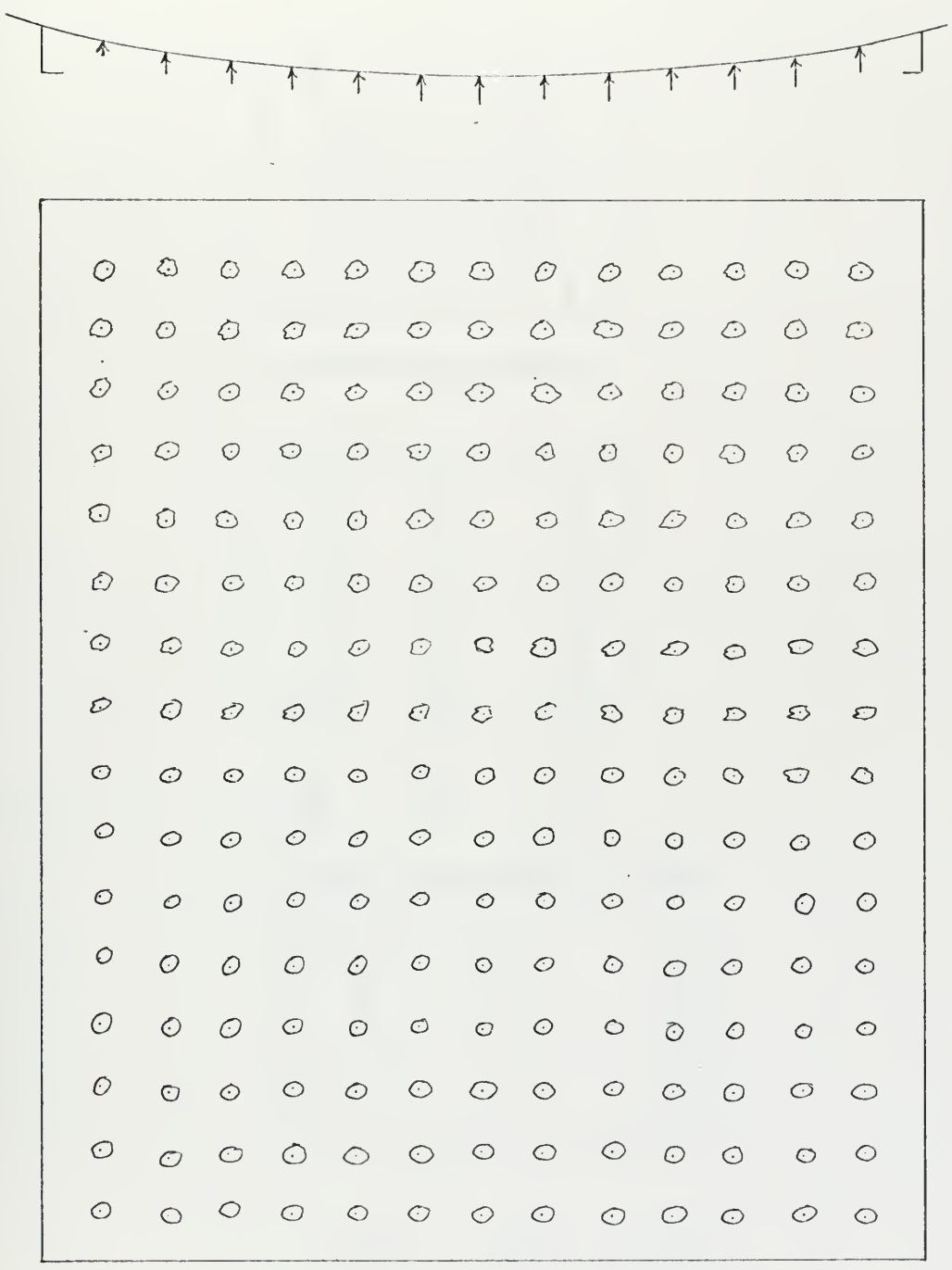

Figure 1: Example of spot flame heating as actually used in shipyard

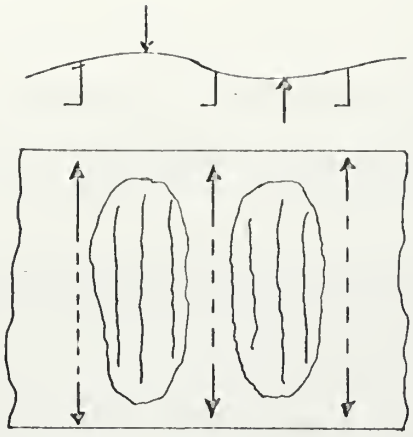

a. Line Heating Panel

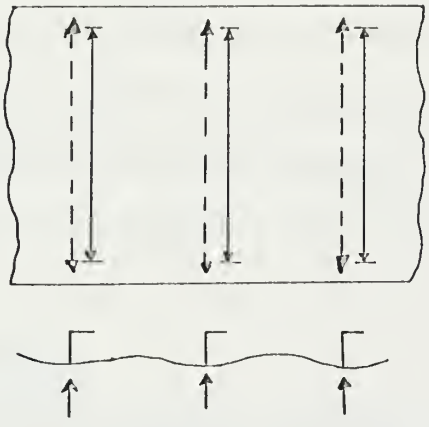

b. Line Heating Back of Welds

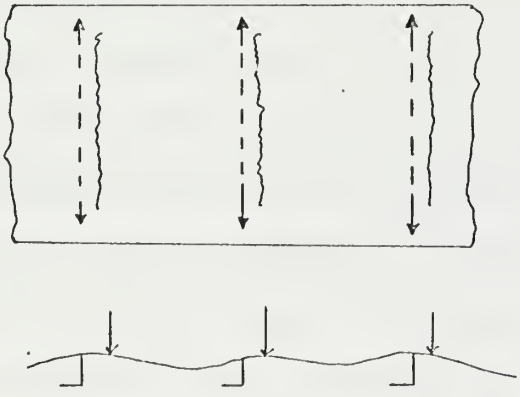

c. Line Heating Parallel to Weld

Figure (2)

These methods are shown in Figure (2).

Richard Holt[5], an authority on flame heating in this country, states that the three basic factors which influence flame bending are:

(1) The thermal expansion of the material with rise in temperature.

(2) The variation of the yield strength of the material with rise in temperature.

(3) The behavior of the modules of elasticity at elevated temperatures.

These are the same factors which influence the stresses induced by welding. Thus, if a satisfactory model for line heating with an acetylene torch can be found to determine the temperature changes in the material, the methods developed for analyzing the welding situation should work for flame heating. A discussion of the model used for the heat source in the welding analysis and selection of a model for the flame heating is contained in Appendix A. Appendix B is a survey of the methods used in analyzing thermal stresses during welding.

B. Previous Investigations

A search for pertinent literature revealed that very little has been published on either experimental or analytical studies of flame heating of steel whether for bending or straightening. Two recent investigations have been carried out at M.I.T. and a third at Battelle Memorial Institute.

Richard Walsh[6] performed a series of investigations to study deformation changes resulting from flame straightening techniques on welded plates and structures made of mild steel and HY-80 steel. The models constructed represented structures found in shipbuilding. Spot heating and water quenching were employed in removing distortion from the welded models.

The conclusions reached in this investigation were:

(1) Flame straightening procedures are two to three times more effective on mild steel than HY-80 steel.

(2) Varying the position of flame straightening techniques from plate mid-span to fillet weld area produces no significant differences in reducing distortion.

Essentially, Walsh found that flame heating does reduce distortion and determined some relative values of distortion reduction for the model types used. There is no indication that the heating technique used could be applied to a full scale structure with the same results. Walsh further indicates that there may be a band of material strength where flame straightening is most effective.

David Duffy[7] continued the work started by Walsh. He chose as materials: mild steel, U.S. Steel Corten, and U.S. Steel T-1. He constructed a model for each of the three types of metal (Figure (3)). Distortion was induced in the panels during the welding of the models. These panels were then flame heated using the line heating technique. Three separate line heats were performed on each panel with distortion measurements taken after each heating.

Duffy concluded that:

(1) When using flame straightening techniques on panel structures, it is necessary to use a water quench to achieve removal of distortion.

(2) There is no definite corridor of steel with yield strengths where the use of flame straightening is more effective than in others.

Battelle Memorial Institute[8] conducted experiments to determine the effects of flame heating and mechanical straightening on base metal properties. Figure (4) from the Battelle report shows that above approximately

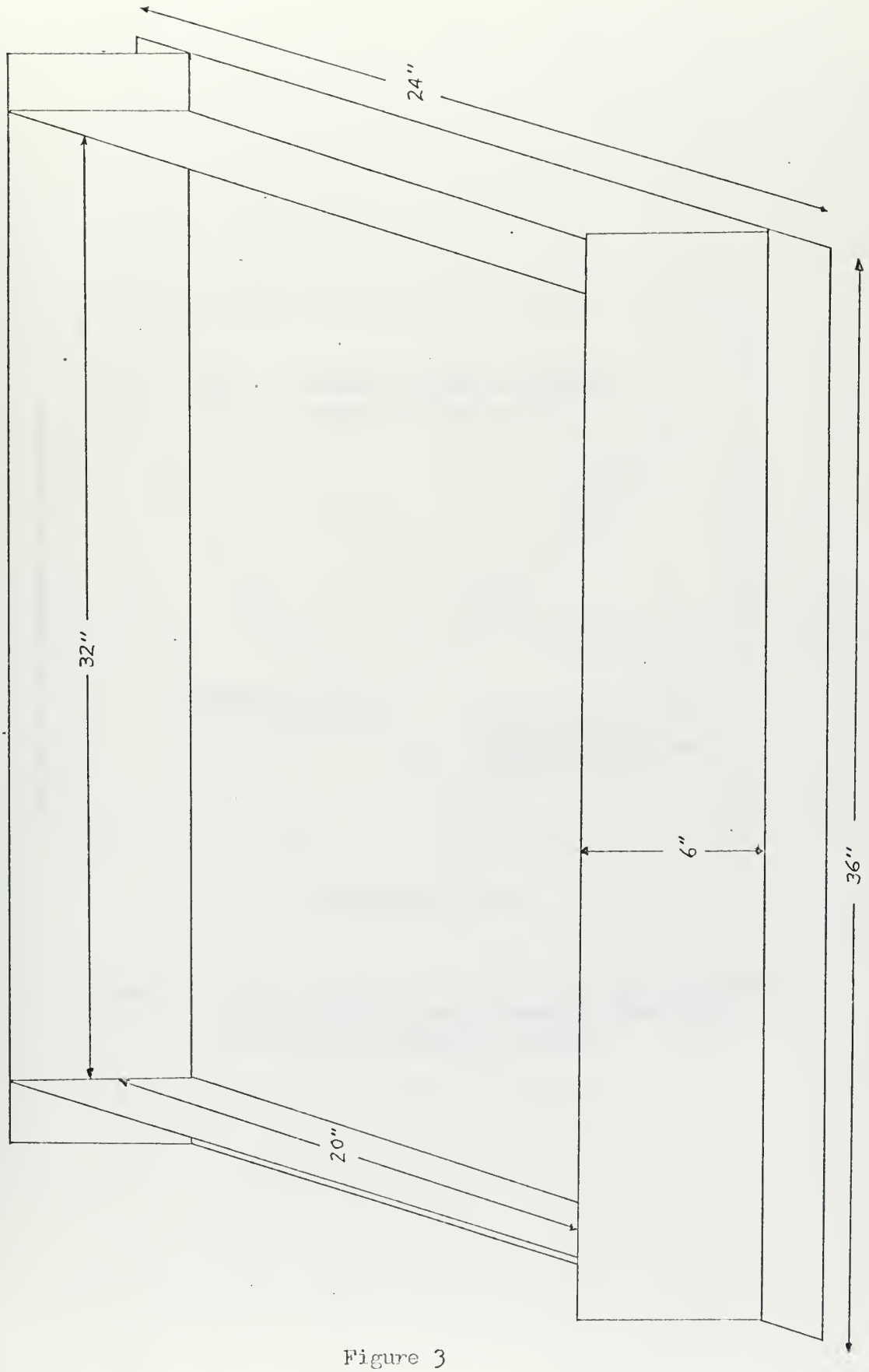

Figure 3

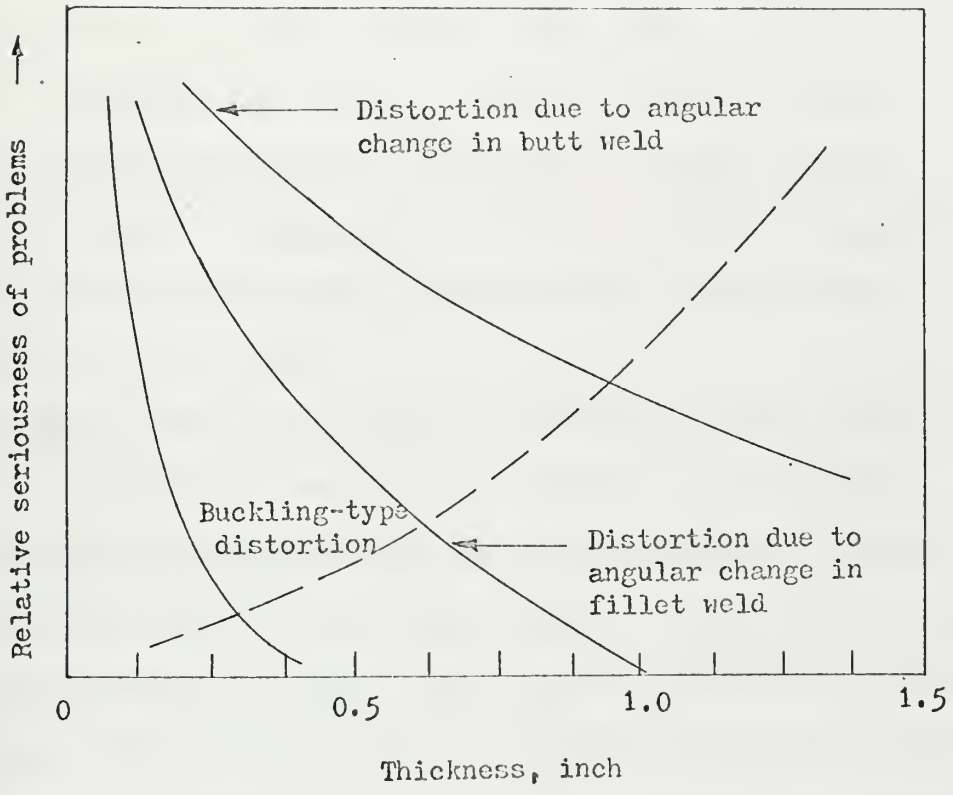

Figure 4: Illustration of the effects of plate thickness on the relative seriousness of distortion problems and material problems

3/8 inch plate thickness, buckling type distortion does not occur. This figure also demonstrates that as plate thickness decreases the distortion problem increases. The major effects observed in the flame straightening were:

(1) Distortion in welded and unwelded plates was generally removed with equal facility.

(2) 3/8 inch thick A517, Grade A plate was more difficult to straighten than 1/2 and 3/4 inch thick A517 plate.

(3) In general A517, Grade A plate was easiest to flame straighten and AB5-B plate (mild steel) was the most difficult.

(4) Attempts to straighten by spot heating were unsuccessful. The major cause was attributed to the fact that the plates were restrained on only one edge.

Conclusion number 3 is exactly the opposite of that observed by Walsh. Duffy did not find flame heating more effective on any material.

The above investigations show that flame heating does remove distortion and gives some measure of what results might be expected if the procedures in the investigations are used. There was no optimization of the heating procedure to most effectively remove distortion and from the results of these investigations no generalization of the best method of heating can be made. In fact, Duffy points out that not only is optimization of heating procedures much needed but an analytical investigation of flame heating is mandatory for this optimization to limit the cost of experimental data.

C. Purpose of Study

The purpose of this study was:

(1) To experimentally observe the effects of line flame heating on steel plate. This will be done by continuously measuring temperatures

and strains induced in the steel plates when flame heating is applied. A better understanding of the flame heating process and how to use this process for bending or straightening are expected results. Also, the question of how material strength affects the effectiveness of this process may be resolved.

(2) Compare the experimental data to the M.I.T. developed one dimensional analysis for welding, modified for flame heating. This will determine if programs developed for welding can be used to analyze flame heating.

(3) If the two dimensional analysis of welding presently being developed at M.I.T. is available, the data will also be compared with this program. If this program is not at the stage where it can be used, a search for any other existing programs that may be used for analysis of the flame heating will be made and the programs utilized if available.

D. Selection of Parameters

Material selection was made with the work performed by both Walsh and Duffy in mind. In order that a continuity be maintained in these studies and because of the availability of materials, the three metals used by Duffy; low carbon steel AISI 1020 (mild steel), low alloy high strength steel ASTM A-242 (U.S. Corten), and quenched and tempered steel ASTM A-514 (U.S. Steel T-1), were also used in this investigation.

The choice of system model was dictated by the decision to compare the experimental and analytical results. The analysis of welding is developed for infinite unconstrained flat plates. Accordingly, the unconstrained flat plate is used for this investigation. It is recognized that this model is not found in production except in the case where flame heating might be

used as a bending technique. However, it is expected that the welding program will evolve to the analysis of more complicated structures and if it can be shown that the simple analysis presently available is applicable for flame heating, the analysis of flame heating can be carried forward with the welding analysis.

The choice of plate thickness was made with Figure (4) and existing production problems in mind. In production much of the distortion that must be removed occurs in internal bulkheads. The thickness of plating used for these bulkheads ranges from 1/4 inch to 1/2 inch and up. The Battelle report indicated that for material thickness of 1/2 inch and greater the distortion problem was not great and, also, that in the thickness range of 1/4 inch or less buckling type distortion occurs. Thus, a thickness of 3/8 inch was chosen because in actual use this will give major distortion problems and yet will not enter the buckling domain.

Material compositions and physical properties are given in Appendix C.

The method of heating used in this study was line heating which is similar to a bead-on-plate weld. The torch tip and speed of heating were chosen to give a 1500°F maximum temperature, and a width of heating zone approximately the same as that seen in previous use of this heating technique.

The results from the welding analysis and the experimental results, so far obtained, show that the longitudinal strain (in the direction of the weld bead) is much higher than the transverse strain (perpendicular to the weld bead) and that the shear strain is very small. Because of this, and also due to the cost of installing gages, transverse and longitudinal strains are the only ones measured in this investigation.

In order that the accuracy of temperatures predicted by assuming a

source of constant strength with thickness can be determined and to observe the bending strains induced by the flame heating, measurements of temperature and strain on both the upper and lower surface of the plate are made.

E. Measuring Strain and Temperature

To analyze what is taking place during the flame heating process it is necessary to measure the temperature and stress that is induced by the heating. Stress cannot be measured directly, therefore, some type of strain measurement is necessary. Since the flame heating technique used is a continuous line heating with the flame moving at a constant speed across the material, continuous readings of strain and temperature are desired.

The measurement of temperature at points on the plate is easily accomplished. A thermocouple can be placed at the point of interest and the temperature determined directly from this gage. In this investigation, BLH type GTM-CA (Chromel/Alumel) thermocouples were an integral part of the strain gages used.

The measurement of strain is more difficult. Due to the temperatures that will be incurred during heating, it is necessary to select a high temperature strain gage so that the probability of gage failure will be minimized. The gages available for temperatures above 500°F are BLH type 1212-5B and 1212-5A. The A designates that the strain gage has a thermo-sensing element included.

An uncompensated potentiometric circuit was used in measuring strain. Since temperature compensation was not possible, the strains measured may have varied non-linearly as the gage temperature moved far from the temperature at which the gage factor for this particular gage was determined. This non-linear deviation can affect the accuracy of the

strain measurement.

The strain measured consists of several components. These component strains are normally superimposed to give a total measured strain[9].

$$e = e_m + e_p + \alpha\Delta T + \Delta R\Delta T$$

This equation shows that the total strain is composed of mechanical (elastic) strain, plastic strain, thermal expansion, and component due to the change in resistance of the strain gage with change in temperature. The last two terms can be combined and referred to as apparent strain. A plot of apparent strain versus temperature for the type 1212-5A strain gage mounted on mild steel is shown in Figure (5). This figure clearly shows the very large apparent strain that occurs with this type of gage. Under these conditions it is doubtful that the superposition of the different components of strain is exactly correct. However, lacking any better method of handling this problem the superposition will be used but some error will probably be induced.

This large value of apparent strain also introduces another problem in measuring the strain. The visicorder used will allow approximately five inches for the measurement of strain from zero to the maximum value. At the maximum safe temperature of 700°F for which the 1212-5A gage can be used, an apparent strain of approximately 27,000 micro-inch per inch will be encountered. In calibrating the recording equipment, 15,000 micro-inch per inch was set equal to five inches of displacement. The scale could be halved to 30,000 micro-inch per five inches if larger values were encountered. With this large a scale, any error when reading displacement of the recording from the zero value can induce considerable error in the value of the strain determined.

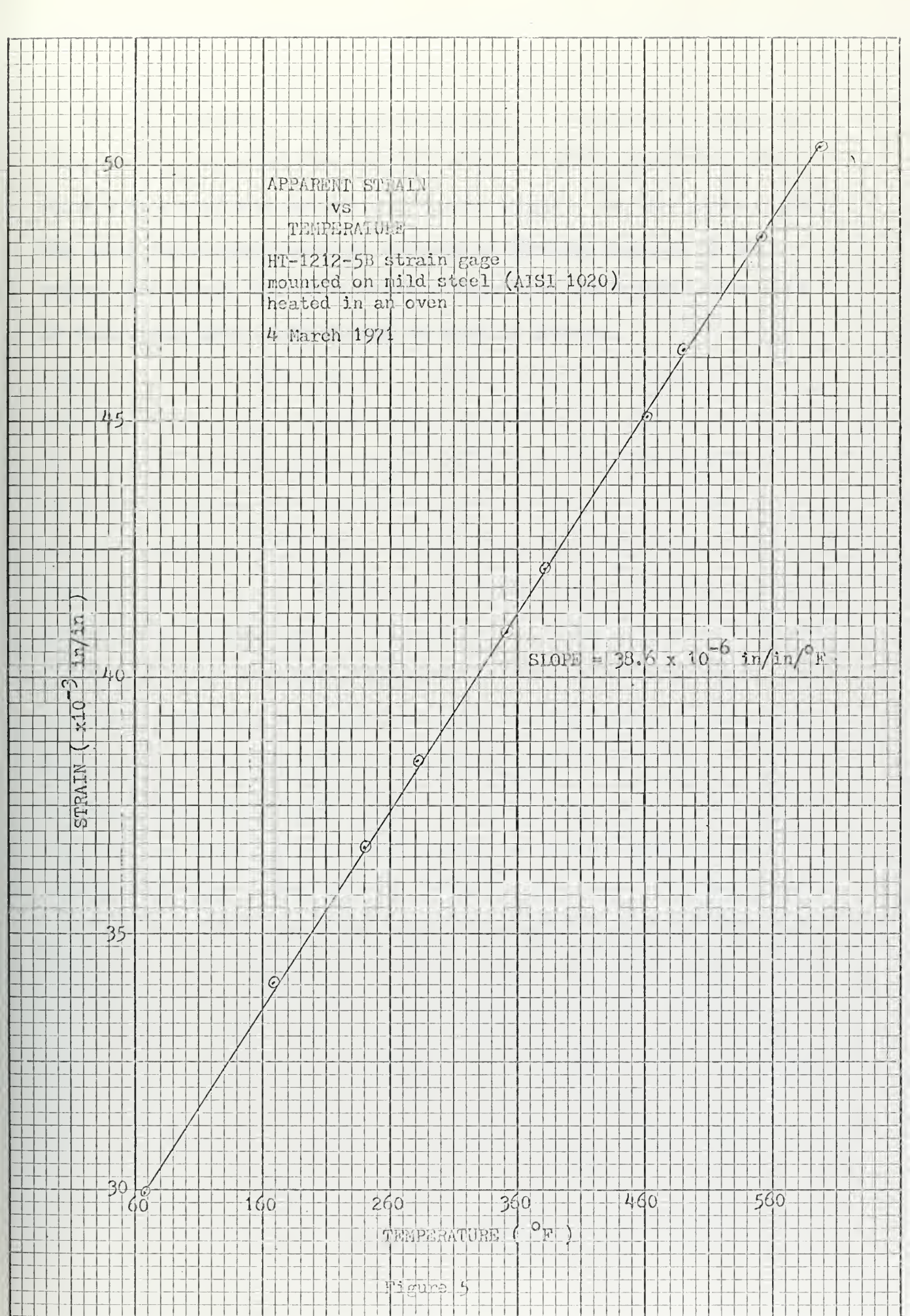
APPARENT STRAIN
vs
TEMPERATURE
HT-1212-5B strain gage
mounted on mild steel (AISI 1020)
heated in an oven
4 March 1971
SLOPE = 38.6 x 10^-6 in/in/°F
STRAIN (x10^-3 in/in)
50
45
40
35
30
60
160
260
360
460
560
TEMPERATURE (°F)

Figure 5

In the reduction of the experimental data, the recorded reading was corrected by subtracting the apparent strain to give experimental strain which consists of both plastic and elastic strains. For the above reasons, the values determined cannot be utilized as absolute measures of the strain encountered, but their relative magnitudes and trends can be used in determining what occurs during the heating process.

II. PROCEDURES

A. Scope of the Research

A series of investigations were made of the strain and temperature changes that occur in mild steel, Corten, and T-1 steel plates as a result of line flame heating on the surface of the plates. Flat unconstrained plates were used as models so that the results could be compared with predicted values. The heating value used in the flame heating was selected to agree with the data available for use in predicting the thermal strains as stated in Appendix A. The speed of heating was selected to give a maximum temperature of 1500°F in the steel plates. Three heats were performed on each plate. The first heat was used for comparison with the predicted values of strain and temperature. The other two heats were used to observe the effect of water quenching and as a check on the first run. The second heat can also be used to see if superposition of strains from heats occurring at different locations is possible.

B. Description of Specimens

For this study 3/8 inch thick plates, one each of AISI 1020 (mild steel), U.S. Steel Corten, and U.S. Steel T-1 were used. The plate size of 36 inch by 27 inch was chosen for all specimens. The 36 inch length was chosen to give a distance sufficient for the heating to reach a quasi-stationary state before readings of temperature and strain were taken. The 27 inch width was chosen to allow three passes of flame heating to be made and minimize the effects from one pass to the next.

The plates were instrumented by BLH Electronics, Incorporated; 42 Fourth Avenue; Waltham, Massachusetts as indicated in Figure (2-1). The pass lines indicated on the figure are representative of the three

Figure 2-1: Diagram of instrumentation

line heats performed on the mild steel plate. Gages were placed on the tops and bottoms of the plates, the bottom gages being mirror images of the top gages. The longitudinal gages (X direction) are BLH type 1212-5A strain gages with BLH type GTM-CA (Chromel/Alumel) thermocouples included. The transverse gages (Y direction) are BLH type 1212-5B strain gages. These gages were attached to the plates by the BLH Rokide Process. This process uses a ceramic cement which is applied by flame spraying. The maximum operating temperature for this type cement is 1500°F. Since this process has a poor humidity resistance, a moisture proofing was applied after the strain gages were installed.

C. Heating Procedures

A torch was mounted on the automatic welding machine in M.I.T. Materials Joining Laboratory as shown in Figure (2-2). The automatic welding machine was used to give a constant speed during heating. The rig used for mounting the torch also allowed precise adjustment of the vertical position of the torch so that the distance between the torch tip and surface of the plate could be maintained at the proper value for most effective heating. This height adjustment was essential for the second and third passes on a plate since distortion induced during the first pass was present in the latter passes. The height adjustment was manually performed and the height maintained such that the inner core of the flame was as close to the plate surface as possible without impinging on the surface. An oxygen-acetylene torch was utilized. The nameplate data on the torch and tip is: Oxweld Torch, Type W-17, Tip Size #10.

The steel plate was rested on fire bricks to minimize the heat conduction away from the plate due to this contact. The fire bricks supported the entire bottom surface except in the area of the bottom

Figure 2-2: Torch mounted on automatic welding machine

strain gages as shown in Figure (2-2) in order to minimize any bending effects due to the plate not being uniformly supported.

Heating started at the leading edge of the plate and proceeded at a constant speed down the length of the plate. Plastic refractory was placed around the strain gages on the heated surface to protect the gages from the flame wash of the torch. This technique proved very successful as no gages were lost due to the heating.

Oxygen and acetylene pressures were adjusted at the tanks by two stage regulators. The amount of acetylene consumed was measured by a flow meter in the acetylene line just downstream from the acetylene regulator. Oxygen and acetylene pressures were adjusted to give the desired acetylene flow rate and the proper flame length.

D. Experimental Procedures

During the flame heating the temperature and strains observed at the different gage positions were recorded. The recorded data was presented as tape outputs from the Honeywell Visicorder. The circuitry used for the thermocouple circuits and the strain gage circuits along with the calibration data are shown in Figures (2-3), (2-4), and (2-5).

The Honeywell Visicorder is limited to twelve channels so that input from eight strain gages and four thermocouples was all that could be recorded for each pass. Therefore, data from two top gage positions and two bottom gage positions was recorded for each pass.

Each plate had all gages calibrated before any heating passes were performed on the plate. The calibration data was included as output on the tape for each plate tested so that the output data could be read as accurately as possible.

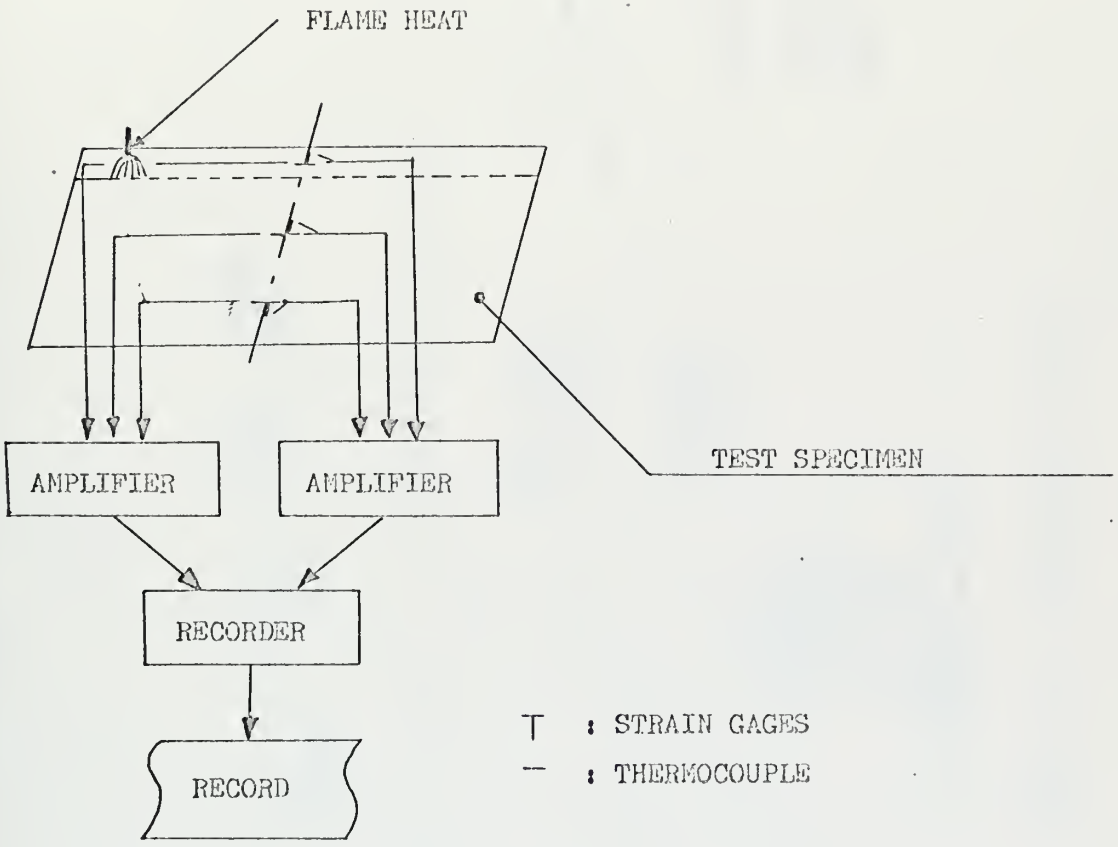

Figure 2-3: Outline of Experimental Set-Up

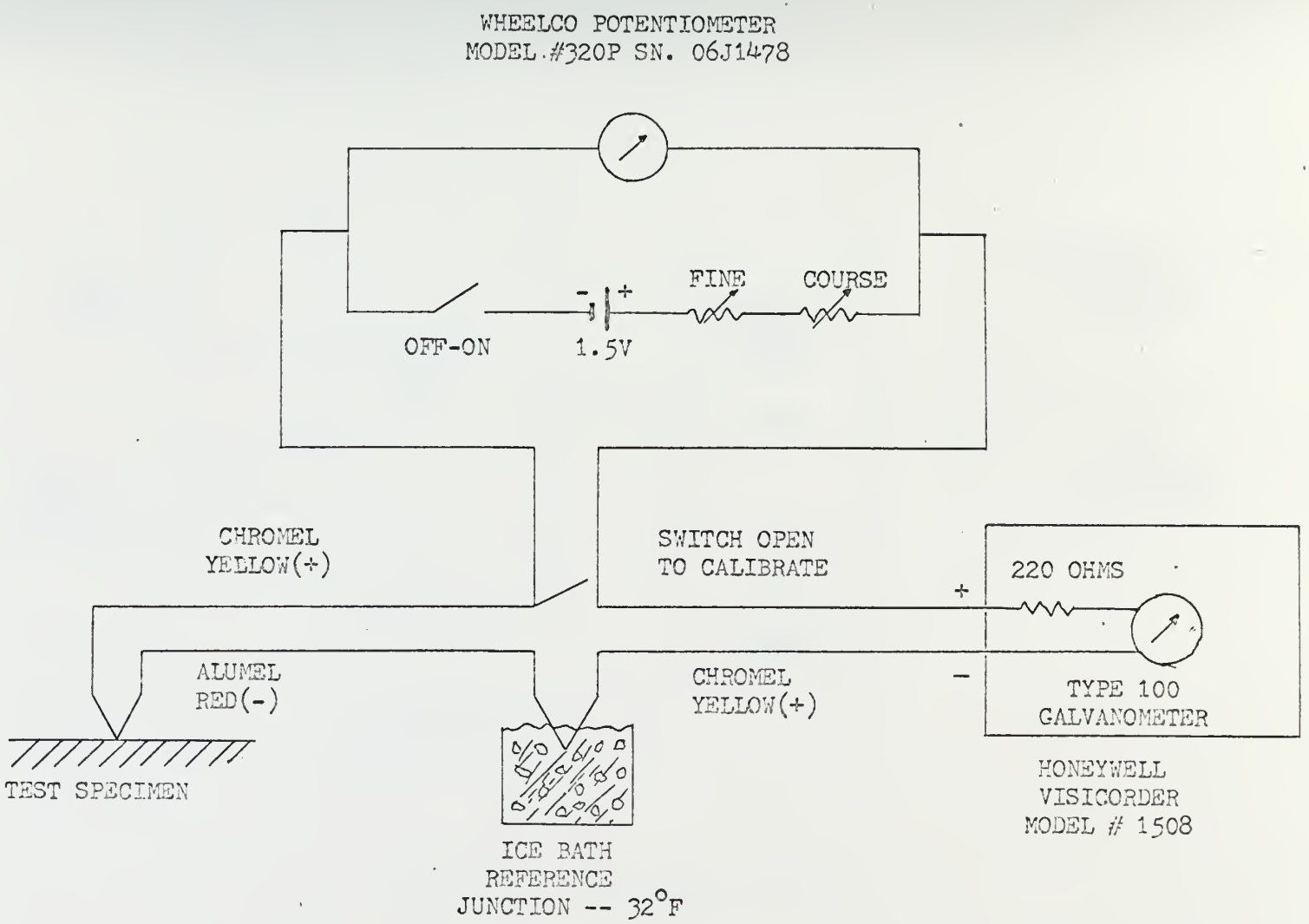

Figure 2-4: Thermocouple Circuit

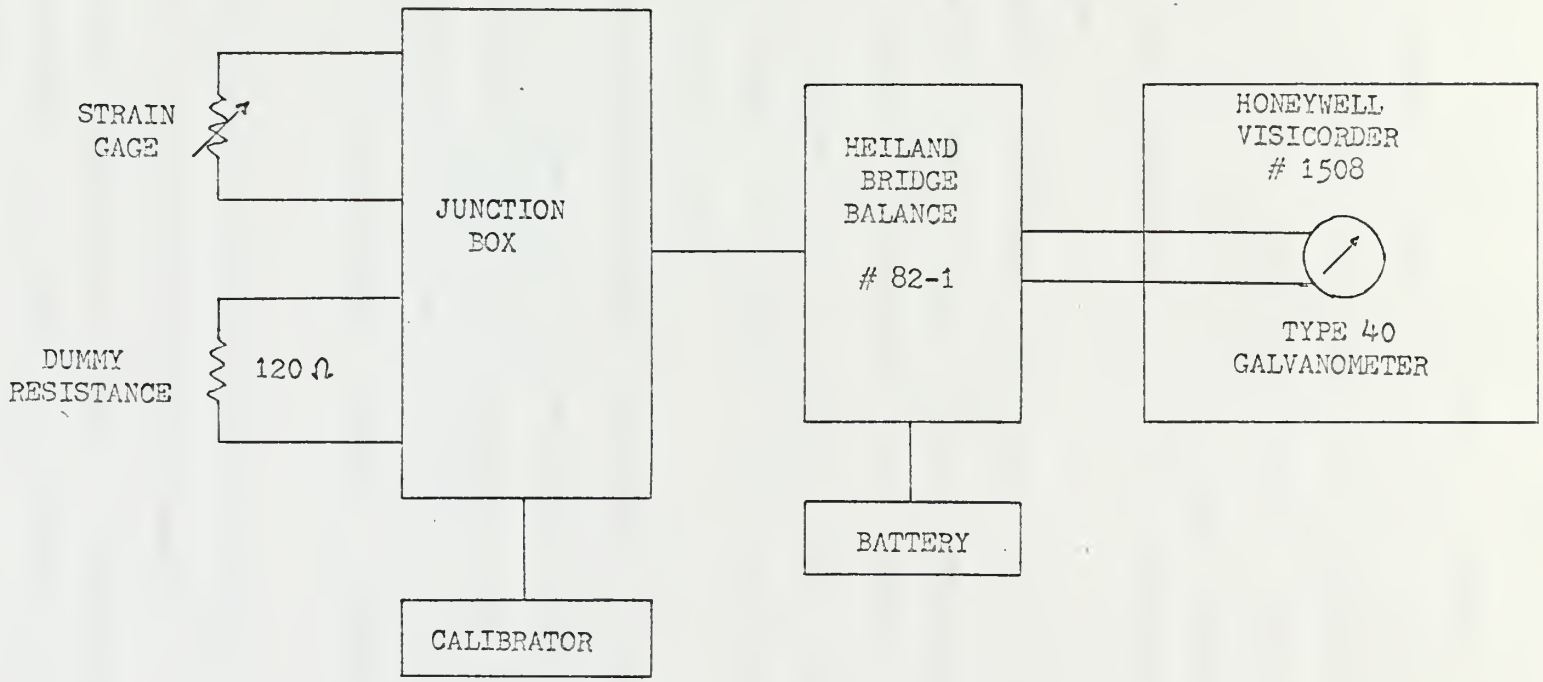

Figure 2-5: Strain Gage Circuit

Temperature and strain measurements commenced for each pass when the flame reached a longitudinal position $6\frac{1}{2}$ inches from the transverse gage positions (Figure (2-6-b)). This allowed the heating to be in a quasi-stationary state before readings were commenced. Temperatures different from initial temperature of the plate were not recorded at the gages until the flame has passed this longitudinal position. Once the readings of temperature and strain were initiated they were continued until the temperatures fell to approximately $100^{\circ}F$ and the strains had stabilized to final values.

The location of the flame on the plate surface is specified by its transverse position from the gage locations on the heated surface at which experimental readings will be recorded. The transverse measurement is taken as shown in Figure (2-6-b). Temperature and strain measurements are also made at the gages on the opposite side of the plate from those specified in the transverse position.

Oxygen and acetylene pressures and acetylene consumption are recorded for each pass. The flame length (l), as shown in Figure (2-6-a), is recorded for each pass. Where water cooling is used, the water temperature, rate of application and the distance the water is applied behind the flame (d) (Figure (2-6-a)) are recorded. The water is applied to the surface as a fine spray.

Also recorded are the effective values of heating (q_e) and a time constant (TC) for the observed acetylene consumption. These values are used in predicting the theoretical values of temperature and strain as explained in Appendix A. The values of q_e and TC are determined from Rykalin's data[13].

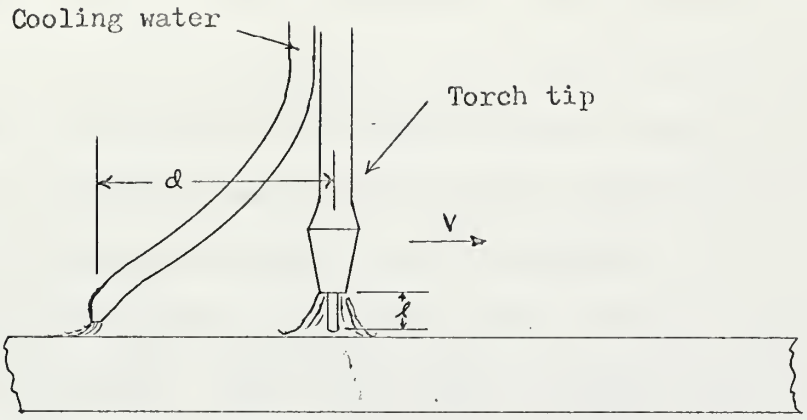

(a) Diagram of torch tip and water cooling attachment

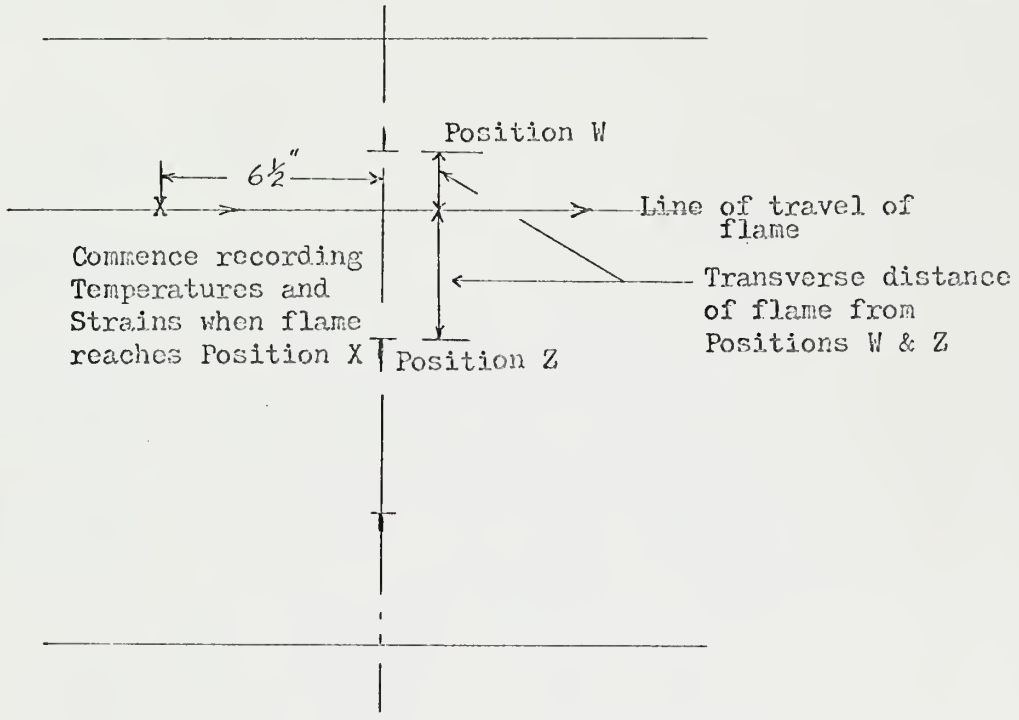

(b) Diagram of dimensions used to specify location of the flame for each pass

Figure 2-6

Tables (2-1), (2-2), and (2-3) list the above values for each of the three passes performed on each specimen. Testing was performed on mild steel first, T-1 second, and Corten last. All three passes were made on each plate before the next was investigated. The location of the flame heating for the first pass was uniform for all three plates. The location and type of pass was varied for the second and third passes. This was done to observe the differences in readings with location and to see if superposition of strains from pass to pass is possible.

Figure (2-7) shows the equipment setup for recording experimental temperatures and strains. Figure (2-8) shows the gage layout and a trace left by one pass of flame heating.

TABLE 2-1

SPECIMEN - MILD STEEL

Pass No.	Transverse Location	Speed of Flame (IPM)	Act. Cons. (ft^3/hr)	Oxy. Press. (PSI)	Act. Press. (PSI)	Flame Length(l) (in)	Water Temp. (^oF)	Rate of Water Appl. (ft^3/hr)	Dist.(d) (in)	q_e (cal/sec)	TC (sec)
1	2" from EX1 5 1/16" from EX2	3	13.7	20	3.25	12/32"	--	----	-	720	10
2	2" from EX2 5 1/16" from EX1	3	13.7	24	3.5	13/32"	--	----	-	720	10
3	2" from EX3 5 3/8" from EX2	3	13.7	24	3.5	13/32"	45	.757	3	720	10

TABLE 2-2

SPECIMEN - U.S. STEEL T-1

Pass No.	Transverse Location	Speed of Flame (IPM)	Act. Cons. (ft^3/hr)	Oxy. Press. (PSI)	Act. Press. (PSI)	Flame Length(l) (in)	Water Temp. (^oF)	Rate of Water Appl. (ft^3/hr)	Dist.(d) (in)	q_e (cal/sec)	TC (sec)
1	2" from EX1 5 3/8" from EX2	3	13.7	24	3.5	13/32"	--	---	-	720	10
2	2" from EX2 5 3/8" from EX1	3	13.7	24	3.5	13/32"	--	---	-	720	10
3	2" from EX3 5 1/4" from EX2	3	13.7	24	3.5	13/32"	46	1.27	3	720	10

TABLE 2-3

SPECIMEN - U.S. STEEL CORTEN

Pass No.	Transverse Location	Speed of Flame (IPM)	Act. Cons. (ft^3/hr)	Oxy. Press. (PSI)	Act. Press. (PSI)	Flame Length(l) (in)	Water Temp. (^oF)	Rate of Water Appl. (ft^3/hr)	Dist.(d) (in)	q_e (cal/sec)	TC (sec)
1	2" from EX1 5 1/4" from EX2	2.8	13.7	24	3.5	13/32"	--	----	----	720	10
2	2" from EX3 5 1/4" from EX2	3.0	13.7	24	3.5	13/32"	45	.775	2.75	720	10
3	2" from EX2 5 1/4" from EX1	3.0	13.7	24*	3.5	13/32"	--	----	----	720	10

*Ran out of oxygen when flame was $5\frac{1}{2}$" past the transverse line through the strain gages.

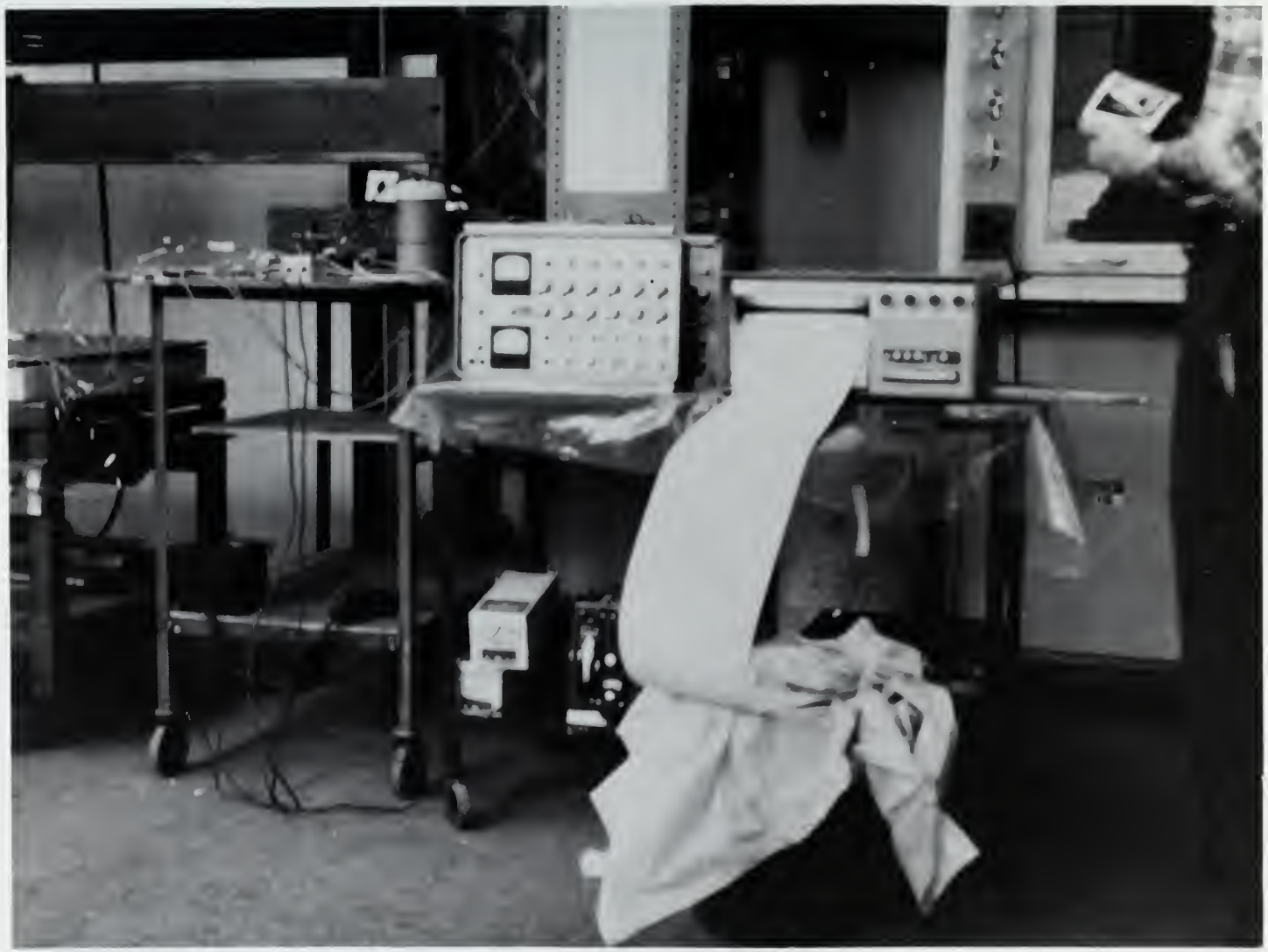

Figure 2-7: Equipment setup for recording experimental results

Figure 2-8: Steel plate after one pass of flame heating

III. RESULTS

The results of experiments on test specimen are in the form of strain plots and a photograph of the distortion induced in one specimen. Appendix D contains tabulated values of the experimental data.

A. Presentation of Data

The plotted results show the strains and temperatures encountered at various positions versus time. Due to the large period of time involved in heating and cooling the steel plate back to room temperature, time is plotted logarithmically. Figures (3-1a) to (3-9b) show the experimental values of temperature and strain measured for the different passes on the specimen. The data is presented for the heated surface first followed by the plot for the opposite side of the plate. This was done because of limits in the computer plotting routine and also for a clearer presentation of the data. All the plots are marked with the symbol T/F indicating the time at which the flame reaches the transverse line connecting the gages.

Figures (3-10) to (3-12) show the temperatures and longitudinal strains predicted by the one dimensional welding program and the experimental temperatures and longitudinal strains observed on the heated surface of the test specimen during the first pass.

Figure (3-13) is a photograph of the mild steel specimen after three passes of flame heating has been performed. This photograph gives an indication of the amount of distortion incurred. The near edge is the edge closest to the third pass which was water cooled.

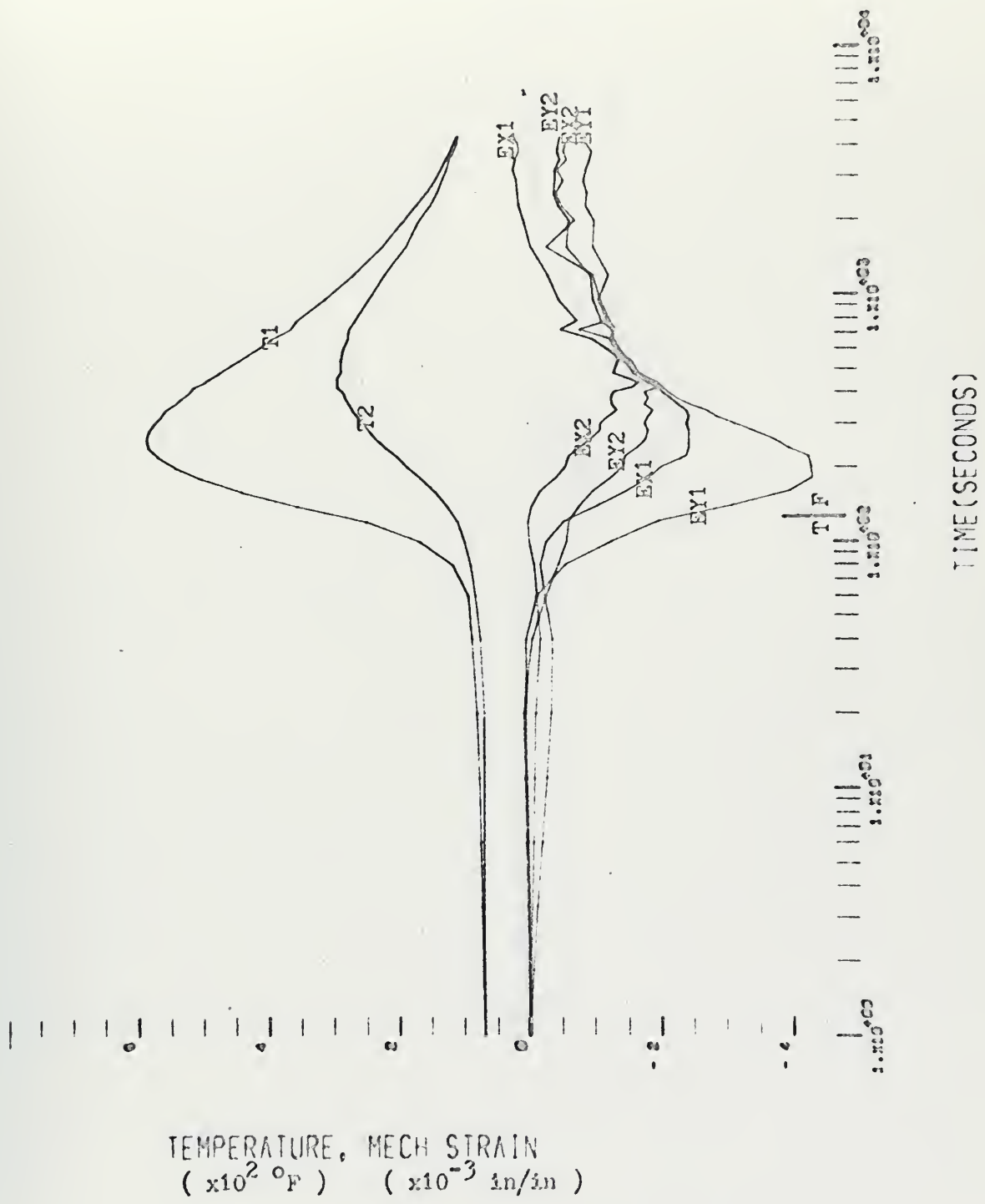

FIGURE 3-1-a: Mild Steel Pass #1, Heated Surface

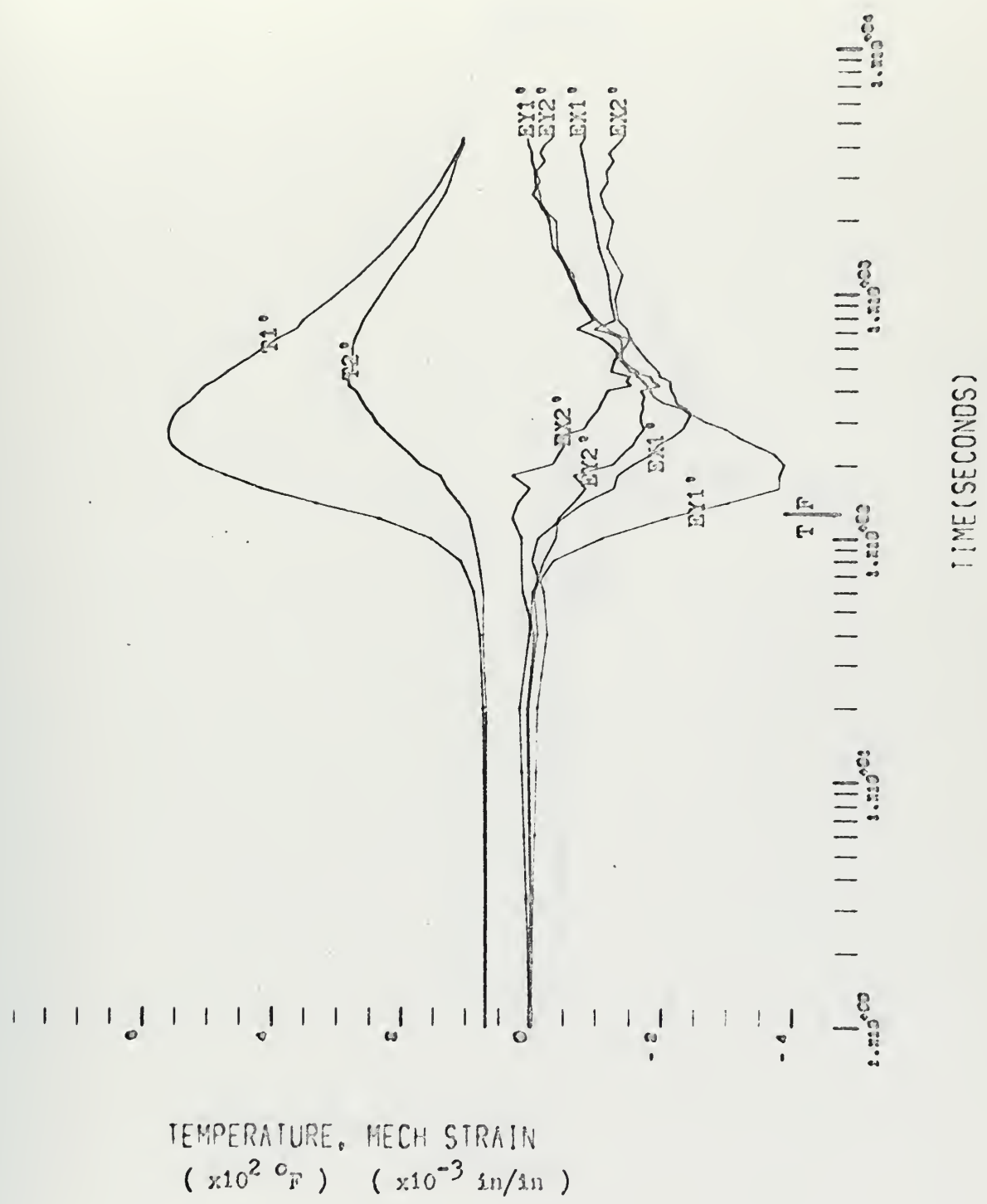

FIGURE 3-1-b: Mild Steel Pass #1, Bottom Surface

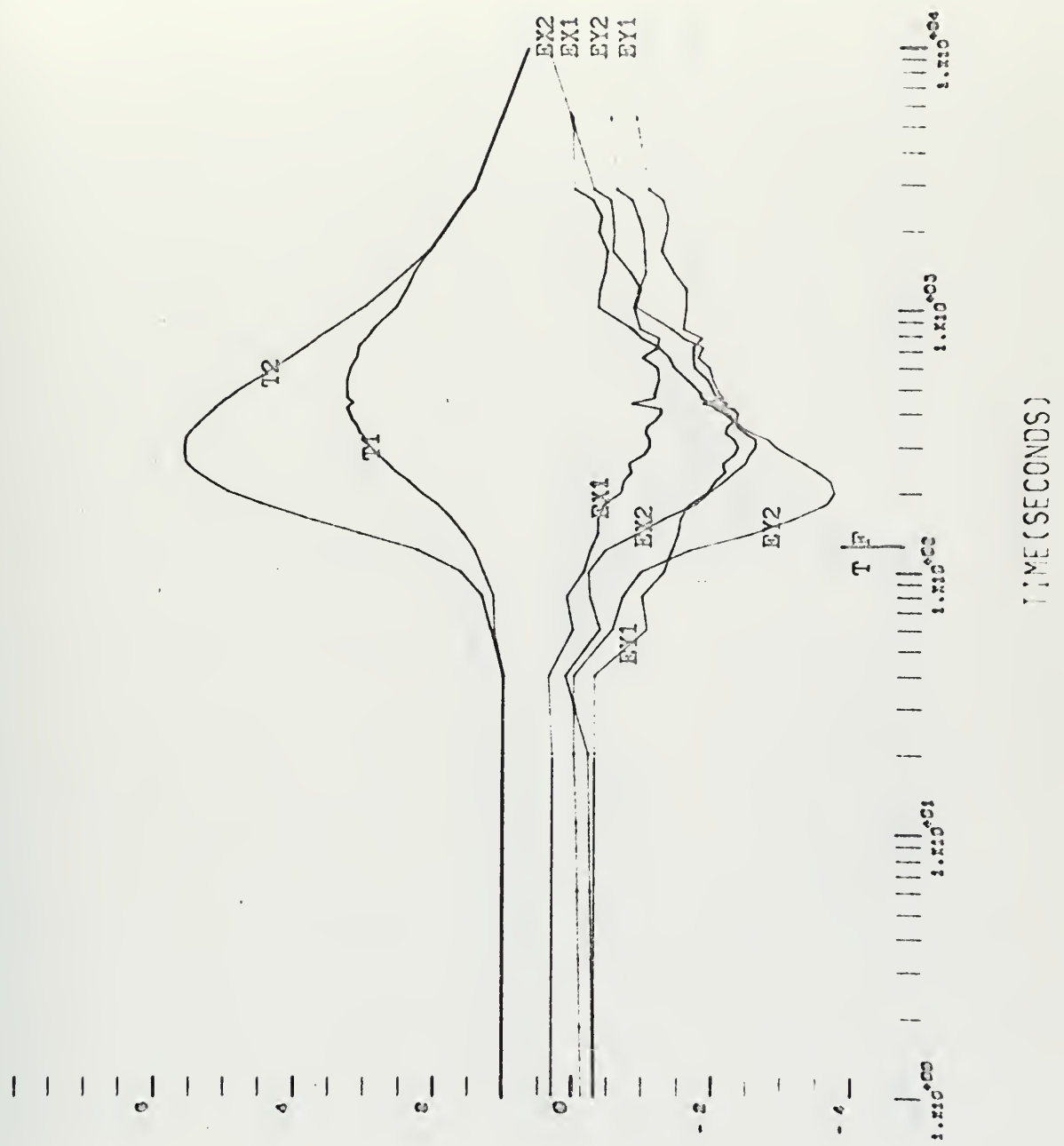

FIGURE 3-2-a: Mild Steel Pass #2, Heated Surface

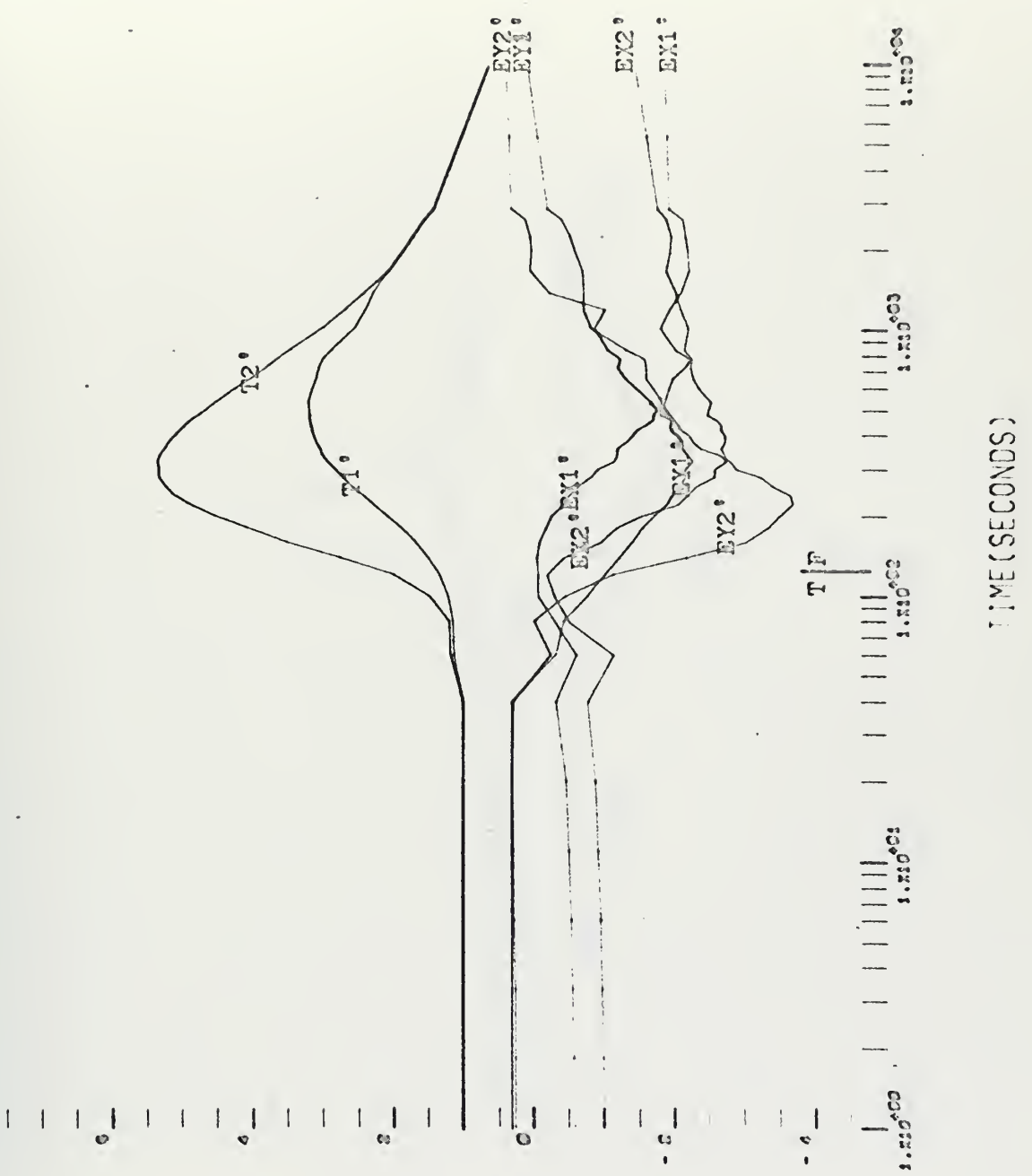

FIGURE 3-2-b: Mild Steel Pass #2, Bottom Surface

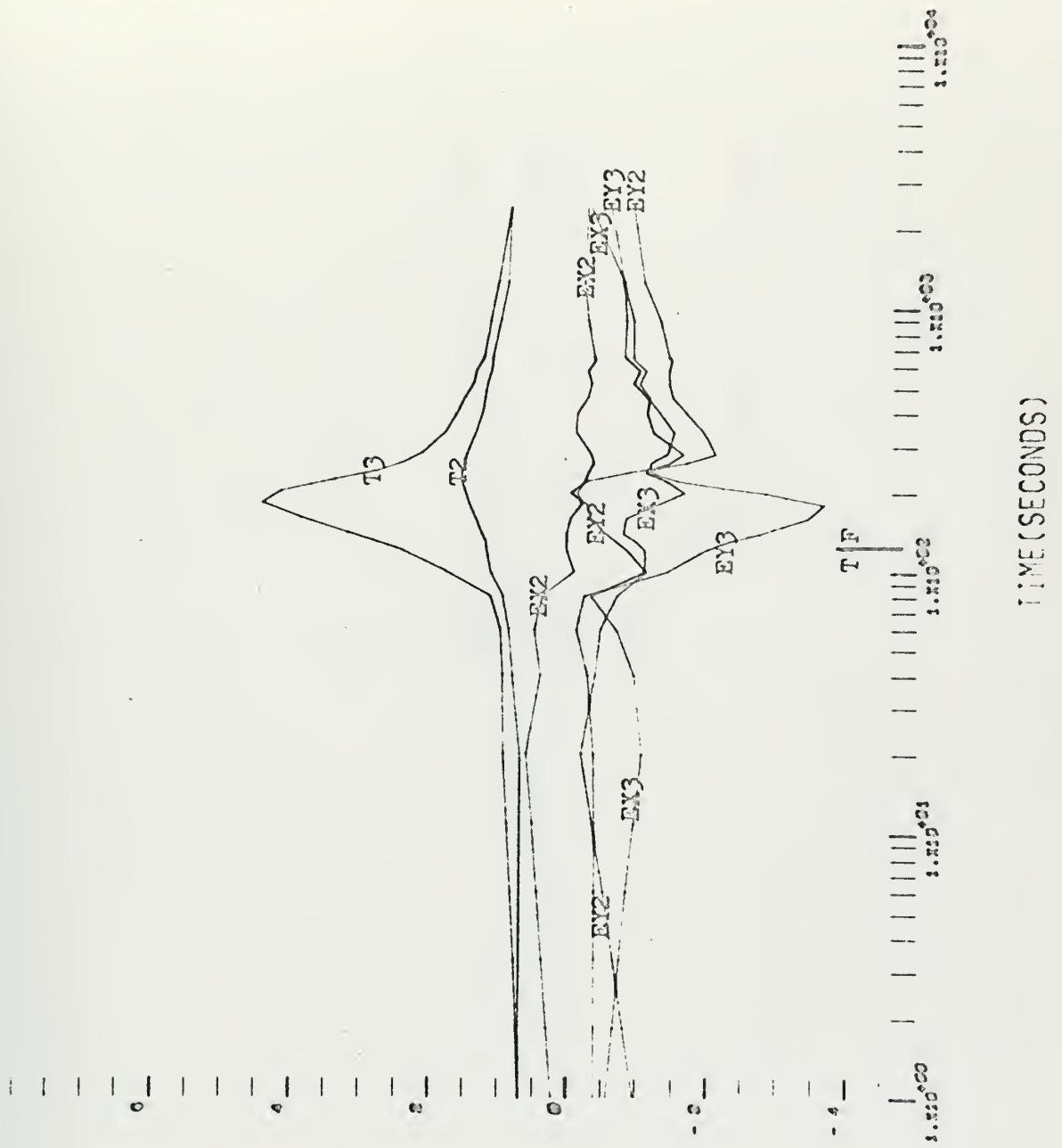

TEMPERATURE, MECH STRAIN

($x10^2$ ^oF) ($x10^{-3}$ in/in)

FIGURE 3-3-a: Mild Steel Pass #3, Heated Surface

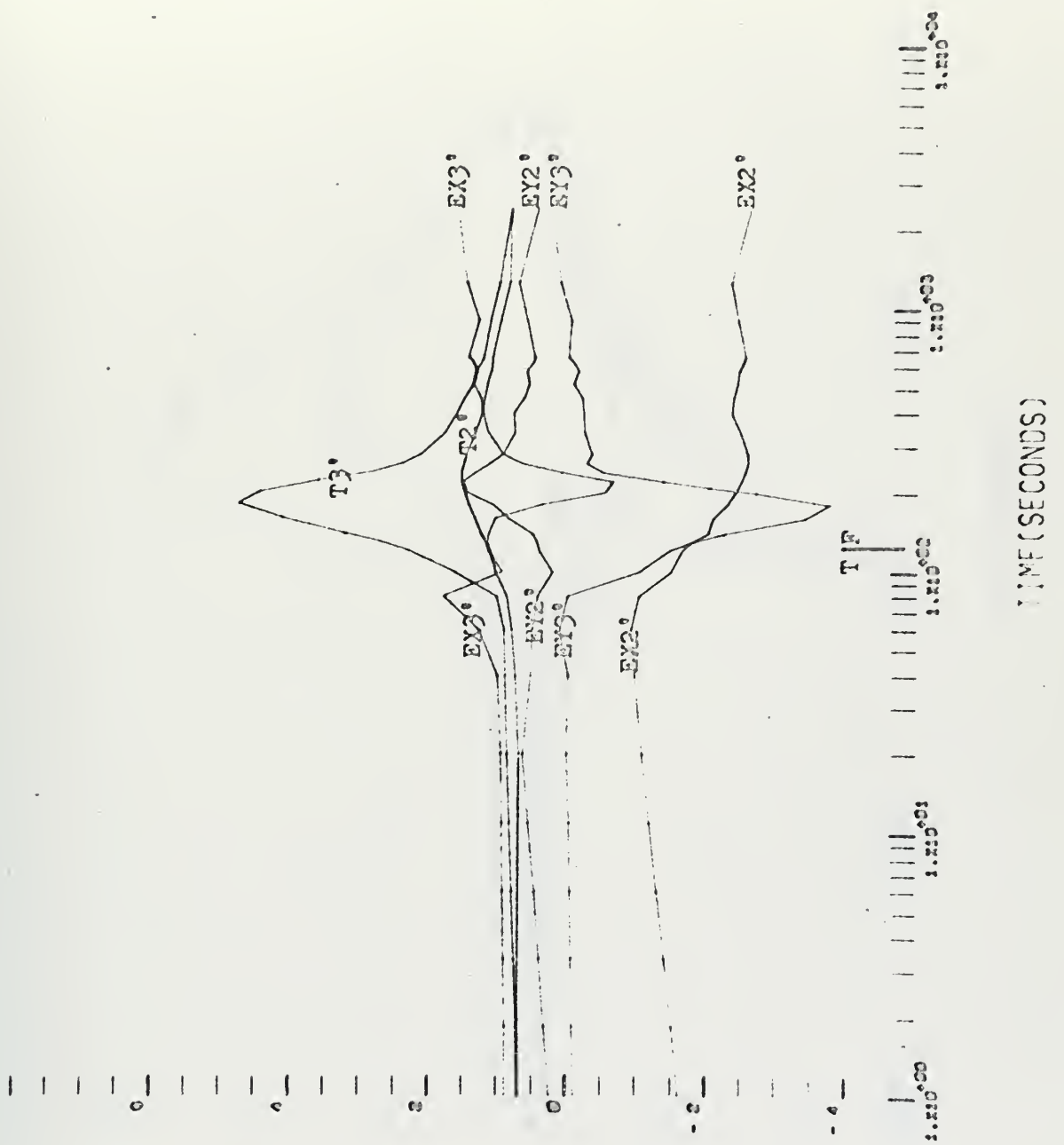

FIGURE 3-3-b: Mild Steel Pass #3, Bottom Surface

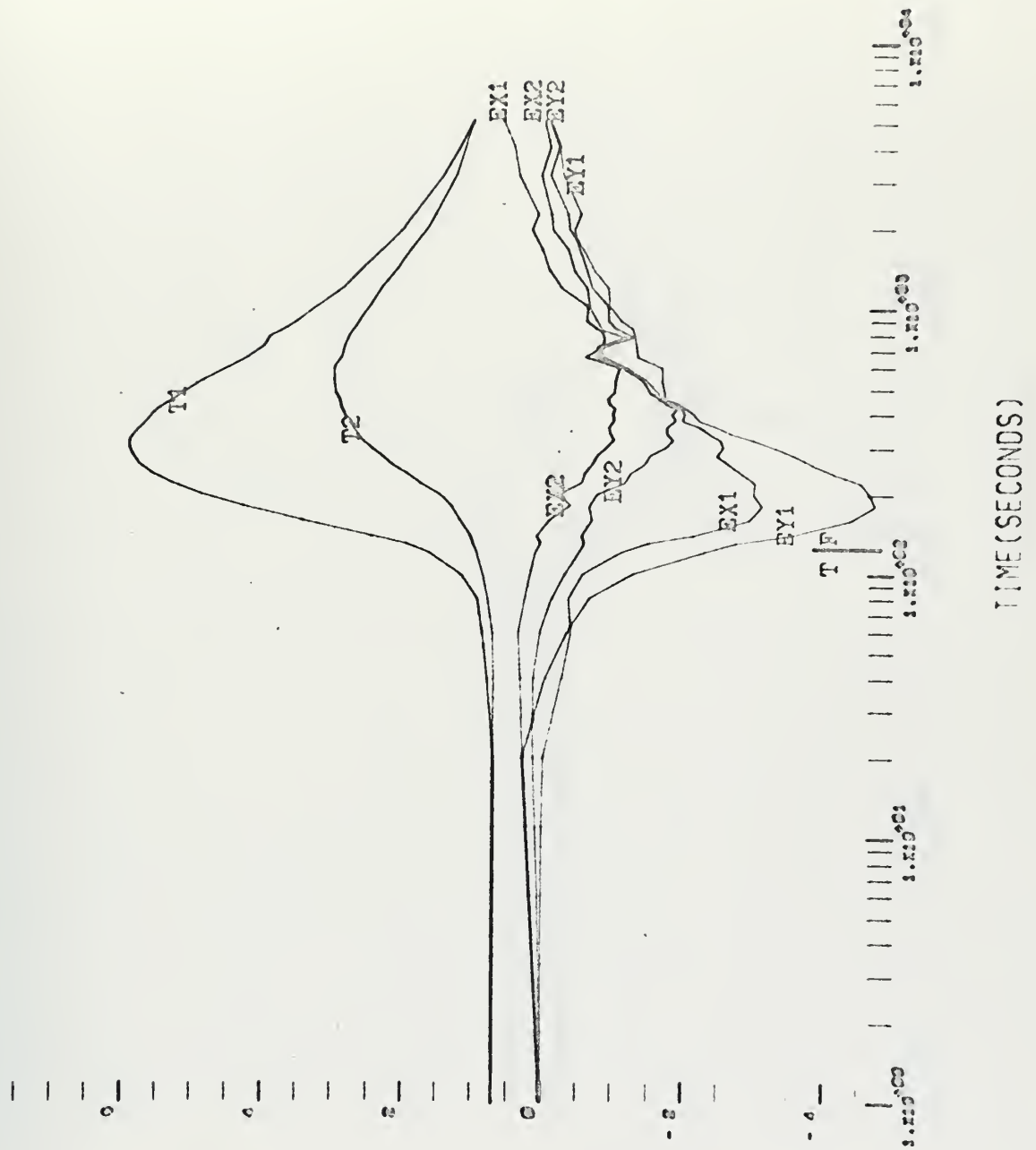

FIGURE 3-4-a: T-1 Pass #1, Heated Surface

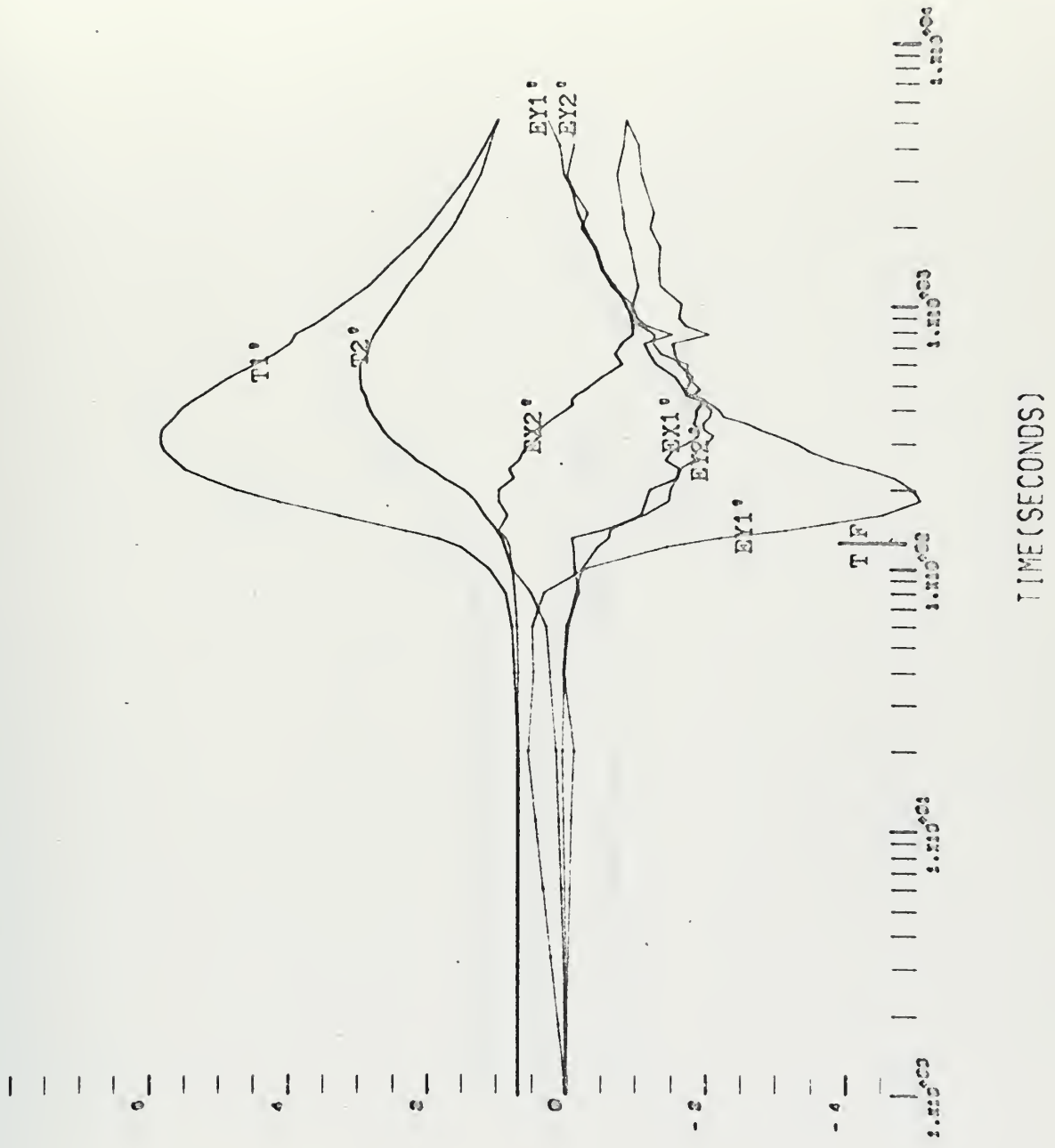

FIGURE 3-4-b: T-1 Pass #1, Bottom Surface

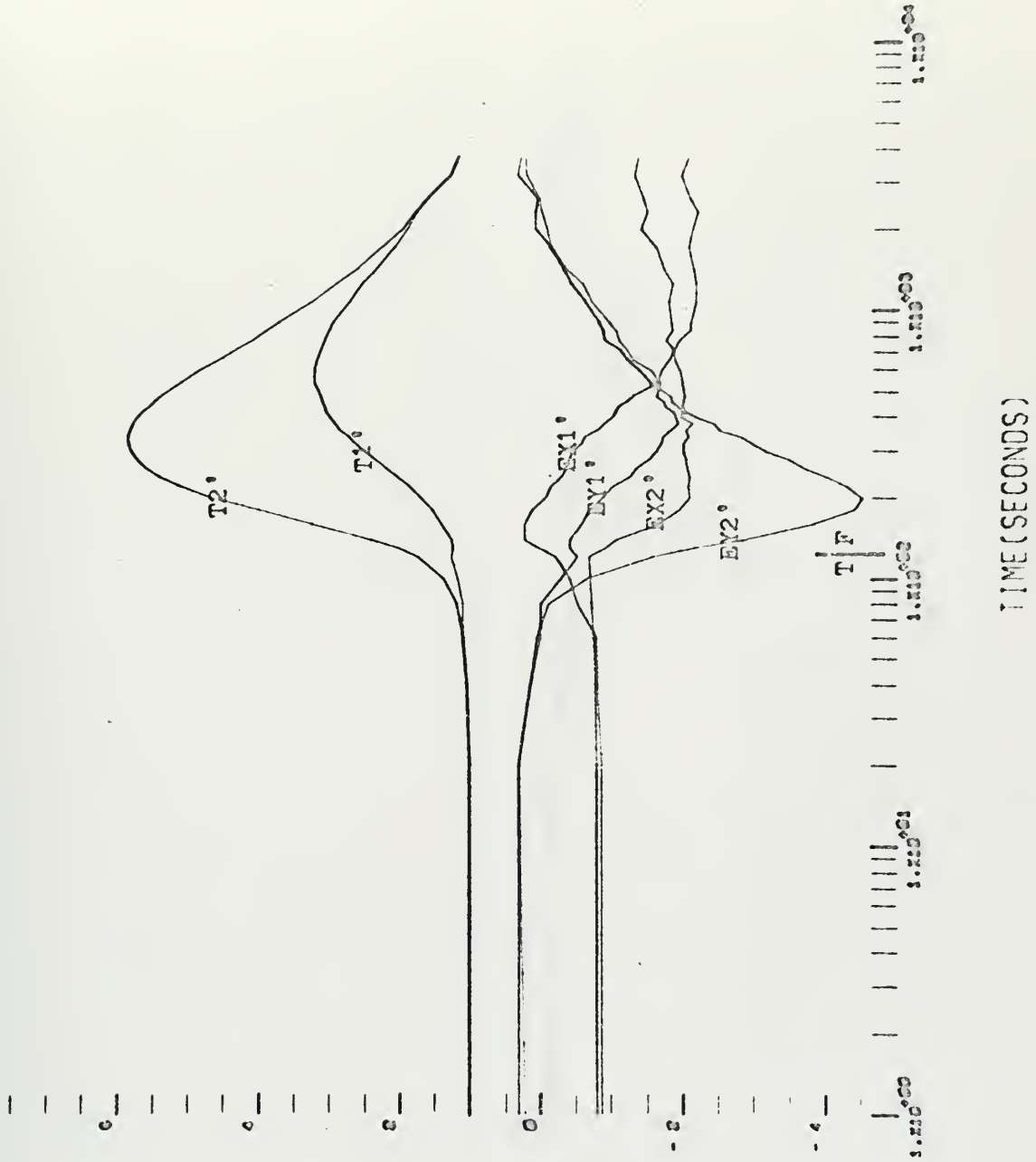

TEMPERATURE, MECH STRAIN

($x10^2$ ^oF) ($x10^{-3}$ in/in)

FIGURE 3-5-a: T-1 Pass #2, Heated Surface

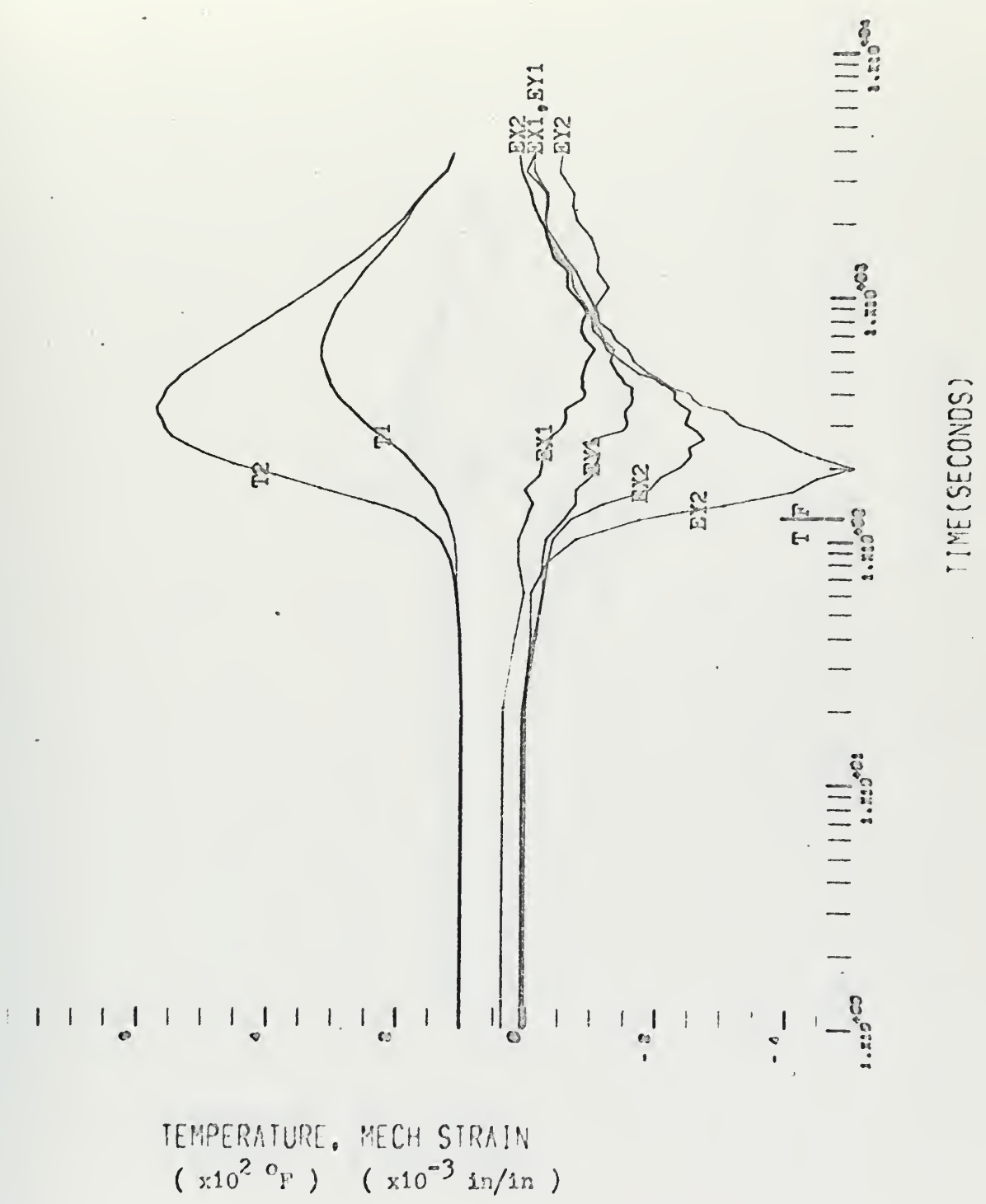

FIGURE 3-5-b: T-1 Pass #2, Bottom Surface

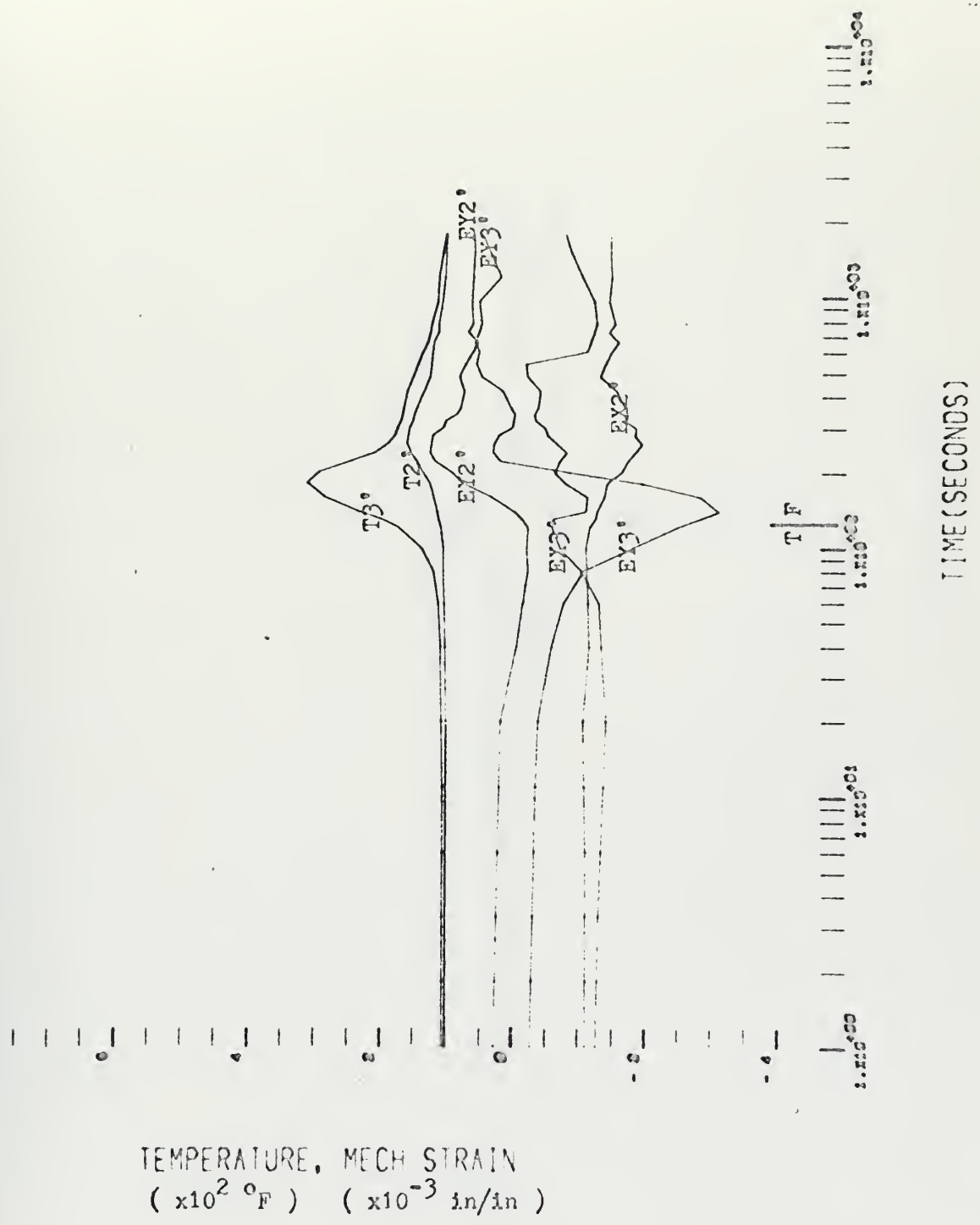

FIGURE 3-6-a: T-1 Pass #3, Heated Surface

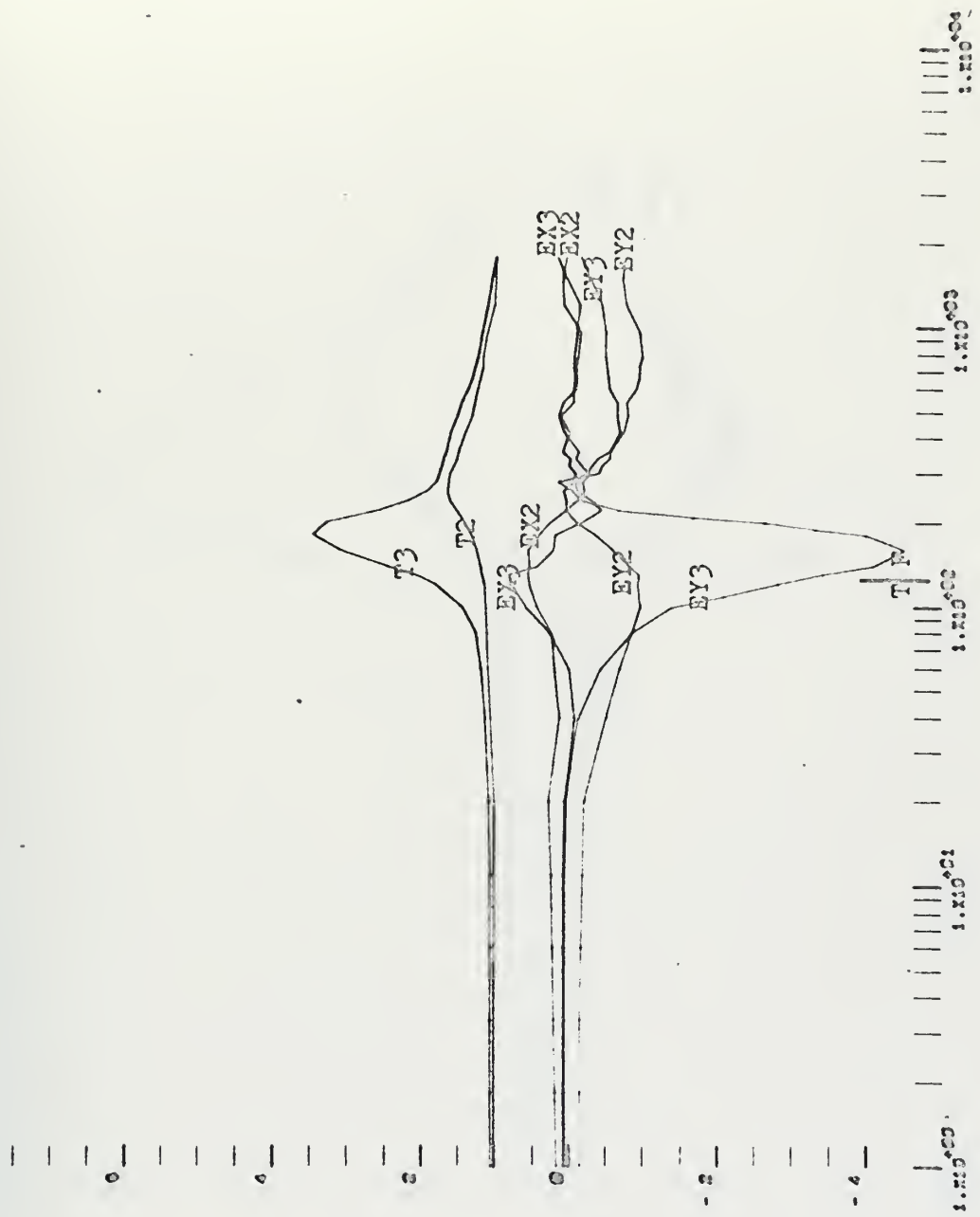

FIGURE 3-6-b: T-1 Pass #3, Bottom Surface

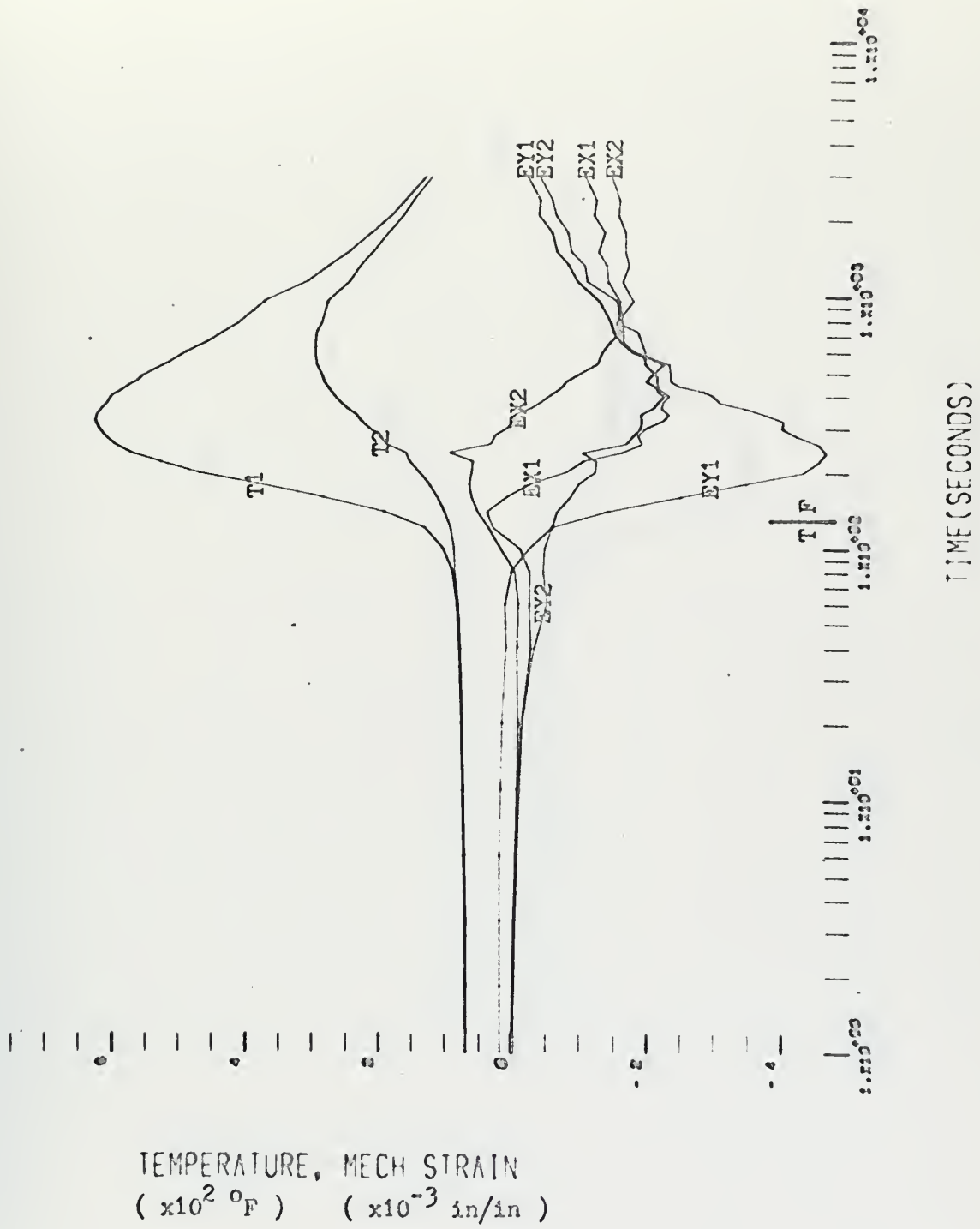

FIGURE 3-7-a: Corten Pass #1, Heated Surface

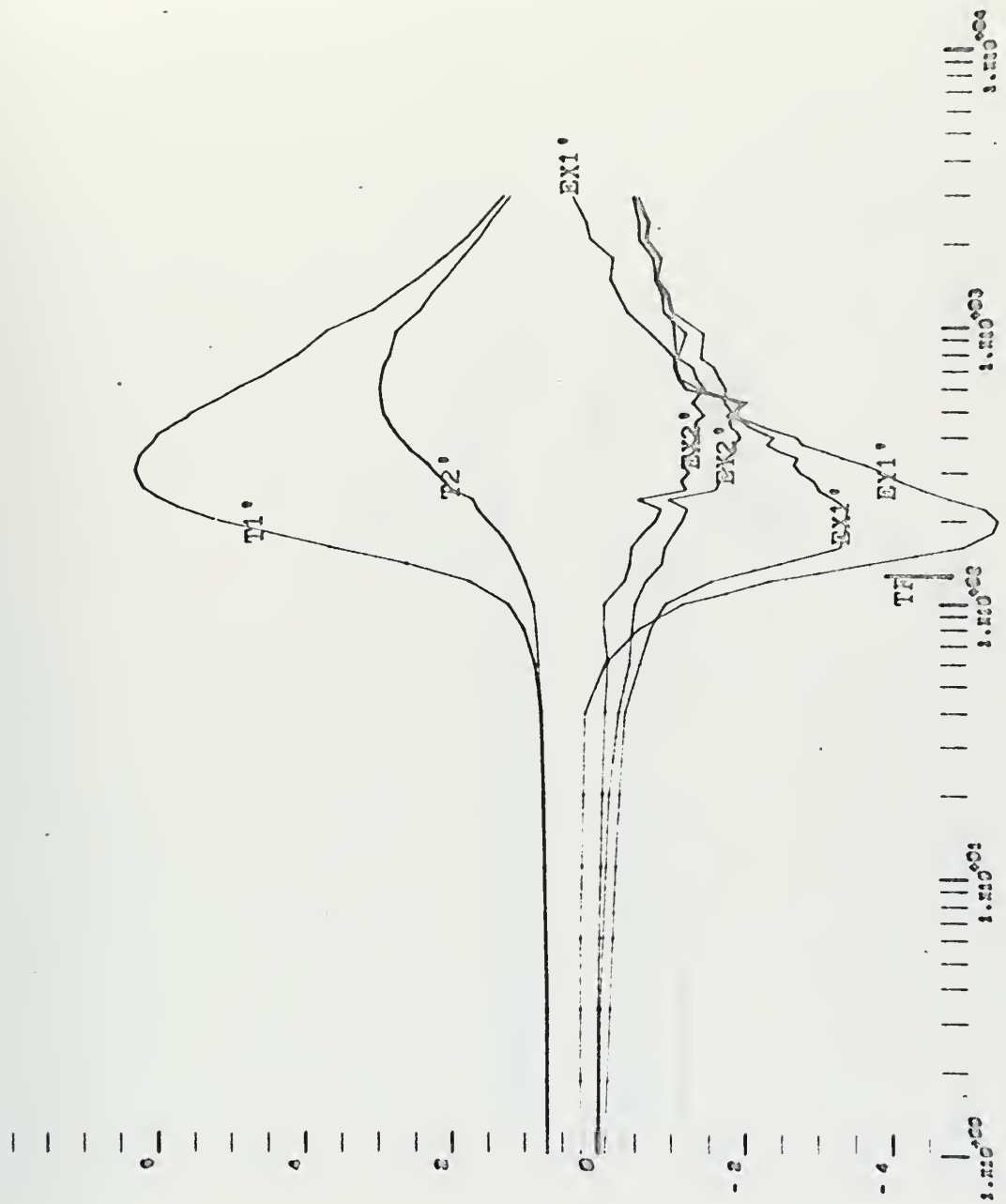

FIGURE 3-7-b: Corten Pass #1, Bottom Surface

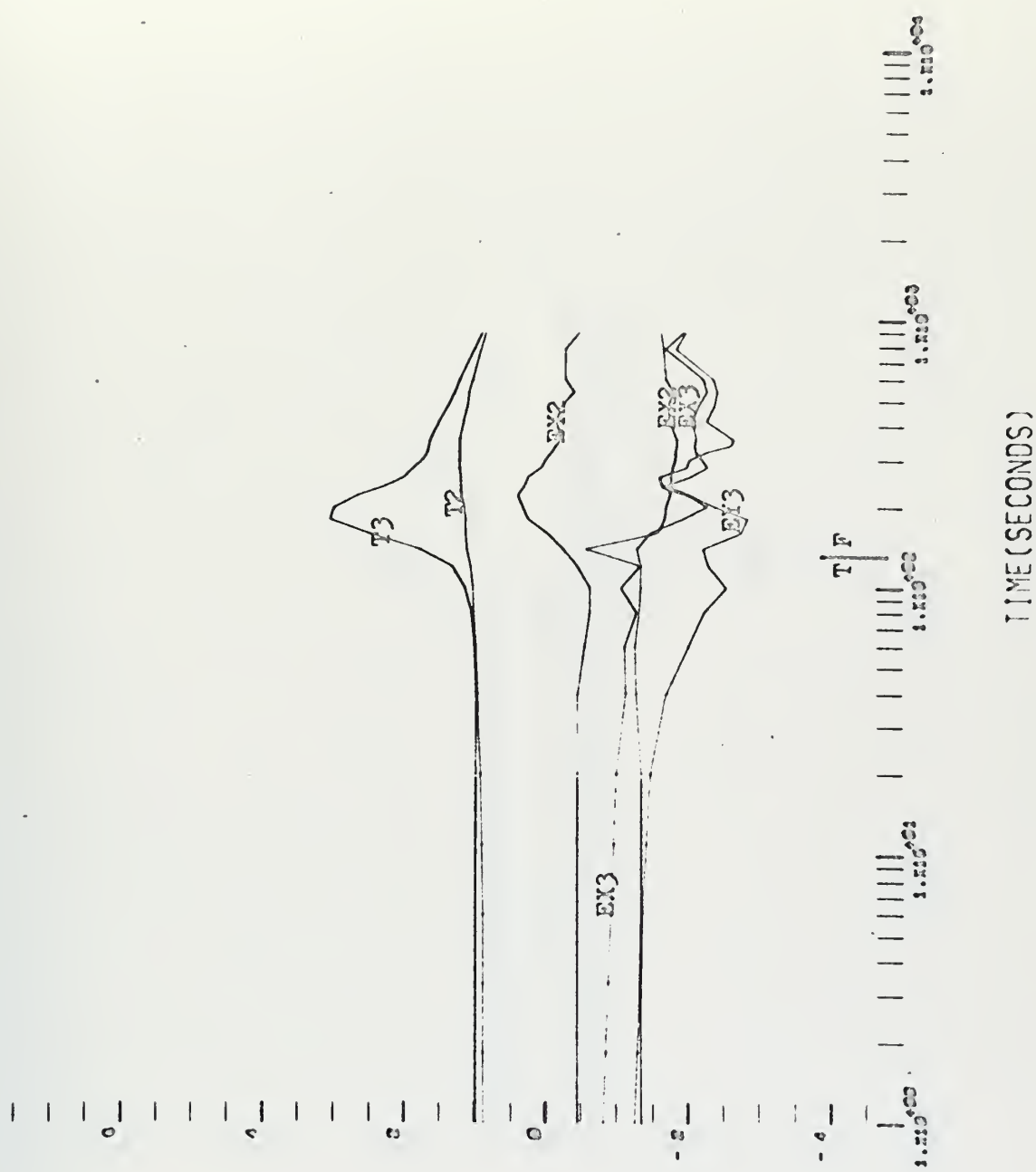

TEMPERATURE, MECH STRAIN
($x10^2$ °F) ($x10^{-3}$ in/in)

FIGURE 3-8-a: Corten Pass #2, Heated Surface

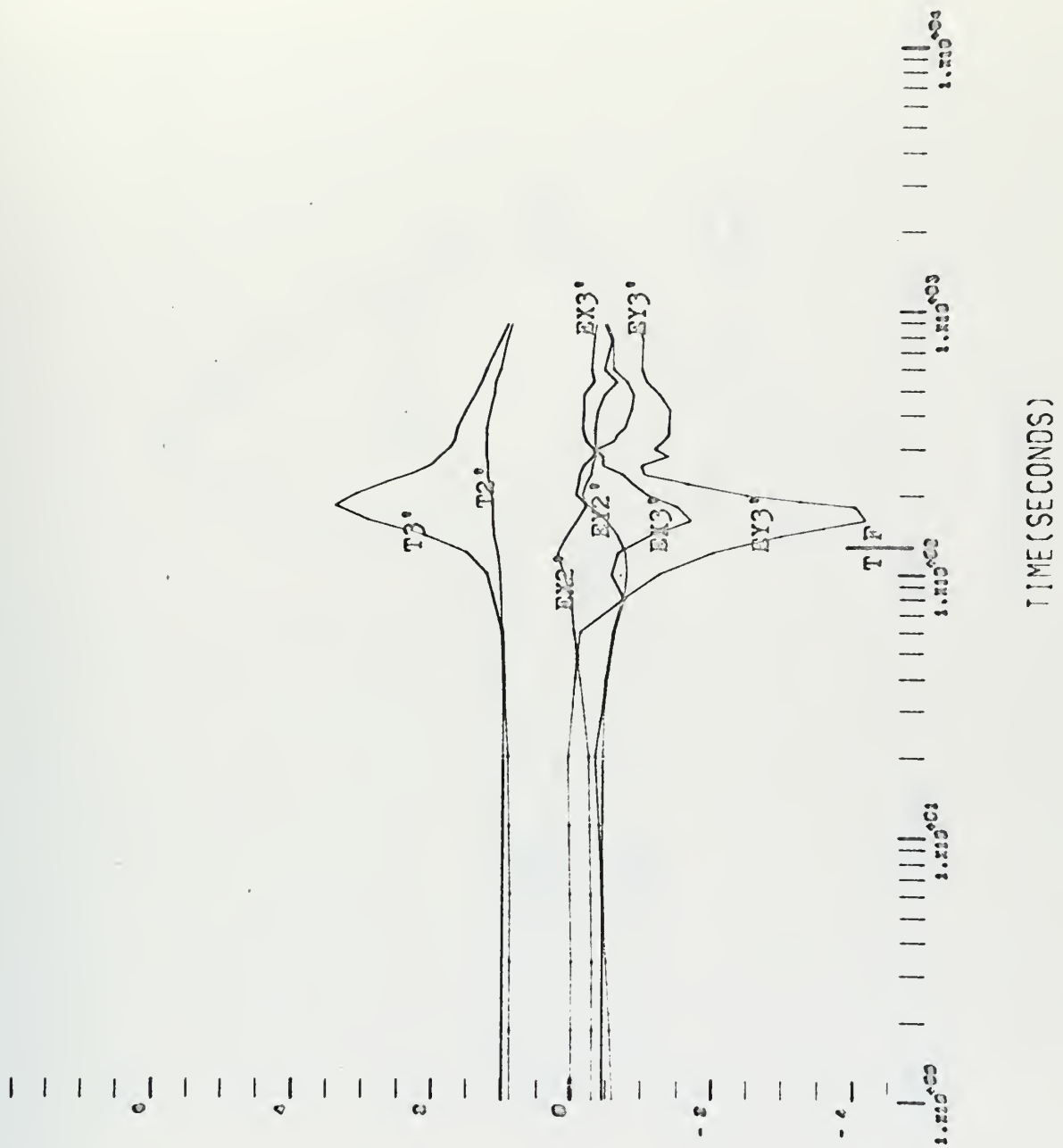

FIGURE 3-8-b: Corten Pass #2, Bottom Surface

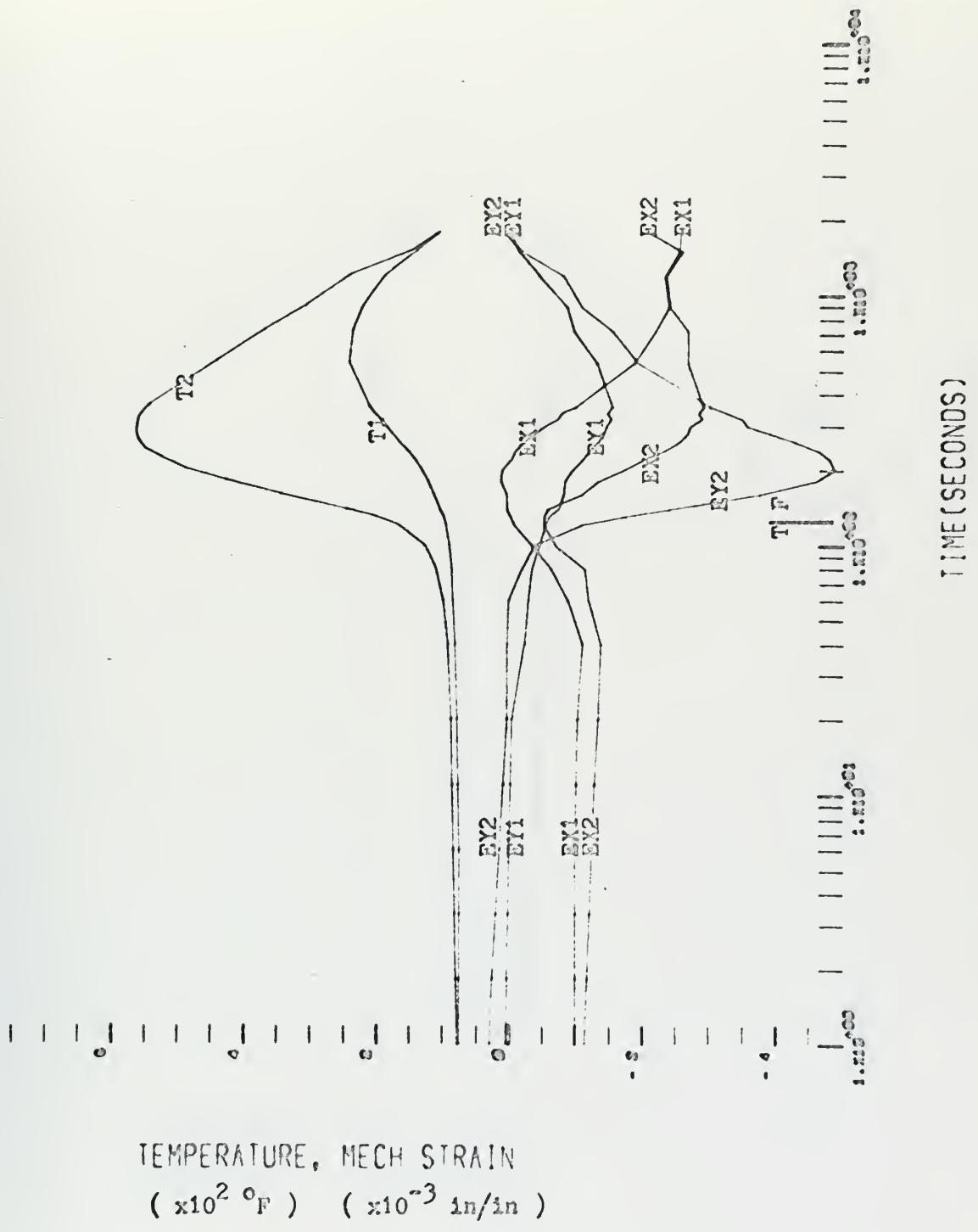

FIGURE 3-9-a: Corten Pass #3, Heated Surface

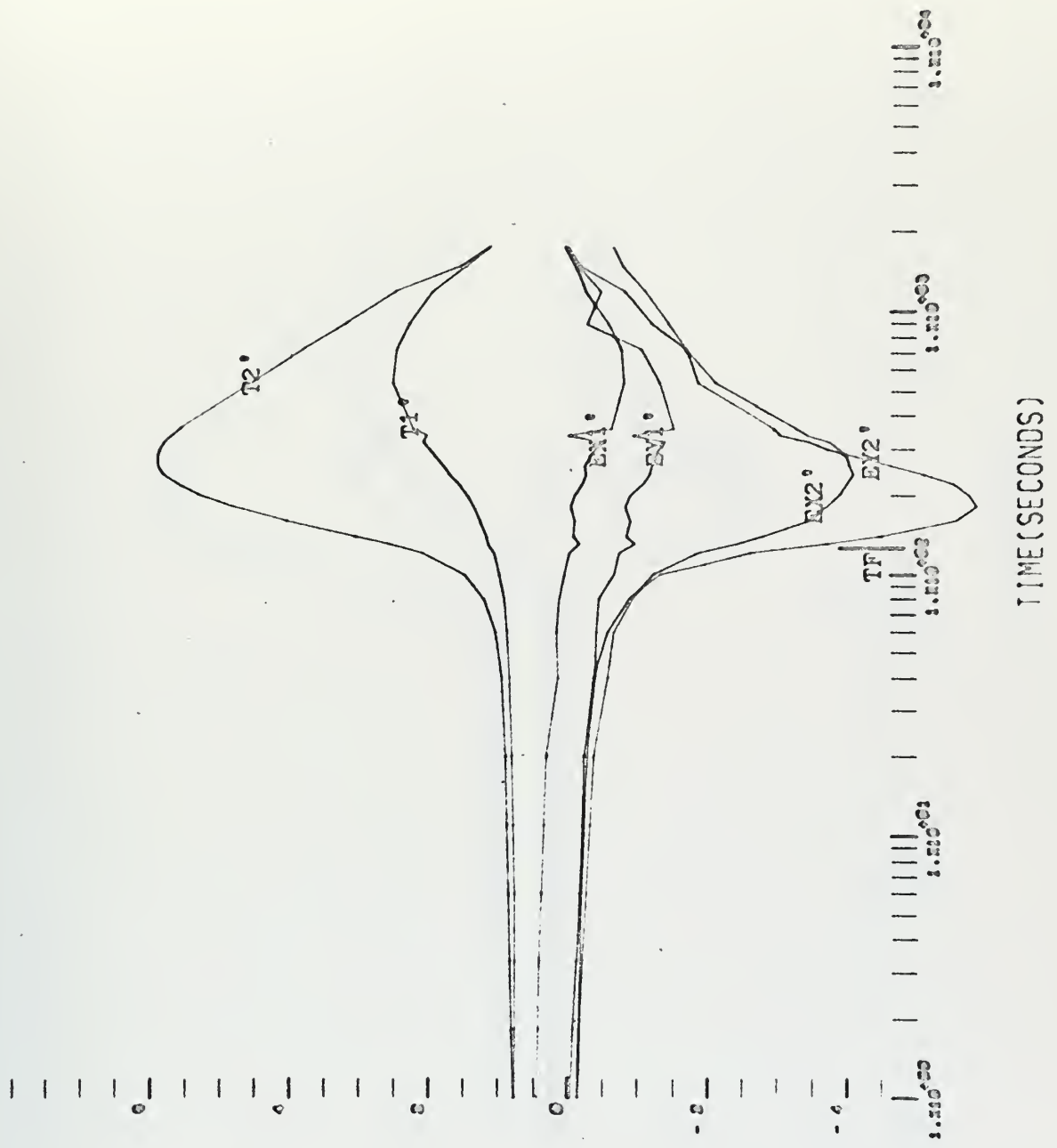

FIGURE 3-9-b: Corten Pass #3, Bottom Surface

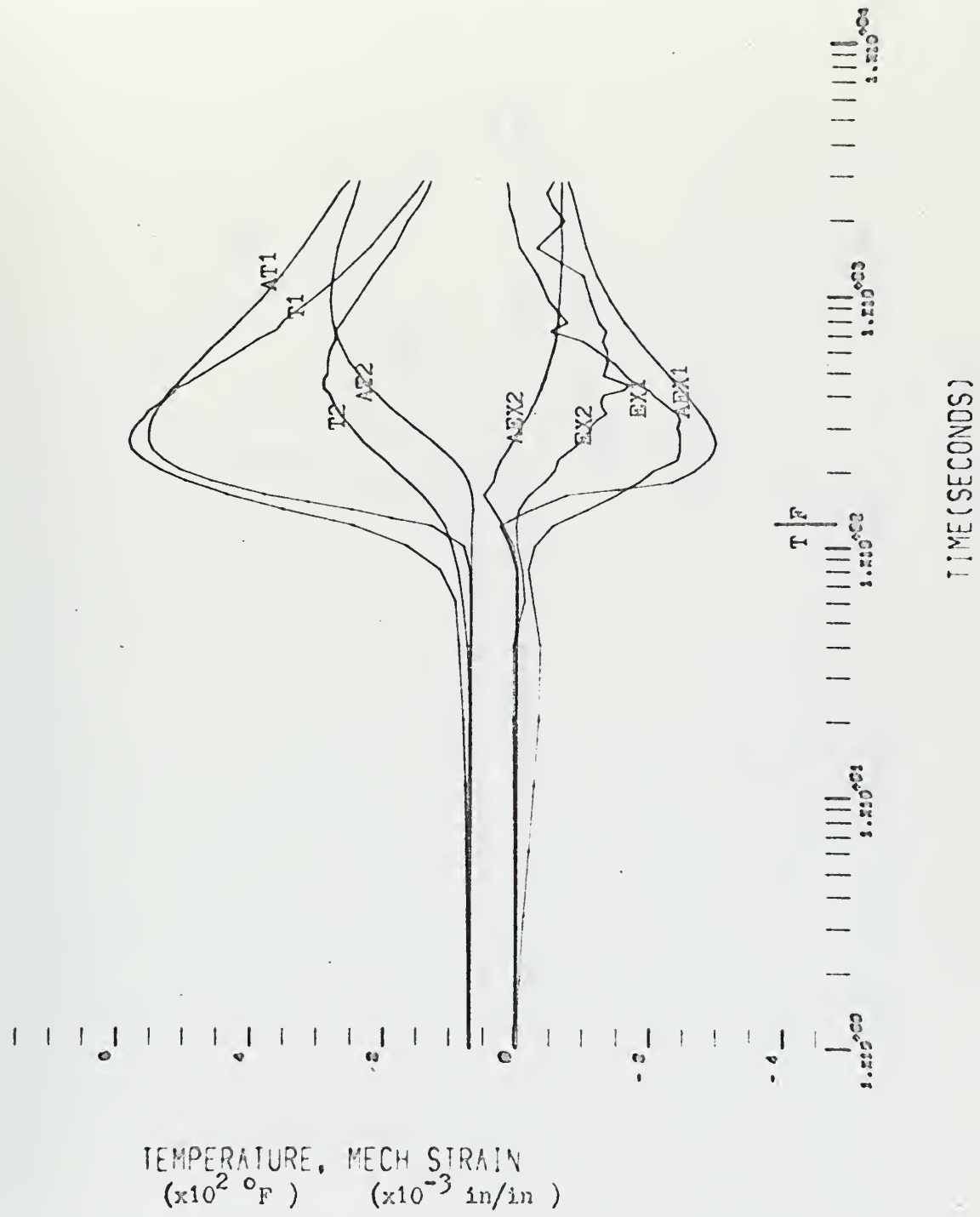

FIGURE 3-10: Analytical Results and Heated Surface Mild Steel Pass #1

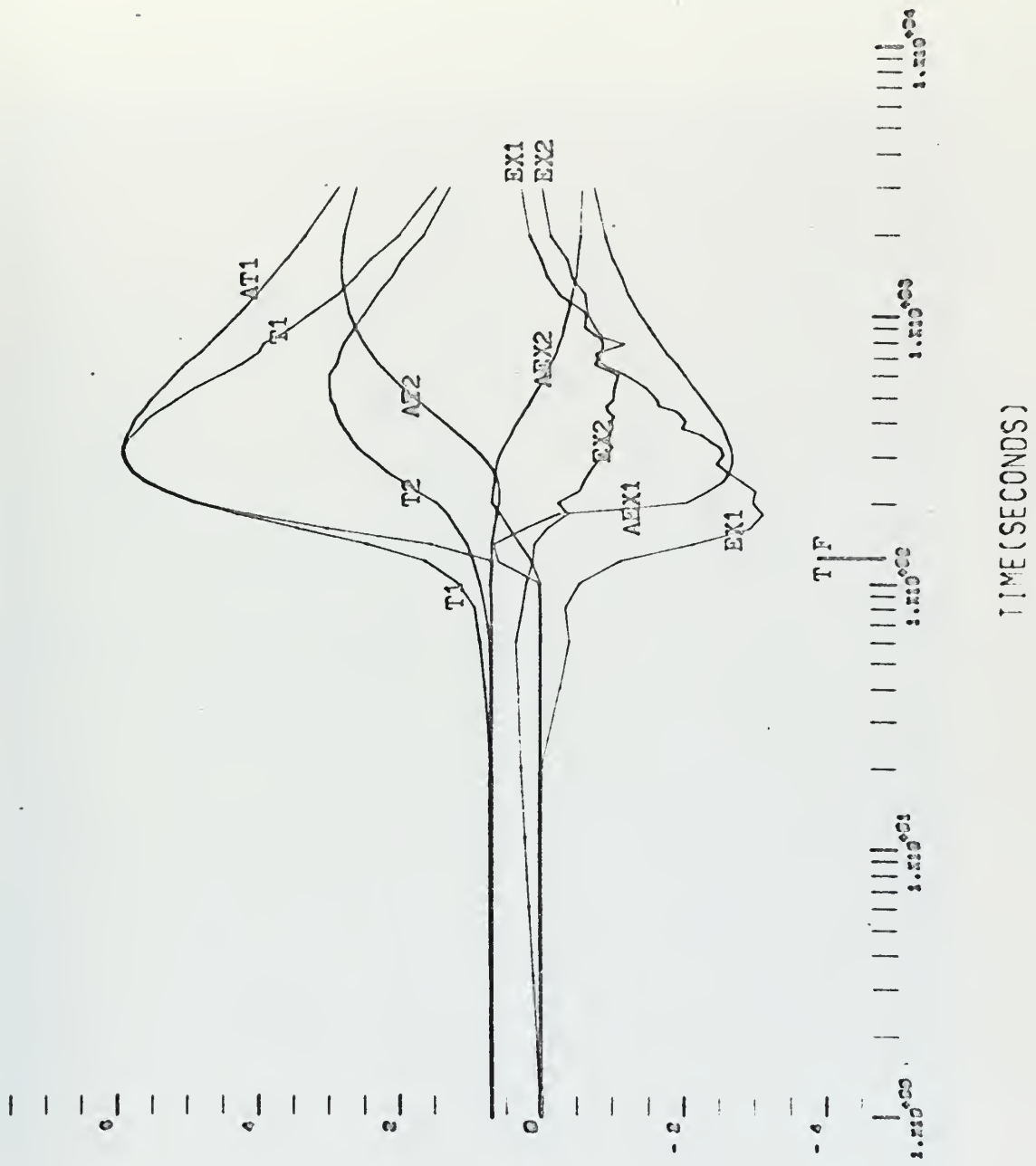

FIGURE 3-11: Analytical Results and Heated Surface T-1 Pass #1

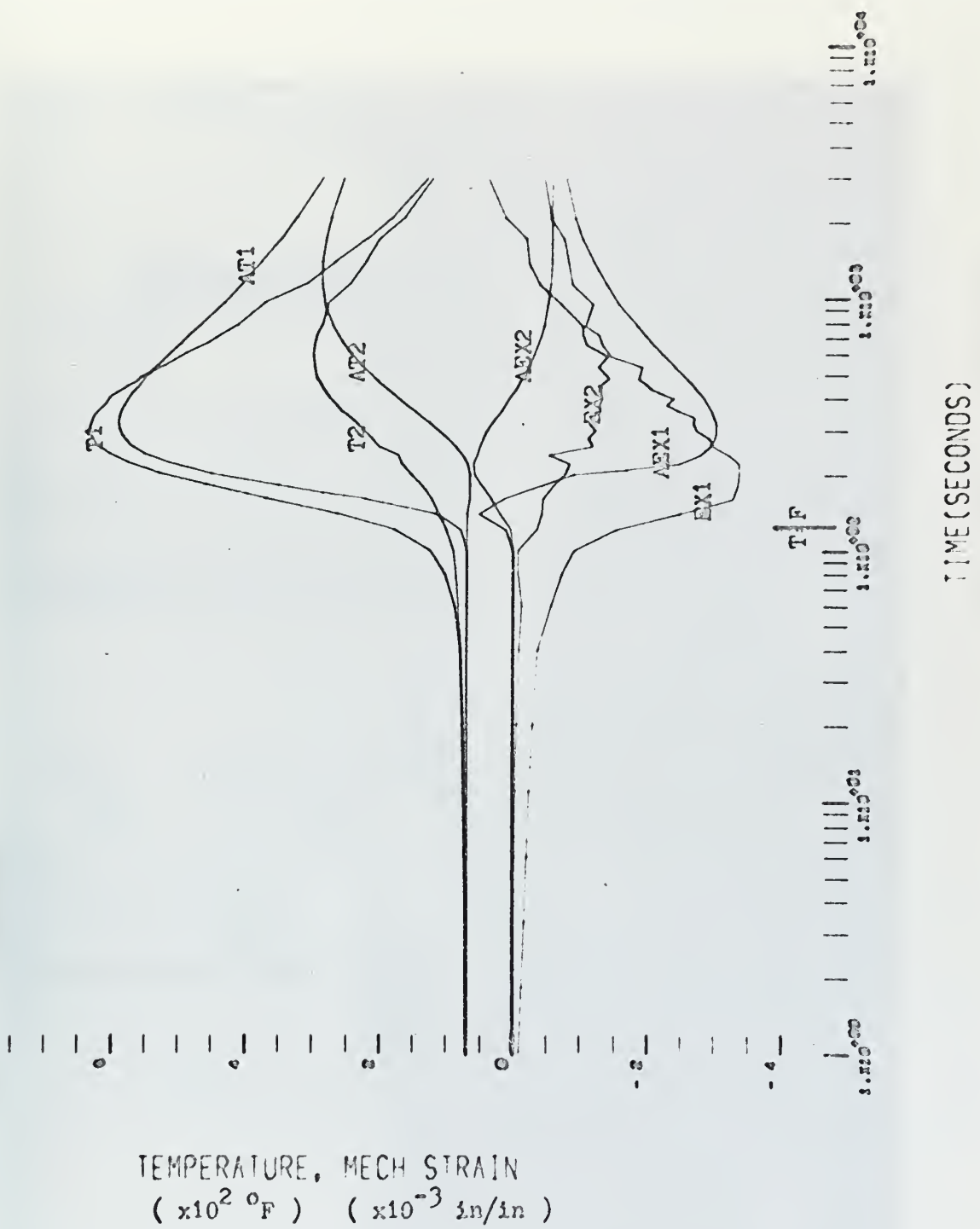

FIGURE 3-12: Analytical Results and Heated Surface Corten Pass #1

Figure 3-13: Mild steel plate after three passes of flame heat

IV. DISCUSSION OF RESULTS

In the experimental procedures, the speed of the flame was to be maintained constant for all passes. The automatic welding machine was used for this purpose. However, the speed adjustment on the welding machine is very coarse especially at the low speed used for these experiments. This made it necessary to preset the desired speed prior to each pass by timing an interval of travel and making fine adjustments to get the desired value of speed. The speed was preset prior to the first pass on the Corten specimen but upon engagement of the drive mechanism for this pass the speed adjustment changed and the speed, calculated from the timing marks on the output data, was 2.8 in./min. versus the desired value of 3.0 in./min. Comparison of data for the first pass on each steel is made difficult since the speed was different for the first pass on Corten.

The results from the first pass on the Corten specimen, and also the other pass where water cooling was not used, show that for this steel the highest temperature was recorded on the side opposite the heating. This is contrary to what occurs for the other two steels where water cooling is not used and intuitively this appears wrong. There is no great difference between the thermal conductivities of the different steels so it is expected that maximum temperature for the Corten should occur on the heated surface.

There are several possible reasons why this apparent inversion of the maximum temperature occurred. These reasons, in the order that they were investigated, are:

(1) Incorrect recording of the experimental data.

(2) The surface below the gages on the heated surface was not sandblasted clean prior to installation of the gages.

(3) The observed results actually occurred.

All the strain gage and thermocouple leads were tagged with channel input numbers and the tags were left on after the experiments were performed. Examination of these leads and the channel tags shows that the hookup of the leads to the input junction box was correct.

The surface directly under the flame had an oxide layer loosened during the heating. The surfaces under the strain gages were to have been sandblasted clean prior to installation of the gages. Thus, the oxide coating noticed on the flame path should not be present under the gages. Examination of the area around the strain gages on the heated surface confirms that the sandblasting was performed prior to gage installation. Therefore, the gages were properly mounted.

Since no equipment failure or incorrect experimental procedures could be detected, the temperatures measured must have actually occurred. There are several factors that could have influenced the heat flow from the source out to the measuring positions. This would influence the temperatures at the measuring points.

The experiments on the mild steel were performed first. There was a period of approximately twelve hours from the finish of the experiments on mild steel until the investigation of the T-1 was begun. Thus, the experiments performed on mild steel and T-1 started with essentially the same initial ambient temperature of the fire brick supporting the plates. The investigation of the Corten was begun immediately after the investigation of the T-1 was completed. Thus, the supporting fire brick may have had a higher initial temperature than for the T-1 and mild steel. This could

result in less heat loss to the fire brick from the lower surface of the Corten plate.

The experiments performed on the Corten were done in the evening and ambient room temperature was less than during experiments on the other steels. The first pass performed on the Corten was made at a slower speed and this could have affected the movement of the air at the plate surface. The combination of these two factors could give a higher heat loss at the heated surface than experienced with the other two steels.

Melting occurred on the heated surface of the Corten during the first pass due to the slower speed of the flame. Thus, a metal transformation occurred which was localized to an area near the flame. This could have influenced the heat flow because of heat absorbed during the melting transformation.

A combination of some or all of the above factors could have influenced the heat flow from the source and caused greater heat losses at the heated surface and less heat loss at the lower surface than during heating of the other two steels. This could result in the temperatures measured at two and five inches from the source being higher on the bottom than at the heated surface.

Since all three steels are heated in the same manner, the temperatures in close to the flame will be essentially the same for all the steels. During heat-up the metal near the flame will experience higher temperatures on the heated surface and then equalization of temperature across the thickness of the plate will occur during cool down.

All the strains induced in the steel plate are the results of the unequal heating performed on the plate. As the plate is heated by the oxyacetylene flame, the heated area will expand. This expansion will be

resisted by the cold rigid surrounding metal. When the compressive stress exerted on the heated area equals the yield stress of the heated area, which is less at the higher temperature, the heated area will experience plastic yielding. Since in the experiments the plate appears a dull red on both the heated and lower surface in near the flame, the plastic yielding will take place throughout the thickness of the material. The only direction that the plastic yielding can take place is perpendicular to the plate surface. Thus, the very hot zone becomes plastically unstable and plastic upset will occur. The direction of this upset will be influenced by many factors including the plate condition prior to heating. Duffy[7] found that the initial conditions of the steel plate and the boundary conditions determined the direction in which plastic upset would occur.

Upon cool down the metal that experienced plastic upset will begin to shrink as will the rest of the plate, until the initial temperature of the plate is reached. The plastic strains that occurred will cause a mismatch of strains upon cool down and result in residual stresses and strains. These residual stresses and strains will cause the bending. The difference between the temperatures on the top and bottom of the plates away from the source will cause a variation in the amount of plastic strain experienced at the surfaces. This will also contribute to the bending effect of the flame heating.

The exact analysis of how the bending is produced in the plates is very complicated. Since the flame is moving, the temperature at a point on the plate varies with time. Plasticity is time dependent, therefore, it is necessary to know the time a metal is at a temperature where plastic yielding will occur as well as the variation of the material properties

with temperature. The above discussion is very general but does serve to point out the mechanism of how bending is induced.

Examination of the strains upon cool down after the first pass shows that for mild steel and T-1 the plate is bent up around the flame path, and in the longitudinal direction the center of the plate lifts and the ends are bent down. Hence, the bending strains induced are opposite for the transverse and longitudinal directions. The Corten experienced bending exactly opposite that observed for the T-1 and mild steel. Thus, the plastic upset occurred in the opposite direction for the Corten.

There was no attempt made to insure that the steel plates were perfectly flat. In fact, during the installation of the strain gages the plates were baked and some bending was noticeable in all three plates but especially in the Corten. This prior bending of the Corten probably caused the direction of the plastic upset to be different and was further amplified by the temperatures being exactly opposite those experienced in the other two steels.

The difference in residual transverse strain between the top and bottom of the three specimen at two inches from the flame path is: 0.99×10^{-3} in./in. for mild steel, $.36 \times 10^{-3}$ in./in. for T-1 and 0.30×10^{-3} in./in. for Corten. This indicates that flame heating without water cooling is more effective for bending mild steel. This agrees with Walsh's observation[6] that flame heating is more effective for straightening mild steel.

The maximum transverse strains recorded during the first pass are: -4.33×10^{-3} in./in. for mild steel, -4.76×10^{-3} in./in. for T-1 and -5.43×10^{-3} in./in. for Corten. These high values of strain, when compared to the difference in residual strains resulting upon cool down, show

that flame heating without water cooling is inefficient as a bending method. Also, the direction of the resulting bending is dependent on the initial plate conditions and is not controlled by the flame.

When straightening welded panels with edge constraints, the maximum deflection that must be removed is usually near the midspan of the panel. Also, the fillet welds used will cause deflection as shown in Figure (4-1). The line flame heating could be used most effectively to remove this type distortion by heating parallel to the weld but on the opposite side of the plate from the weld. The flame path should not be directly opposite the weld but moved in a slight distance toward the center of the panel. This location of the flame line will give a maximum moment arm for the induced bending strains to cause deflection. The flame is not placed directly opposite the weld so the edge constraint will not reduce the bending effect.

The difference between longitudinal residual stresses in the two surfaces during flame heating is large, 1.05×10^{-3} in./in. for mild steel. If the direction of flame travel is the same as that used for welding, this should relieve some of the welding residual stresses too. The distance from the weld could be adjusted to maximize this stress removal.

If plastic behavior of the metal is assumed to be localized near this hot zone trailing the flame during heating, it should be possible to predict the strains that will result if another pass is performed with the measuring positions of the strains at the same distance from the flame. This would be done by superimposing the strains that would result at the location on those already present. This was attempted during pass number 2 on T-1 and mild steel. The predicted and experimental values of strain

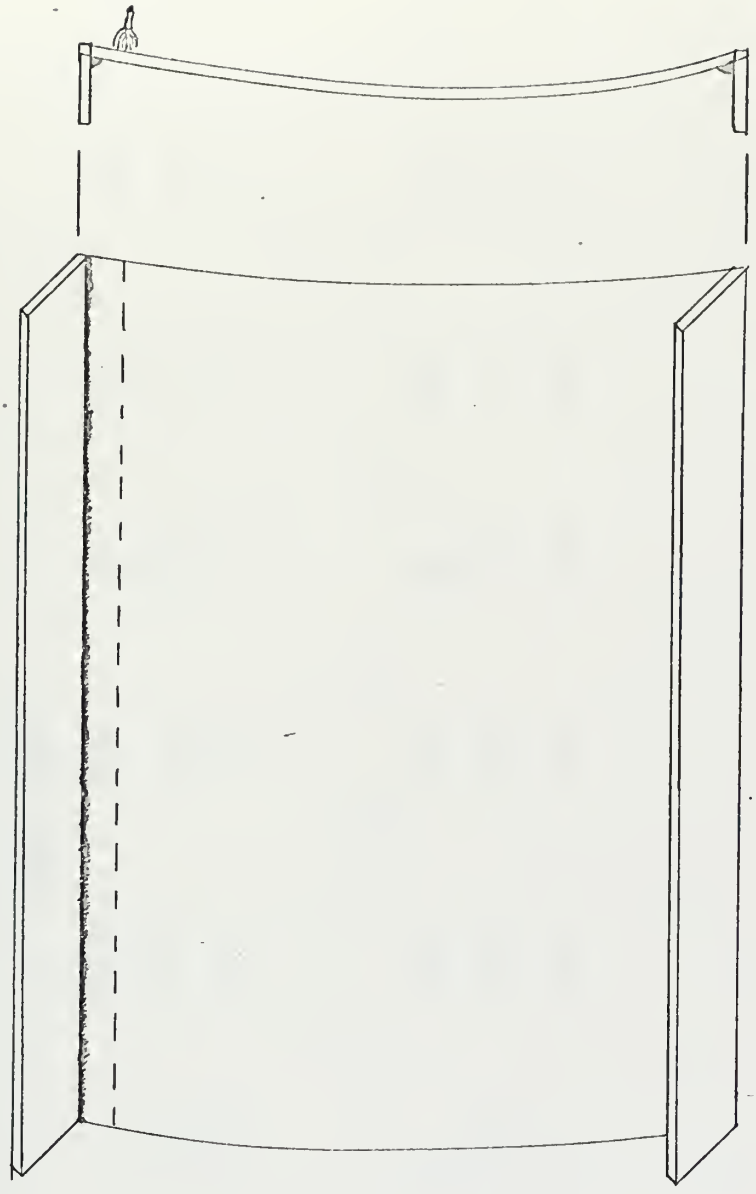

Figure 4-1: Illustration of how flame heating should be applied to remove distortion from welding

TABLE 4-1

PREDICTED VALUES OF STRAIN FOR THE SECOND PASS VERSUS MEASURED STRAIN

MILD STEEL

	EX1	EY1	EX1'	EY1'	EX2	EY2	EX2'	EY2'
Predicted	-0.39	-1.35	-2.17	-0.19	-0.39	-1.35	-2.17	-0.19
Measured	0.09	-0.39	-1.8	0.15	0.42	-0.69	-1.38	0.45

T-1

	EX1	EY1	EX1'	EY1'	EX2	EY2	EX2'	EY2'
Predicted	-0.23	-0.08	-0.23	-0.08	-0.83	0.25	-0.83	0.25
Measured	-0.05	-0.05	-2.06	0.25	0.19	-0.47	-1.34	0.31

are given in Table (4-1). There is no correlation of the predicted and measured values. This indicates that the strain induced during flame heating is highly dependent on the plate condition at the time of heating and that the plastic behavior is not localized to the hot zone near the flame.

The third pass on mild steel and T-1 and the second pass on Corten were made with water cooling employed. The strains of primary interest are the transverse strains, since these cause bending along the entire length of the plate and the line flame heating would utilize those strains in straightening or bending. The difference between the transverse strains on the heated surface and bottom surface two inches from the flame path is: 0.87×10^{-3} in./in. for mild steel and 1.02×10^{-3} in./in. for Corten. This shows a large increase in the bending strain induced in the Corten. The bending strain induced in the mild steel is less than where water cooling was not used. These values probably differ considerably from what one pass of flame heating would produce due to the large initial strains in the plates from previous passes. The bending of all plates is the same as described for pass number 1 on mild steel. The T-1 pass was performed on the side opposite the initial pass and the bending strain is larger than for cases where no water cooling was employed.

Water cooling limits the thermal effects experienced by the plate. The temperatures measured are less than half the temperatures recorded with no water cooling. Thus, the very hot zone will be more constrained than when no water cooling is used. The water cooling also prevents temperature equalization across the thickness of the plate. Since all the plates bent in the same direction when water cooling was used, even though the plates had entirely different initial conditions, the water

cooling forces the direction of plastic upset and hence, the bending. Temperature equalization across the thickness of the plate was not permitted since water cooling was applied directly after the flame. Thus, plastic yielding could take place only in one direction.

The values of maximum strains recorded are much smaller when water cooling is employed. Comparing the maximum strains with the residual bending strains shows that line flame heating with water cooling is more efficient than without. The maximum temperatures recorded with water cooling are much lower. This shows that the heat affected zone is much narrower and, for metallurgical reasons, the water cooling should be employed during flame heating. The ability to achieve bending in a specified direction is a desirable feature of the water cooling.

The large values of transverse strain observed during flame heating are contrary to the assumption of negligible transverse strains in the one dimensional welding program. Therefore, this program is not suitable for predicting the effects of flame heating. However, the one dimensional analysis was performed to check the validity of the model of the flame heat source and to see if the program can be used to estimate the longitudinal strains.

At two inches from the flame path, the predicted temperatures agree until the maximum temperature occurs. During cool down, the rate of temperature change is much less for the predicted temperatures. This is due to two factors:

(1) The analytical model does not include heat losses to the atmosphere and the supporting surface.

(2) The temperatures are predicted for a plate symmetric about the line flame heating, but in the experimental model this is not the case.

This second reason is the major factor in causing a faster cool down in the experimental specimen.

At a distance of approximately five inches from the flame path, the correlation is not as good for the temperatures. The slope of the two curves during temperature build-up is approximately the same and the maximum temperature is the same for both curves. The two curves are separated by a constant time factor during the build-up of temperatures. This is due to the fact that at increased distance from the flame, the heat source will appear to be a point source. This change with increased transverse distance is not incorporated in the mathematical model. The cool down rates are different for the same reasons as above.

The correlation of temperatures is sufficient to give an estimate of the strains that could be expected. If the strain for position two is shifted by the time separating the temperatures at position two, an estimate of the strains at this position can be obtained. One other problem is encountered with the model. At points near the heat source and directly under the source, the predicted temperatures will be very large. This can be seen by examination of the temperature equation in Appendix A. In the program, the maximum temperature was limited to 1500°F.

The mild steel results show the best correlation especially when AEX2 is shifted. The predicted maximum values are close to what is observed. The difference in residual strain is due to the different cool down rates for the analytical and experimental temperatures. The correlation for the other two steels is not as good, but a good estimate

of the strains that occur can be obtained from the program. The residual strains differ as for the mild steel and for the same reason.

This simple one dimensional analysis shows that computer programs developed for welding can be used for flame heating. Two dimensional programs for welding analysis use a finite element solution. Thus, the solution for temperatures should be changed so that better correlation is obtained throughout the plate.

The same temperature solution was used to alter the two dimensional program for welding which is being developed at M.I.T. The results from this program were not plotted because the predicted transverse strains were very small. The longitudinal strains were about the same as given by the one dimensional analysis. The program has not been completely perfected and great difficulty was experienced in trying to perform a run. It appears that the analysis used is correct, but there is an error in the program in predicting the transverse strains.

From the analysis of flame heating, one does not desire the residual stress for one surface. The variation of residual stresses across the thickness of the plate is needed to estimate the bending that will be induced. The two dimensional program will not yield this information. What is required is a full three dimensional analysis of the flame heating process. Until this analysis becomes a working reality, the analytical programs developed for welding are of very little use for studying flame heating.

V. CONCLUSIONS

The conclusions of this investigation based on the preceding discussion are:

A. Experimental Observations

(1) Line flame heating without water cooling is most effective for bending the mild steel. The amount of bending depends on the material yield strength and variation of the yield strength with temperature. The direction of bending without the water cooling is dependent on initial plate conditions and not the flame location. Thus, the direction of bending cannot be controlled by the heating.

(2) Line flame heating with water cooling is more efficient as a bending process. The location of the flame controls the direction of the bending and the heat affected zone is much smaller than without cooling.

(3) The large values of transverse strain necessitate at least a two dimensional analysis for predicting the effects of flame heating.

B. Observations From Analysis of Results

(1) Line flame heating when used for straightening should be applied parallel to the weld line, but on the opposite side and displaced slightly toward the center of the panel. Water cooling should be used to cause bending in the direction which will remove the distortion induced by the welding. The heat is not applied directly opposite the weld to prevent the edge constraint from restricting the bending effect of the flame heat and to relieve longitudinal residual stresses induced by the welding.

(2) The one dimensional welding program gives a fair estimate of the longitudinal strains that occur during flame heating for the heated surface. However, transverse strains are assumed to be zero in this

program while experimental data shows that these strains are large. Thus, the program is of no use for predicting the results of flame heating although the comparison does indicate that analytical programs developed for welding may be used for line flame heating if modified for the proper heat source.

(3) Analytical methods that presently exist for welding cannot be used to optimize the flame heating techniques. The desired result of flame heating is bending in a specified direction. Present programs do not evaluate the bending that will be induced by flame heating. Thus, they give no useful data about the primary function of the flame heating.

VI. RECOMMENDATIONS

It is recommended that efforts in the study of flame heating be directed toward solving the heat flow problem. Since a three dimensional analysis is necessary for predicting bending strains, a three dimensional analysis of the heat transfer will be necessary. An analysis of this type will require the use of the computer and finite element techniques.

There exists the need in the welding field for the development of a three dimensional stress analysis. Work is going forward in this area and will not stop with a two dimensional analysis. Thus, a three dimensional analysis will probably be available in the future. The thermal analysis developed for the flame heating can then be utilized with the three dimensional stress analysis for predicting the effects of flame heating.

It is further recommended that experimental studies of the flame heating methods be discontinued until the three dimensional analysis becomes available. There is enough data available from the studies so far performed at M.I.T. to improve the flame heating practiced in industrial applications. At most, the flame straightening is a problem of secondary importance to industry and there exists no pressing need to carry forward any further investigations of the straightening that particular heating techniques will yield. However, once a three dimensional analysis becomes available, more experimental studies will be needed to determine the accuracy of the analytical solution.

APPENDIX A

THERMAL ANALYSIS

The mathematical technique used in solving the heat transfer part of the welding analysis was developed by Rosenthal[10] in 1941. The differential equation of heat transfer is:

$$\frac{\partial^2 t}{\partial x^2} + \frac{\partial^2 t}{\partial y^2} + \frac{\partial^2 t}{\partial z^2} = 2\lambda \frac{\partial t}{\partial s}$$

If the welding is carried out over a sufficient length, a state is created in the welded piece which is called quasi-stationary. In the quasi-stationary state, an observer stationed at the moving heat source will notice no temperature change around the heat source. The differential equation of heat can be shifted to a new coordinate system whose origin is at the heat source. If the X axis lies in the direction of welding, replacing X by a new coordinate w where $w = x - vs$ leads to the equation:

$$\frac{\partial^2 t}{\partial w^2} + \frac{\partial^2 t}{\partial y^2} + \frac{\partial^2 t}{\partial z^2} = -2\lambda v \frac{\partial t}{\partial w}$$

This is the differential equation of the quasi-stationary state of welding and cutting.

In the welding analysis, a line source of constant strength through the thickness of the material and constant material thermal properties are assumed. The problem then becomes two dimensional. The solution of the heat transfer equation is then:

$$t - t_o = \frac{Q}{2\pi K g} e^{-\lambda v w} K_o(\lambda v r)$$

where $r = \sqrt{w^2 + y^2}$ and Ko is the so called Bessel function of the second kind and zero order.

The thermal properties of metals are not constant with temperature variation and this variation with temperature may be considerable. In the

M.I.T. analysis of the welding problem this variation of thermal properties is included by an iterative method. The temperature is first solved for - with assumed thermal properties and then thermal properties corresponding to this temperature are used for the next solution. This process is continued until the error in temperature calculated is a specified minimum.

The flame heating problem is different from the welding problem in that the heat source is not a point source on the surface, but a distributed source of varying strength (Figure A-1-a).

The differential equation of heat transfer is the same, but the boundary conditions imposed by the source are different than those of a line source. Research of available literature shows that there is not a closed form solution to this problem as is used in the welding analysis. Nakada and Hashimoto[11] have solved the problem in the form of Fourier integrals which can be solved using a computer. They also developed a method of direct numerical integration by digital computer. Both of these methods require extensive computer space and a great amount of computer time in order to solve the equations.

Since the strain analysis developed at M.I.T. (Appendix B) requires a minimum of computer space and time, the thermal solutions discussed above seem incompatible with this program. The large space requirements and cost of these solutions for temperatures of an accuracy not matched in the strain analysis make the above solutions unacceptable as models for the flame heating.

Rykalin[13] has developed a simpler analysis of the flame heating problems which should give the desired accuracy in solving the heat transfer problem. The model he uses for the flame heating process is shown in Figure (A-1-b). In this model he assumes an imaginary heat source at a

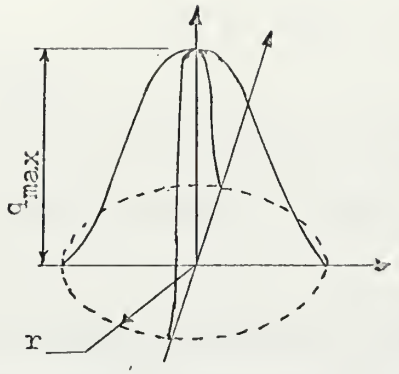

(a) Heat flux distribution of the standard torch flame along radius r

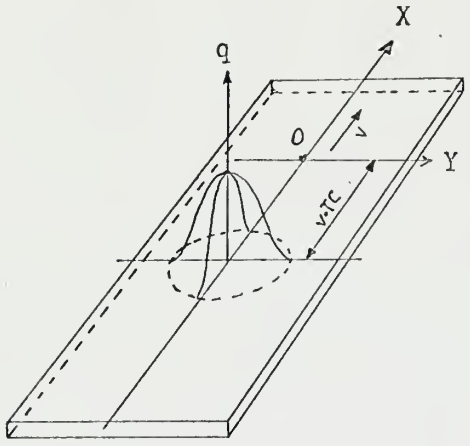

(b) Model of flame heating with imaginary heat source located at point O

Figure A-1

distance, equal to a time constant times the speed of the flame, in front of the actual source. The solution to the heat transfer problem then becomes:

$$t - t_o = \frac{q_e}{2\pi K g} e^{\left[-\lambda v w + \frac{2\alpha}{c\rho g}(TC)\right]} K_o(\lambda v r)$$

q_e is an effective heat input for the imaginary source. A table of experimental values of q_e and TC (time constant) is found in Reference 13, page 19.

In modifying the M.I.T. welding program for flame heating Rykalin's model of the flame heating is used. Since the two solutions are similar, the modification of the program is very slight.

APPENDIX B

ANALYSIS OF THERMAL STRESSES AND METAL MOVEMENT

Because a weldment is locally heated by the welding arc, the temperature distribution in the weldment is not uniform and changes as welding progresses. This non-uniform temperature distribution causes thermal stresses in the weldment, which also change as welding progresses. A computer program has been developed at M.I.T.[2] to analyze thermal stresses during welding and the resulting residual stresses.

Masubuchi describes the welding process as follows[14]. Figure (B-1) shows schematically how welding thermal stresses are formed. Figure (B-1-a) shows a bead-on-plate weld in which a weld bead is being laid at a speed v. O-xy is the coordinate system; the origin, O, is on the surface underneath the welding arc and the x-direction lies in the direction of welding.

Figure (B-1-b) shows temperature distribution along several cross sections. Along Section A-A, which is ahead of the welding arc, the temperature change due to welding, T, is almost zero (Figure B-1-b-1). Along Section B-B, which crosses the welding arc, the temperature distribution is very steep (Figure B-1-b-2). Along Section C-C, which is some distance behind the welding arc, the distribution of temperature change is as shown in Figure (B-1-b-3). Along Section D-D, which is very far from the welding arc, the temperature change due to welding again diminishes (Figure B-1-b-4).

Figure (B-1-c) shows the distribution of stresses along these sections in the x-direction, σ_x. Stress in the y-direction, σ_y, and shearing stress, τ_{xy}, also exist in a two dimensional stress field (Figure B-1-a).

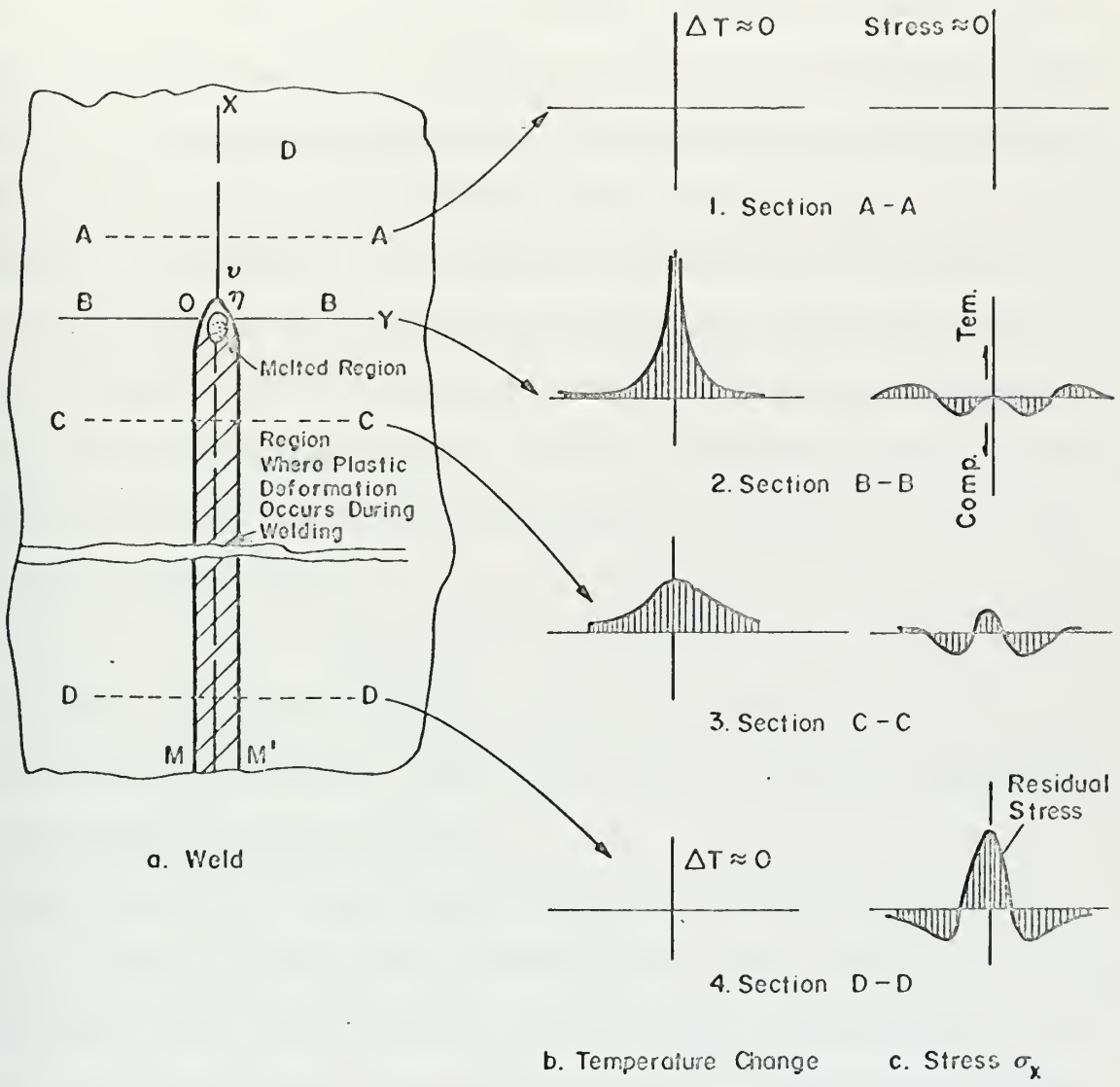

Figure B-1: Schematic Representation of Changes of Temperature and Stresses During Welding

Along Seetion A-A, thermal stresses due to welding are almost zero (Figure B-1-e-1). The stress distribution along Section B-B is shown in Figure (B-1-c-2). Stresses in areas underneath the welding are are close to zero, beeause molten metal does not support loads. Stresses in areas somewhat away from the are are compressive, because the expansion of these areas is restrained by surrounding areas that are heated to lower temperatures. Sinee the temperatures of these areas are quite high and the yield strength of the material is low, stresses in these areas are as high as the yield strength of the material at eorresponding temperatures. The amount of compressive stress increases with inereasing distance from the weld or with deereasing temperature. However, stresses in areas away from the weld are tensile and balanee with eompressive stresses in areas near the weld. In other words,

$$\int \sigma_x \, dy = 0$$

across Seetion B-B. This equation negleets the effects of σ_y and τ_{xy} on the equilibrium eondition. Thus, the stress distribution along Section B-B is as shown in Figure (B-1-e-2).

Stresses are distributed along Section C-C as shown in Figure (B-1-e-3). Since the weld-metal and base-metal regions near the weld have eooled, they try to shrink causing tensile stresses in areas close to the weld. As the distanee from the weld inereases, the stresses first ehange to compressive and then beeome tensile.

Figure (B-1-e-4) shows the stress distribution along Seetion D-D. High tensile stresses are produced in areas near the weld, while eompressive stresses are produced in areas away from the weld. The distribution of residual stresses that remain after welding is eompleted as shown in the figure.

The cross-hatched area, MM', in Figure (B-1-a) shows the region where plastic deformation occurs during the welding thermal cycle. The ellipse near the origin, O, indicates the region where the metal is melted. The region outside the cross-hatched area remains elastic during the entire welding thermal cycle.

The M.I.T. analysis of thermal stresses includes plasticity, variation of coefficient of linear expansion and loading history. A plane stress formulation is used, with stress and strains being considered uniform in the thickness direction, and σ_z, the stress in this direction is assumed to be zero. The analysis is then reduced to one dimension by the assumption that only the longitudinal stress is non-zero. The detailed equations and computer program developed are found in Reference (2).

The assumption of constant stresses across the thickness preclude any bending effects. The analysis does not include changes of stress-strain characteristics and expansion characteristics due to metallurgical changes which may take place during welding. The analysis first calculates the temperatures that will be present in the plate at various times and then uses these temperatures and times as inputs to the stress program. Thus, the analysis is split into two separate parts.

The line flame heating is similar to the bead-on-plate weld for which the analysis was developed. The major difference is the heat source for which a mathematical model has already been developed. Due to the finite width of the source, the width of the hot zone around the flame will be larger than in welding. This width and the fact that more heat must be used to raise the zone to the desired temperatures will undoubtedly introduce transverse strains. However, if these transverse strains are still reasonably small the welding analysis should give estimates of how

the longitudinal strains act and reasonable values of residual thermal stresses.

At present, a two dimensional plane stress program is being developed by Andrews and Masubuchi. This analysis includes the complete two dimensional stress equations and equilibrium equations. The material assumptions and analysis are similar to the one dimensional program except a finite element solution is used and the thermal and stress analysis are combined. The program is currently at the stage where past welding data is being compared with the program outputs to check the program. It is still in the stage of being continually refined and debugged.

Only the results of the computer programs will be presented in this report. No attempt at developing a suitable program is being made. The flame heating data will be compared with the analytical results to see if the welding programs, modified for the heat source, can be used for analysis of flame heating.

APPENDIX C

MATERIAL COMPOSITION AND PHYSICAL PROPERTIES

1. Chemical Composition[20]

Specimen	C	Mn	P	S
AISI 1020 (mild steel)	0.06	.31	.002	.024
ASTM A-242 (Corten)	0.09	.36	.09	.032
ASTM A-415 (T-1)	0.18	.90	.010	.023

2. Physical Properties[20,21,22]

A. AISI 1020

Temperature (^{o}F)	70	200	300	400	500	600	800	1000	1200	1500
Young's Modulus ($x10^{6}$ psi)	29.3	28.5	27.6	27.4	27.3	27.2	26.0	22.8	14.2	0
Yield Strength ($x10^{3}$ psi)	35.0	32.0	28.0	26.0	23.5	21.5	18.0	14.0	8.0	0
Strain Hardening Parameter ($x10^{6}$ psi)	0	0	0	0	0	0	0	0	0	0
Specific Heat ($\frac{cal}{^{o}F\text{-}lb}$)	26.2	28.8	30.2	31.7	32.9	33.6	37.2	38.2	40.0	40.5
Conductivity ($\frac{cal}{in\text{-}sec\text{-}^{o}F}$)	.165	.165	.165	.157	.154	.150	.143	.136	.128	.118
Density ($\frac{lb}{in^{3}}$)	.284	.284	.284	.284	.284	.284	.284	.284	.284	.284
Coef. of Thermal Expansion ($\frac{in/in}{^{o}F}$)	6.8	6.8	6.9	7.0	7.10	7.20	7.60	8.0	8.5	9.0

B. ASTM A-514

Temperature (^{o}F)	70	200	400	600	800	1000	1200	1400	1800	2000
Young's Modulus ($x10^{6}$ psi)	30.5	28.5	27.3	27.1	25.7	22.8	14.8	8.2	1.3	0
Yield Strength ($x10^{3}$ psi)	100.0	97.0	87.0	84.0	80.0	66.0	43.0	20.0	4.0	0
Strain Hardening Parameter ($x10^{6}$ psi)	1.5	1.5	1.4	1.3	1.1	.9	.8	.7	.6	.5
Specific Heat ($\frac{cal}{F\text{-}lb}$)	28.9	30.03	31.7	32.6	33.6	34.1	33.6	33.1	31.7	28.4
Conductivity ($\frac{cal}{in\text{-}sec\text{-}^{o}F}$)	.102	.111	.118	.118	.113	.111	.103	.098	.091	.078
Density ($\frac{lb}{in}3$)	.283	.283	.283	.283	.283	.283	.283	.283	.283	.283
Coef. of Thermal Expansion ($\frac{in/in}{^{o}F}$)	6.30	6.32	6.39	6.50	6.70	7.00	7.39	7.70	8.22	8.40

C. ASTM A-242

Temperature (^{o}F)	70	200	300	400	500	600	800	1000	1200	1500
Young's Modulus ($x10^{6}$ psi)	29.3	28.5	27.6	27.4	27.3	27:2	26.0	22.8	14.2	0
Yield Strength ($x10^{3}$ psi)	53.3	49.9	49.0	48.0	47.9	47.8	28.5	18.5	10.0	0
Strain Hardening Parameter ($x10^{6}$ psi)	1.5	1.5	1.4	1.4	1.3	1.2	1.0	.8	.6	.5
Specific Heat ($\frac{cal}{^{o}F\text{-}lb}$)	26.4	29.1	30.5	31.4	32.4	33.4	34.7	35.5	35.9	34.8
Conductivity ($\frac{cal}{in\text{-}sec\text{-}^{o}F}$)	.137	.139	.141	.140	.138	.136	.132	.126	.119	.107
Density ($\frac{lb}{in}3$)	.284	.284	.284	.284	.284	.284	.284	.284	.284	.284
Coef. of Thermal Expansion ($\frac{in/in}{^{o}F}$)	6.32	6.55	6.70	6.84	7.04	7.25	7.70	8.00	8.30	8.47

APPENDIX D

TABULATED EXPERIMENTAL RESULTS

MILD STEEL PASS #1

TIME	T1	T1'	T2	T2'	EX1	EY1	EX1'	EY1'	EX2	EY2	EX2'	EY2'
1	70	70	70	70	0.0	0.0	0.0	0.0	0.0	0.0	0.0	0.0
20	81	74	70	70	-0.33	-0.09	-0.09	0.18	0.06	0.09	0.06	0.06
40	87	81	74	74	-0.36	-0.18	-0.24	0.03	0.06	-0.03	-0.03	-0.09
60	94	89	83	75	-0.24	-0.12	-0.19	-0.01	-0.11	-0.26	0.14	-0.04
80	117	109	90	82	-0.16	-0.55	-0.01	-0.34	-0.08	-0.44	0.17	-0.19
100	166	155	98	89	-0.26	-1.25	-0.10	-1.09	-0.00	-0.57	0.17	-0.37
120	250	237	110	97	-0.53	-1.97	-0.48	-2.07	0.02	-0.61	0.31	-0.41
140	355	335	126	114	-1.04	-3.11	-0.81	-3.03	-0.03	-0.78	0.22	-0.65
160	442	420	145	132	-1.49	-3.98	-1.27	-3.82	-0.17	-0.98	0.04	-0.83
180	504	475	167	142	-1.84	-4.33	-1.32	-3.81	-0.41	-1.25	0.31	-0.65
200	543	516	187	173	-2.03	-4.31	-1.56	-3.90	-0.56	-1.43	-0.32	-1.25
220	570	544	203	190	-2.41	-4.27	-1.86	-3.75	-0.60	-1.47	-0.40	-1.39
240	584	560	220	205	-2.44	-3.97	-1.93	-3.46	-0.78	-1.65	-0.50	-1.55
260	588	567	235	220	-2.44	-3.73	-2.17	-3.19	-0.94	-1.78	-0.39	-1.62
280	584	567	246	233	-2.44	-3.43	-2.32	-2.98	-1.09	-1.81	-0.80	-1.73
300	577	563	255	243	-2.41	-3.16	-2.38	-2.68	-1.08	-1.77	-0.86	-1.67
320	567	557	263	250	-2.44	-2.86	-2.45	-2.49	-1.21	-1.81	-0.95	-1.67
340	560	550	272	259	-2.41	-2.71	-2.39	-2.33	-1.35	-1.89	-1.03	-1.72
360	547	535	276	264	-2.27	-2.45	-2.23	-2.02	-1.26	-1.77	-1.07	-1.70
380	535	526	282	270	-2.17	-2.26	-2.21	-1.88	-1.25	-1.82	-1.12	-1.72
400	523	516	285	274	-2.04	-2.13	-2.16	-1.83	-1.28	-1.76	-1.15	-1.66
420	517	510	295	285	-1.98	-2.04	-2.13	-1.77	-1.58	-2.03	-1.52	-1.97
440	500	495	295	285	-1.84	-1.90	-2.13	-1.71	-1.67	-1.97	-1.46	-1.85
460	489	484	295	288	-1.71	-1.77	-1.97	-1.61	-1.49	-1.79	-1.51	-1.81
480	477	474	290	280	-1.61	-1.67	-1.94	-1.61	-1.29	-1.59	-1.21	-1.51
540	448	445	290	280	-1.45	-1.57	-1.76	-1.37	-1.35	-1.50	-1.27	-1.39
600	418	418	286	280	-1.19	-1.31	-1.61	-1.25	-1.35	-1.38	-1.42	-1.39

MILD STEEL PASS #1 (Continued)

TIME	T1	T1'	T2	T2'	EX1	EY1	EX1'	EY1'	EX2	EY2	EX2'	EY2'
660	396	396	279	277	-0.97	-1.27	-1.51	-1.06	-1.26	-1.29	-1.51	-1.36
720	366	366	277	270	-0.48	-0.78	-0.96	-0.69	-1.33	-1.27	-1.45	-1.15
780	358	358	268	263	-0.74	-1.19	-1.28	-0.95	-1.22	-1.10	-1.33	-0.99
960	313	313	246	241	-0.44	-1.07	-1.19	-0.74	-1.09	-0.97	-1.26	-0.72
1200	270	270	222	217	-0.28	-1.21	-1.15	-0.55	-0.98	-0.95	-1.38	-0.63
1560	225	225	188	185	-0.01	-0.97	-1.00	-0.37	-0.26	-0.56	-1.14	-0.30
1980	192	192	168	164	0.09	-0.99	-0.93	-0.36	-0.69	-0.60	-1.23	-0.24
2280	173	173	152	150	0.16	-0.86	-0.89	-0.11	-0.50	-0.44	-1.08	-0.15
2580	158	158	141	138	0.17	-0.88	-0.85	-0.10	-0.40	-0.37	-1.03	0.02
2880	145	145	133	130	0.20	-0.83	-0.83	-0.02	-0.51	-0.39	-1.15	-0.10
3180	135	135	126	124	0.25	-0.86	-0.80	-0.02	-0.42	-0.39	-1.12	-0.04
3480	128	128	123	120	0.22	-0.92	-0.78	0.03	-0.58	-0.46	-1.24	-0.16
3780	121	118	116	113	0.16	-0.95	-0.74	0.04	-0.52	-0.43	-1.15	-0.10
4080	115	112	110	108	0.18	-0.87	-0.72	0.09	-0.55	-0.43	-1.29	-0.18
4380	110	109	110	109	0.26	-0.88	-0.79	0.11	-0.64	-0.46	-1.39	-0.31

Temperature - ^{o}F

Strain - $x10^{-3}$ in/in

MILD STEEL PASS #2

TIME	T2	T2'	T1	T1'	EX2	EY2	EX2'	EY2'	EX1	EY1	EX1'	EY1'
1	100	100	100	100	-0.32	-0.14	-1.01	0.25	0.28	-0.32	-0.59	0.31
20	100	100	100	100	-0.23	-0.02	-0.89	0.31	0.28	-0.32	-0.47	0.31
40	100	100	100	100	0.10	-0.02	-0.77	0.28	0.34	-0.32	-0.32	0.31
60	118	118	113	113	-0.38	-0.56	-1.13	-0.23	-0.01	-1.06	-0.61	-0.31
80	132	120	116	116	-0.23	-0.71	-0.49	-0.01	0.08	-1.00	-0.31	-0.43
100	163	149	130	123	-0.23	-0.98	-0.29	-0.44	-0.16	-1.30	-0.07	-0.76
120	225	200	143	136	-0.46	-1.66	-0.19	-1.12	-0.24	-1.41	-0.06	-1.02
140	309	276	159	152	-0.92	-2.57	-0.42	-2.16	-0.35	-1.52	-0.05	-1.22
160	389	353	177	170	-1.30	-3.19	-0.96	-3.03	-0.35	-1.55	-0.08	-1.40
180	453	410	198	190	-1.76	-3.65	-1.18	-3.34	-0.44	-1.67	-0.16	-1.54
200	498	456	222	210	-1.94	-3.77	-1.52	-3.50	-0.68	-1.94	-0.24	-1.71
220	528	493	240	230	-2.17	-3.69	-2.05	-3.70	-0.71	-2.03	-0.42	-1.89
240	548	515	258	246	-2.31	-3.54	-2.17	-3.65	-0.84	-2.19	-0.49	-1.96
260	560	528	271	262	-2.47	-3.34	-2.32	-3.40	-0.80	-2.15	-0.63	-2.07
280	563	537	286	275	-2.53	-3.10	-2.58	-3.24	-1.02	-2.31	-0.80	-2.15
300	563	537	297	286	-2.62	-2.92	-2.58	-2.88	-1.08	-2.37	-0.90	-2.16
320	560	538	305	297	-2.62	-2.80	-2.73	-2.79	-1.09	-2.32	-1.14	-2.25
340	553	535	311	304	-2.47	-2.56	-2.70	-2.65	-1.02	-2.19	-1.17	-2.19
360	544	527	315	308	-2.37	-2.40	-2.67	-2.37	-1.06	-2.20	-1.18	-2.11
380	536	522	323	313	-2.33	-2.30	-2.72	-2.27	-1.19	-2.33	-1.31	-2.12
400	525	514	327	317	-2.20	-2.20	-2.71	-2.20	-1.25	-2.36	-1.40	-2.06
420	516	506	330	319	-2.04	-2.16	-2.67	-2.10	-1.25	-2.30	-1.45	-1.96
440	508	498	320	321	-1.99	-2.21	-2.66	-2.03	-0.83	-1.85	-1.59	-1.95
460	497	489	330	323	-1.84	-2.08	-2.61	-1.98	-1.16	-2.15	-1.70	-1.97
480	487	478	330	323	-1.82	-2.03	-2.46	-1.80	-1.16	-2.09	-1.70	-1.91
540	459	454	330	324	-1.64	-1.94	-2.52	-1.65	-1.22	-2.00	-1.85	-1.82
600	431	428	325	319	-1.42	-1.72	-2.36	-1.46	-1.20	-1.95	-1.90	-1.69
660	409	405	316	313	-1.36	-1.72	-2.25	-1.29	-0.98	-1.79	-1.97	-1.58
720	387	385	313	310	-1.19	-1.71	-2.23	-1.18	-1.22	-1.85	-2.12	-1.58
780	371	368	300	304	-1.21	-1.84	-2.23	-1.21	-0.96	-1.56	-2.22	-1.56
840	350	350	292	292	-0.94	-1.57	-2.14	-1.03	-0.83	-1.40	-2.00	-1.31
1020	304	304	259	259	-0.84	-1.59	-2.19	-0.84	-0.34	-0.88	-1.78	-0.79

MILD STEEL PASS #2 (Continued)

TIME	T2	T2'	T1	T1'	EX2	EY2	EX2'	EY2'	EX1	EY1	EX1'	EY1'
1200	273	273	244	244	-0.94	-1.60	-2.08	-0.99	-0.36	-0.93	-1.92	-0.69
1380	246	246	232	232	-0.79	-1.42	-1.99	-0.19	-0.43	-1.00	-2.08	-0.67
1680	210	210	210	210	-0.54	-1.23	-1.86	0.09	-0.45	-0.99	-2.19	-0.66
1980	190	190	190	190	-0.55	-1.30	-1.90	0.08	-0.34	-0.97	-2.17	-0.55
2280	175	175	175	175	-0.54	-1.32	-1.92	0.09	-0.36	-0.90	-2.13	-0.48
2640	160	160	160	160	-0.50	-1.25	-1.85	0.16	-0.23	-0.80	-2.09	-0.35
2880	146	146	146	146	-0.26	-1.04	-1.73	0.37	0.01	-0.59	-1.88	-0.14
9999	70	70	70	70	0.42	-0.69	-1.38	0.45	0.09	-0.39	-1.80	0.15

MILD STEEL PASS #3

TIME	T3	T3'	T2	T2'	EX3	EY3	EX3'	EY3'	EX2	EY2	EX2'	EY2'
1	70	70	70	70	-0.57	-0.39	0.87	-0.12	0.21	-0.96	-1.62	0.24
20	93	85	70	70	-1.07	-0.38	0.95	-0.01	0.60	-0.18	-1.08	0.63
40	95	89	80	75	-0.97	-0.28	1.01	-0.01	0.39	-0.39	-0.97	0.53
60	98	92	85	80	-0.69	-0.12	1.28	0.11	0.50	-0.46	-0.93	0.51
80	113	102	95	88	-0.34	-0.22	1.79	-0.01	0.39	-0.70	-1.02	0.45
100	178	162	113	104	-1.11	-1.41	0.95	-1.03	-0.07	-1.12	-1.49	0.22
120	243	230	119	113	-1.10	-1.97	1.14	-1.47	0.03	-0.84	-1.66	0.41
140	320	323	126	126	-0.80	-2.75	1.15	-2.27	0.03	-0.54	-2.01	0.51
160	390	415	135	135	-0.83	-3.44	1.05	-3.42	-0.02	-0.32	-2.09	0.85
180	446	479	145	145	-1.28	-3.68	0.38	-3.79	-0.20	-0.26	-2.30	1.10
200	418	448	150	150	-1.67	-2.84	-0.52	-2.71	-0.12	-0.03	-2.40	1.47
220	340	362	155	155	-1.42	-1.57	-0.65	-1.37	-0.22	-0.25	-2.50	1.52
240	278	284	155	155	-1.13	-1.16	0.08	-0.49	-0.28	-0.88	-2.56	1.34
260	239	239	152	152	-1.45	-1.18	0.68	-0.25	-0.35	-1.67	-2.59	1.24
280	214	214	148	148	-1.66	-1.42	0.95	-0.34	-0.31	-2.11	-2.59	0.95
340	179	179	136	136	-1.21	-1.51	1.16	-0.22	-0.09	-1.95	-2.49	0.78
400	163	163	126	126	-1.13	-1.31	1.24	-0.20	-0.12	-1.68	-2.34	0.80
460	152	152	122	122	-1.16	-1.13	1.27	-0.20	-0.27	-1.50	-2.37	0.66
520	139	139	118	118	-1.01	-0.92	1.39	-0.05	-0.32	-1.43	-2.42	0.57
580	135	135	114	114	-1.10	-1.01	1.33	-0.14	-0.26	-1.43	-2.45	0.61
640	126	126	112	112	-0.93	-0.84	1.41	-0.03	-0.36	-1.47	-2.52	0.51
900	115	115	100	100	-0.93	-0.81	1.32	-0.03	-0.26	-1.31	-2.42	0.61
1260	104	102	90	87	-0.77	-0.77	1.49	0.14	-0.20	-1.07	-2.31	0.75
2460	85	85	85	85	-0.28	-0.58	1.64	0.29	-0.25	-0.91	-2.59	0.47

T-1 PASS #1

TIME	T1	T1'	T2	T2'	EX1	EY1	EX1'	EY1'	EX2	EY2	EX2'	EY2'
1	70	70	70	70	0.0	0.0	0.0	0.0	0.0	0.0	0.0	0.0
20	70	70	70	70	-0.03	0.27	-0.12	0.54	0.27	0.12	0.15	0.06
40	78	74	70	70	-0.28	-0.04	0.02	0.47	0.30	0.12	0.24	0.03
60	86	78	72	72	-0.41	-0.35	-0.01	0.50	0.34	0.04	0.28	-0.05
80	94	87	78	74	-0.36	-0.66	-0.18	0.33	0.26	-0.13	0.50	-0.13
100	117	111	86	79	-0.56	-1.28	-0.12	-0.27	0.19	-0.32	0.79	-0.23
120	163	152	95	89	-1.12	-2.29	-0.09	-1.44	0.11	-0.52	0.82	-0.44
140	246	232	105	100	-2.15	-3.53	-0.52	-3.16	0.08	-0.55	0.99	-0.62
160	345	330	119	119	-2.96	-4.40	-1.12	-4.54	-0.10	-0.70	0.86	-1.06
180	430	417	131	131	-3.14	-4.76	-1.46	-5.09	-0.39	-0.66	0.99	-1.14
200	490	478	148	148	-3.00	-4.68	-1.48	-4.97	-0.24	-0.78	0.99	-1.20
220	534	522	177	177	-3.03	-4.56	-1.57	-4.72	-0.55	-1.18	0.77	-1.60
240	561	553	196	196	-2.85	-4.17	-1.64	-4.34	-0.60	-1.26	0.84	-1.62
260	580	569	217	217	-2.65	-3.85	-1.42	-3.82	-0.69	-1.44	0.69	-1.83
280	588	582	233	233	-2.48	-3.59	-1.50	-3.48	-0.77	-1.52	0.64	-1.85
300	594	588	248	248	-2.57	-3.32	-1.73	-3.29	-0.91	-1.75	0.50	-2.01
320	593	589	260	260	-2.53	-3.01	-1.89	-3.03	-1.01	-1.85	0.40	-2.12
340	586	586	267	267	-2.38	-2.68	-1.90	-2.77	-0.95	-1.76	0.40	-1.97
360	578	578	273	273	-2.25	-2.49	-1.83	-2.58	-0.95	-1.76	0.29	-1.97
380	568	568	281	281	-1.98	-2.22	-1.86	-2.25	-1.02	-1.89	0.15	-2.07
400	560	560	286	286	-2.03	-2.15	-1.85	-2.18	-0.99	-1.84	0.02	-2.08
420	551	551	290	290	-1.98	-2.04	-1.92	-2.07	-1.03	-1.90	-0.07	-1.99
440	540	540	292	292	-1.91	-1.91	-1.97	-1.94	-0.93	-1.74	-0.06	-1.92
460	527	527	294	294	-1.65	-1.68	-1.71	-1.77	-0.92	-1.73	-0.14	-1.82
480	516	516	298	298	-1.64	-1.52	-1.70	-1.67	-1.01	-1.73	-0.26	-1.91
540	487	487	300	300	-1.48	-1.42	-1.81	-1.54	-1.03	-1.69	-0.49	-1.72
600	450	450	300	300	-1.18	-1.12	-1.60	-1.27	-1.09	-1.69	-0.79	-1.72
660	423	423	290	290	-0.85	-0.58	-1.54	-1.18	-0.76	-1.33	-0.67	-1.33
720	401	401	285	285	-0.78	-0.87	-1.50	-1.11	-0.84	-1.32	-0.78	-1.23
780	394	394	280	280	-1.17	-1.29	-2.04	-1.49	-0.86	-1.31	-0.95	-1.25
840	368	368	272	272	-0.76	-1.03	-1.69	-1.12	-0.82	-1.26	-0.94	-1.06
900	351	351	264	264	-0.61	-0.91	-1.60	-1.00	-0.75	-1.11	-0.93	-0.93

T-1 PASS #1 (Continued)

TIME	T1	T1'	T2	T2'	EX1	EY1	EX1'	EY1'	EX2	EY2	EX2'	EY2'
1020	325	325	249	249	-0.62	-0.92	-1.64	-0.92	-0.64	-0.94	-0.94	-0.82
1200	288	288	232	232	-0.24	-0.69	-1.32	-0.63	-0.61	-0.91	-1.00	-0.67
1380	263	263	213	213	-0.08	-0.62	-1.31	-0.49	-0.42	-0.72	-0.96	-0.48
1680	230	230	190	190	0.03	-0.51	-1.32	-0.39	-0.34	-0.55	-0.91	-0.40
1980	203	203	169	169	0.18	-0.42	-1.17	-0.18	-0.12	-0.37	-0.81	-0.24
2280	186	186	156	156	0.09	-0.51	-1.23	-0.27	-0.10	-0.34	-0.79	-0.13
3180	144	144	126	126	0.37	-0.26	-1.04	0.07	0.05	-0.07	-0.70	0.02
4080	120	120	113	113	0.43	-0.20	-1.01	0.13	-0.08	-0.20	-0.80	-0.08
5160	100	100	100	100	0.61	-0.05	-0.83	0.31	0.01	-0.05	-0.83	-0.02

T-1 PASS #2

TIME	T2'	T2	T1'	T1	EX2'	EY2'	EX2	EY2	EX1'	EY1'	EX1	EY1
1	100	100	100	100	-0.80	0.22	0.01	0.04	-0.86	0.31	0.37	0.07
20	100	100	100	100	-0.80	0.31	0.01	0.04	-0.86	0.31	0.37	0.07
40	105	105	105	105	-0.78	0.15	-0.15	-0.06	-0.81	0.15	0.18	-0.12
60	109	109	109	109	-0.76	0.05	-0.24	-0.07	-0.79	-0.01	0.05	-0.25
80	119	118	109	109	-0.72	-0.12	-0.32	-0.32	-0.52	-0.01	0.14	-0.22
100	138	135	117	113	-0.70	-0.64	-0.38	-0.74	-0.40	-0.28	0.14	-0.28
120	174	174	126	123	-0.68	-1.55	-0.65	-1.70	-0.21	-0.51	0.02	-0.55
140	240	240	127	135	-1.07	-2.84	-1.16	-3.05	0.23	-0.40	-0.08	-0.74
160	324	322	140	145	-1.64	-3.83	-1.86	-4.12	0.24	-0.57	0.05	-0.74
180	402	393	153	162	-1.96	-4.42	-2.06	-4.46	0.13	-0.68	-0.16	-0.97
200	467	457	171	177	-2.09	-4.52	-2.37	-5.04	-0.06	-0.87	-0.20	-1.04
220	513	502	187	192	-2.07	-4.32	-2.52	-4.50	-0.14	-1.01	-0.21	-1.08
240	545	530	204	209	-2.09	-4.04	-2.49	-4.14	-0.28	-1.24	-0.30	-0.90
260	563	553	220	225	-2.05	-3.70	-2.71	-3.91	-0.36	-1.35	-0.31	-1.00
280	576	565	237	244	-2.04	-3.48	-2.61	-3.66	-0.39	-1.53	-0.48	-1.47
300	582	569	251	257	-2.00	-3.17	-2.43	-3.27	-0.45	-1.62	-0.56	-1.52
320	586	575	263	268	-2.01	-2.97	-2.45	-3.14	-0.58	-1.69	-0.56	-1.49
340	587	577	273	277	-2.08	-2.83	-2.50	-3.04	-0.61	-1.72	-0.55	-1.48
360	583	571	285	288	-2.04	-2.52	-2.36	-2.66	-0.80	-1.82	-0.70	-1.57
380	580	567	294	297	-2.14	-2.44	-2.23	-2.53	-0.88	-1.93	-0.84	-1.59
400	571	563	300	303	-1.97	-2.18	-2.26	-2.47	-1.02	-1.89	-0.86	-1.58
420	565	555	306	308	-2.01	-2.04	-2.19	-2.22	-1.04	-1.88	-0.82	-1.60
440	556	547	308	310	-1.99	-1.93	-2.09	-2.03	-1.09	-1.75	-0.83	-1.46
460	548	540	312	314	-2.01	-1.83	-2.00	-1.94	-1.21	-1.72	-0.81	-1.44
480	539	529	314	316	-2.02	-1.81	-1.85	-1.70	-1.29	-1.62	-0.83	-1.37
540	511	502	323	323	-1.99	-1.54	-1.62	-1.44	-1.64	-1.67	-0.89	-1.25
600	484	475	323	323	-1.94	-1.37	-1.53	-1.20	-1.70	-1.55	-1.01	-1.31
660	456	450	318	318	-1.88	-1.22	-1.32	-1.14	-1.80	-1.29	-0.87	-1.14
720	433	429	313	313	-1.86	-1.11	-1.26	-1.08	-1.88	-1.19	-0.80	-0.98
780	409	406	307	307	-1.75	-0.88	-1.06	-0.99	-1.95	-1.08	-0.81	-0.96
840	391	388	303	303	-1.83	-0.87	-1.05	-0.99	-2.09	-1.04	-0.86	-0.92
900	373	370	296	296	-1.83	-0.81	-0.99	-1.02	-2.09	-0.95	-0.83	-0.86

T-1 PASS #2 (Continued)

TIME	T2'	T2	T1'	T1	EX2'	EY2'	EX2	EY2	EX1'	EY1'	EX1	EY1
1080	326	326	273	273	-1.78	-0.61	-0.82	-1.21	-2.17	-0.70	-0.58	-0.67
1260	291	291	255	255	-1.84	-0.40	-0.70	-1.03	-2.16	-0.57	-0.57	-0.63
1440	262	262	234	234	-1.71	-0.30	-0.54	-1.05	-2.13	-0.33	-0.36	-0.42
1740	227	227	209	209	-1.59	-0.12	-0.33	-0.93	-2.07	-0.12	-0.27	-0.27
2040	198	198	191	191	-1.37	0.09	-0.14	-0.71	-2.12	-0.05	-0.23	-0.23
2340	179	179	177	177	-1.48	0.11	-0.04	-0.64	-2.18	0.01	-0.26	-0.26
2640	162	162	162	162	-1.42	0.08	-0.01	-0.67	-2.08	0.05	-0.25	-0.25
3240	129	129	129	129	-1.29	0.36	0.15	-0.45	-1.95	0.24	-0.06	0.06
3840	118	118	118	118	-1.34	0.30	0.19	-0.47	-2.06	0.25	-0.05	-0.05

T-1 PASS #3

TIME	T3'	T3	T2'	T2	EX3'	EY3'	EX3	EY3	EX2'	EY2'	EX2	EY2
1	106	106	100	100	-1.28	-0.29	0.04	0.07	-1.10	0.28	0.16	-0.14
20	108	108	100	100	-1.41	-0.39	0.03	0.06	-1.07	0.19	0.28	-0.20
40	110	113	103	106	-1.34	-0.59	-0.08	-0.14	-1.16	-0.05	0.13	-0.50
60	113	119	105	109	-1.31	-0.77	-0.01	-0.43	-1.15	-0.16	0.20	-0.67
80	120	126	106	112	-1.04	-1.07	0.26	-0.85	-1.13	-0.23	0.23	-0.85
100	139	144	106	113	-0.73	-1.81	0.58	-1.37	-1.10	-0.20	0.43	-0.95
120	174	181	110	116	-0.58	-2.47	0.79	-2.81	-1.16	-0.23	0.56	-0.91
140	234	246	116	121	-1.11	-3.12	0.43	-4.10	-1.27	-0.01	0.54	-0.81
160	287	312	121	126	-1.13	-2.84	0.21	-4.53	-1.38	0.33	0.56	-0.58
180	313	348	126	134	-0.79	-1.96	0.20	-4.00	-1.42	0.77	0.43	-0.35
200	295	329	137	142	-0.63	-0.87	-0.15	-2.64	-1.64	0.94	0.27	-0.09
220	245	259	146	153	-0.70	0.20	-0.43	-0.67	-1.72	1.19	0.05	0.05
240	209	219	156	162	-0.80	0.31	-0.32	-0.17	-1.84	1.25	0.09	0.06
260	190	194	161	166	-0.67	0.29	-0.10	-0.04	-1.94	1.24	-0.18	0.09
280	179	182	160	165	-0.51	0.21	-0.05	0.16	-1.84	1.22	-0.18	-0.06
300	175	178	158	163	-0.47	0.01	-0.08	-0.38	-1.85	1.06	-0.25	-0.22
320	170	173	152	158	-0.34	-0.01	0.02	-0.43	-1.68	1.02	-0.14	-0.29
340	168	172	150	154	-0.32	-0.02	0.00	-0.54	-1.72	0.86	-0.08	-0.38
360	166	168	146	152	-0.36	0.03	0.10	-0.53	-1.69	0.80	-0.12	-0.54
420	161	163	136	142	-0.41	0.16	0.02	-0.67	-1.57	0.74	0.09	-0.72
480	151	154	127	134	-0.20	0.49	0.13	-0.62	-1.31	0.82	0.16	-0.77
540	145	149	124	129	-0.18	0.57	-0.03	-0.63	-1.37	0.73	0.11	-0.76
600	137	139	122	126	-1.09	0.52	-0.04	-0.52	-1.48	0.62	-0.07	-0.88
660	130	134	120	123	-1.16	0.58	-0.05	-0.50	-1.58	0.55	-0.08	-0.92
720	126	129	114	119	-1.21	0.53	-0.04	-0.49	-1.44	0.69	-0.07	-0.91
780	124	126	113	118	-1.25	0.48	-0.04	-0.46	-1.52	0.61	-0.09	-0.96
960	116	120	107	113	-1.21	0.53	-0.08	-0.47	-1.44	0.63	-0.14	-0.92
1200	113	113	105	105	-1.04	0.19	-0.11	-0.41	-1.48	0.62	0.11	-0.73
1500	107	107	103	103	-0.87	0.36	0.06	-0.24	-1.46	0.61	0.13	-0.68
1800	103	103	103	103	-0.77	0.49	0.19	-0.11	-1.46	0.61	0.07	-0.71

CORTEN PASS #1

TIME	T1	T1'	T2	T2'	EX1	EY1	EX1'	EY1'	EX2	EY2	EX2'	EY2'
1	70	70	70	70	0.0	0.18	-0.09	0.24	0.0	0.0	0.0	0.0
20	74	74	74	74	-0.15	0.15	-0.30	0.21	-0.09	-0.15	-0.06	-0.15
40	78	78	78	78	-0.28	0.08	-0.37	0.17	-0.07	-0.34	-0.10	-0.28
60	82	87	82	82	-0.25	0.11	-0.57	-0.09	-0.10	-0.52	-0.13	-0.43
80	90	102	86	86	-0.26	0.01	-0.73	-0.55	-0.05	-0.47	-0.08	-0.47
100	104	125	88	90	-0.11	-0.26	-0.92	-1.16	0.18	-0.48	-0.08	-0.50
120	131	177	94	100	0.29	-0.58	-1.55	-2.33	0.36	-0.60	-0.35	-0.65
140	192	263	102	112	0.39	-1.41	-2.47	-3.70	0.53	-0.67	-0.42	-0.87
160	286	370	114	122	0.09	-2.52	-3.30	-4.95	0.61	-0.86	-0.45	-0.90
180	385	460	126	137	-0.28	-3.49	-3.38	-5.36	0.66	-0.99	-0.61	-1.03
200	472	530	141	153	-0.79	-4.33	-3.39	-5.43	0.62	-1.24	-0.77	-1.13
220	531	579	156	169	-1.05	-4.56	-3.39	-5.25	0.61	-1.25	-0.85	-1.21
240	575	607	161	174	-1.61	-4.67	-3.24	-4.80	0.96	-1.05	-0.53	-0.95
260	602	626	190	203	-1.94	-4.58	-3.01	-4.42	0.32	-1.69	-1.20	-1.59
280	616	634	202	214	-1.88	-4.25	-2.93	-4.10	0.27	-1.80	-1.12	-1.66
300	625	637	216	227	-1.98	-4.02	-2.75	-3.89	0.09	-1.92	-1.23	-1.74
320	630	635	228	237	-2.24	-4.04	-2.67	-3.63	-0.01	-1.93	-1.14	-1.68
340	628	630	237	248	-2.34	-3.78	-2.72	-3.32	-0.03	-1.92	-1.20	-1.74
360	622	622	250	260	-2.23	-3.49	-2.47	-3.07	-0.26	-2.09	-1.30	-1.87
380	613	613	260	268	-2.24	-3.08	-2.30	-2.78	-0.40	-2.17	-1.28	-1.85
400	606	606	269	276	-2.33	-2.99	-2.39	-2.69	-0.54	-2.25	-1.32	-1.92
420	594	594	274	282	-2.23	-2.83	-2.23	-2.47	-0.64	-2.17	-1.31	-1.88
440	582	582	281	287	-2.12	-2.48	-2.06	-2.24	-0.73	-2.17	-1.30	-1.81
460	569	569	285	291	-1.98	-2.34	-1.98	-2.04	-0.80	-2.15	-1.33	-1.78
480	560	560	288	296	-2.05	-2.35	-1.87	-1.75	-0.91	-2.14	-1.43	-1.85
540	525	525	296	301	-2.26	-2.32	-1.93	-2.02	-1.25	-1.97	-1.27	-1.72
600	493	493	298	302	-1.81	-1.78	-1.36	-1.18	-1.33	-1.96	-1.43	-1.73
660	462	462	299	301	-1.63	-1.60	-1.09	-1.09	-1.43	-1.91	-1.33	-1.63
720	438	438	297	297	-1.63	-1.48	-1.03	-1.03	-1.59	-1.86	-1.26	-1.56
780	416	416	289	289	-1.63	-1.45	-1.03	-1.06	-1.52	-1.58	-1.07	-1.37
960	375	375	280	280	-1.57	-1.27	-0.70	-1.00	-1.78	-1.54	-1.18	-1.42
1140	312	312	248	248	-1.39	-0.94	-0.37	-0.97	-1.62	-1.08	-0.87	-0.99

CORTEN PASS #1 (Continued)

TIME	T1	T1'	T2	T2'	EX1	EY1	EX1'	EY1'	EX2	EY2	EX2'	EY2'
1320	279	279	231	231	-1.38	-0.81	-0.24	-0.90	-1.71	-1.05	-0.84	-0.93
1500	250	250	213	213	-1.25	-0.62	-0.14	-0.77	-1.65	-0.84	-0.75	-0.78
1800	215	215	189	189	-1.34	-0.56	-0.17	-0.83	-1.65	-0.78	-0.72	-0.81
2100	185	185	166	166	-1.17	-0.36	0.15	-0.63	-1.55	-0.62	-0.53	-0.62
2400	165	165	151	151	-1.21	-0.37	0.20	-0.67	-1.57	-0.55	-0.52	-0.64
3000	131	131	122	122	-1.03	-0.16	0.41	-0.49	-1.44	-0.36	-0.42	-0.45

CORTEN PASS #2

TIME	T3	T3'	T2	T2'	EX3	EY3	EX3'	EY3'	EX2	EY2	EX2'	EY2'
1	87	87	98	98	-0.81	-1.26	-0.60	0.0	-1.35	-0.45	-0.30	-0.45
20	91	91	98	98	-0.99	-1.47	-0.33	-0.06	-1.35	-0.45	-0.24	-0.45
40	96	96	98	98	-1.12	-1.69	-0.49	-0.04	-1.26	-0.45	-0.12	-0.48
60	100	100	100	100	-1.09	-1.99	-0.59	-0.11	-1.25	-0.53	-0.02	-0.59
80	106	113	103	103	-1.27	-2.23	-0.73	-0.73	-1.30	-0.61	0.02	-0.73
100	116	123	105	105	-1.06	-2.53	-0.55	-1.24	-1.32	-0.60	0.12	-0.78
120	133	152	108	108	-1.32	-2.28	-0.65	-2.00	-1.32	-0.42	0.21	-0.75
140	180	211	113	113	-1.28	-2.21	-1.09	-2.98	-0.55	-0.22	0.08	-0.64
160	251	294	115	115	-1.47	-2.73	-1.69	-4.18	-1.56	0.00	-0.06	-0.48
180	308	340	116	116	-1.93	-2.83	-1.48	-4.03	-1.66	0.26	-0.19	-0.25
200	302	312	117	117	-2.27	-2.39	-1.06	-2.50	-1.66	0.35	-0.13	-0.04
220	270	270	120	120	-2.02	-2.02	-0.85	-1.63	-1.72	0.41	-0.19	-0.07
240	230	230	122	122	-1.65	-1.62	-0.72	-1.02	-1.74	0.33	-0.27	-0.09
260	204	204	123	123	-2.02	-1.57	-0.43	-0.97	-1.75	0.26	-0.28	-0.16
280	190	190	125	125	-2.26	-1.96	-0.43	-1.36	-1.76	0.10	-0.32	-0.29
300	177	177	125	125	-2.18	-2.00	-0.29	-1.16	-1.79	0.04	-0.32	-0.35
320	171	171	125	125	-2.10	-2.25	-0.18	-1.29	-1.79	-0.05	-0.32	-0.59
340	168	168	125	125	-2.07	-2.58	-0.15	-1.35	-1.82	-0.11	-0.32	-0.62
360	166	166	124	124	-2.09	-2.63	-0.14	-1.37	-1.81	-0.19	-0.31	-0.73
420	153	153	118	118	-2.03	-2.24	-0.14	-1.37	-1.70	-0.11	-0.35	-0.83
480	140	140	114	114	-2.13	-2.34	-0.15	-1.23	-1.70	-0.20	-0.44	-0.86
540	132	132	112	112	-2.24	-2.39	-0.29	-1.04	-1.77	-0.36	-0.63	-0.78
600	125	125	106	105	-2.18	-2.33	-0.26	-0.98	-1.66	-0.25	-0.45	-0.57
780	105	105	95	95	-1.65	-1.80	-0.30	-0.99	-1.63	-0.25	-0.55	-0.58
900	94	94	87	87	-1.92	-1.95	-0.33	-0.93	-1.59	-0.45	-0.45	-0.48

CORTEN PASS #3

TIME	T2	T2'	T1	T1'	EX2	EY2	EX2'	EY2'	EX1	EY1	EX1'	EY1'
1	78	78	74	74	-1.15	0.29	-0.13	-0.04	-0.99	0.06	0.45	-0.15
20	87	87	78	78	-1.35	0.03	-0.39	-0.30	-1.03	-0.04	0.29	-0.25
40	94	94	83	83	-1.38	0.03	-1.60	-0.39	-1.10	-0.23	0.13	-0.41
60	100	103	85	85	-1.19	0.01	-0.67	-0.58	-0.88	-0.28	0.14	-0.43
80	112	119	87	89	-1.14	-0.18	-0.96	-0.90	-0.63	-0.33	0.11	-0.46
100	128	146	91	97	-0.71	-0.38	-1.25	-1.34	-0.33	-0.45	0.04	-0.68
120	169	206	97	105	-0.52	-1.09	-1.89	-2.64	-0.05	-0.53	-0.03	-0.75
140	248	305	106	115	-0.57	-2.40	-2.83	-4.54	0.05	-0.73	-0.09	-0.87
160	347	403	116	125	-1.09	-3.76	-3.49	-5.59	0.05	-0.82	-0.11	-0.92
180	431	480	124	133	-1.33	-4.60	-3.74	-5.90	0.14	-0.82	-0.06	-0.84
200	491	530	133	143	-1.70	-4.88	-3.93	-5.79	0.12	-0.93	-0.12	-0.93
220	528	563	145	156	-2.02	-4.81	-4.03	-5.56	-0.02	-1.10	-0.23	-1.10
240	553	582	156	168	-2.32	-4.63	-4.13	-5.15	-0.08	-1.20	-0.27	-1.20
260	565	590	168	178	-2.55	-4.32	-4.08	-4.68	-0.21	-1.32	-0.27	-1.23
280	569	591	179	188	-2.67	-3.93	-4.03	-4.18	-0.37	-1.42	-0.32	-1.28
300	567	587	189	197	-2.71	-3.58	-3.94	-3.76	-0.51	-1.44	-0.40	-1.33
320	565	580	198	206	-2.91	-3.51	-3.79	-3.49	-0.71	-1.52	-0.51	-1.41
340	557	568	206	202	-2.84	-3.26	-3.47	-3.08	-0.78	-1.47	-0.03	-0.96
360	548	558	214	222	-2.91	-3.03	-3.33	-2.99	-0.99	-1.54	-0.65	-1.55
540	448	453	246	251	-2.68	-1.93	-2.15	-1.88	-1.87	-1.30	-0.84	-1.35
720	374	379	240	246	-2.67	-1.53	-1.73	-1.73	-2.18	-0.95	-0.79	-1.09
900	312	318	225	227	-2.41	-1.06	-1.23	-1.47	-2.38	-0.85	-0.60	-0.30
1200	246	248	192	194	-2.32	-0.79	-0.84	-1.14	-2.34	-0.42	-0.29	-0.50
1500	154	154	145	145	-2.58	-0.15	-0.21	-0.81	-2.54	-0.11	-0.14	-0.17
1800	108	108	108	108	-2.07	0.12	0.03	-0.66	-2.55	0.03	0.03	-0.03

Pan out of oxygen when flame was $5\frac{1}{2}$" past the transverse line through the strain gages.

REFERENCES

(1.) K. Masubuchi, F. B. Simmons and R. E. Monroe, "Analysis of Thermal Stresses and Metal Movement During Welding", RSIC-820, Redstone Scientific Information Center, Redstone Arsenal, Alabama (July 1968).

(2.) J. B. Andrews, M. Arita and K. Masubuchi, "Analysis of Thermal Stress and Metal Movement During Welding", Report No. 71-1, Massachusetts Institute of Technology, Department of Naval Architecture and Marine Engineering, (December 1970).

(3.) R. Tanbakuchi, "Comparison of Measured Metal Temperatures During Arc Welding with Temperature Calculated Using a Finite Heat Source", The University of Wisconsin, Ph.D., (1967), Engineering, engineering, mechanical.

(4.) V. Pauclic, "Temperature Histories in a Thin Steel Plate Welded with Tungsten Inert Gas Process", The University of Wisconsin, Ph.D., (1968), Engineering, engineering, mechanical.

(5.) Richard E. Holt, "Flame Straightening Basics", Welding Engineer, Vol. 50, (September 1965).

(6.) R. A. Walsh, "Investigation of Distortion Removal in Welded Structures", Thesis XIII-A, (May 1970), M.I.T.

(7.) David A. Duffy, "Distortion Removal in Structural Weldments", Thesis XIII-A, (May 1970), M.I.T.

(8.) H. E. Pattee, R. M. Evans and R. E. Monroe, "Experimental Flame and Mechanical Straightening and its Effects on Base Metal Properties", Project SR-185, Battelle Memorial Institute, Columbus, Ohio, (July 1969).

(9.) W. M. Murray, "Stress and Strain Relations", Part of a series of lectures presented at Wayne State University during the NSF Summer Institute on Experimental Strain Analysis for College Teachers, (July 25 to September 2, 1966).

(10.) Daniel Rosenthal, "Mathematical Theory of Heat Distribution During Welding and Cutting", Welding Journal, 20, (5) Supplement 220-S to 234-S, (1941).

(11.) T. Nakada and S. Hashimoto, "Heat Conduction in a Semi-Infinite Solid Heated by a Moving Heat Source Along the Boundary", Bull JSME 6:21, 59-69, (February 1963).

(12.) N. Y. Olcer, "On the Theory of Conductive Heat Transfer in Finite Regions", Internat. J. Heat Mass Transfer, 7, 3, 307-314, (March 1964).

(13.) N. W. Rykalin, "Calculation of Heat Processes in Welding", Moscow, (1960).

(14.) K. Masubuchi, "Control of Distortion and Shrinkage in Welding", WRC Bulletin, (April 1970).

(15.) J. N. Goodier, "On the Integration of Thermo-Elastic Equations", Phil. Mag., 23, (1937), p. 1037.

(16.) Alexander Mendelson, "Plasticity: Theory and Application", McMillan, New York, (1968).

(17.) C. F. Lucks and H. W. Dean, "Thermal Properties of Thirteen Metals", ASTM Special Technical Publication, No. 227, (1958).

(18.) L. L. Lengyel, "An Analytical Correlation of Heat Flux, Nozzle Diameter and Melting Time as Applied to Nozzle Burners", Appl. Sci. Res. (A), 13, 4/5, 393-400, (1964).

(19.) H. S. Carslaw and J. C. Jaeger, "Conduction of Heat in Solids", (2nd Ed.), Clarendon Press, Oxford, (1959).

(20.) "Aerospace Structural Metals Handbook", Mich. Properties Data Center, Air Force Info. Center, Belfour Stulen, Inc.

(21.) U.S.S.C. - "U.S.S. T-1 Steel, A Proven Engineering Material", (1959).

(22.) U.S.S.C. - "U.S.S. Corten High Strength Low Alloy Steel", (1960).